Universitat de Girona

BIOREMEDIATION OF NITRATE-POLLUTED GROUNDWATER USING BIOELECTROCHEMICAL SYSTEMS

Narcís Pous Rodríguez

Dipòsit legal: Gi. 1346-2015
http://hdl.handle.net/10803/302539

DOCTORAL THESIS

Bioremediation of nitrate-polluted groundwater using bioelectrochemical systems

Narcís Pous Rodriguez

2015

EXPERIMENTAL SCIENCES AND SUSTAINABILITY PhD PROGRAMME

Supervisors: Dr. Sebastià Puig Broch, Dra. M. Dolors Balaguer Condom, Dr. Jesús Colprim Galceran.

Tutor: Dr. Sebastià Puig Broch

PhD thesis submitted to aim for PhD degree for the University of Girona

List of publications

This thesis has been written as published peer reviewed articles compendium based on the specific regulations of the PhD program of the University of Girona.

Peer reviewed paper publications presented as chapters of this PhD thesis and the candidate PhD contribution in each publication is listed below:

1. **Pous, N.**; Puig, S.; Coma, M.; Balaguer, M.D.; Colprim, J., 2013. Bioremediation of nitrate-polluted groundwater in a microbial fuel cell. Journal of Chemical Technology and Biotechnology 88 (9) 1690-1696. DOI:10.1002/jctb.4020. Impact factor: 2.494. 1st quartile.

   Author's contribution: Experimental design and performance. Data monitoring and reactor operation. Writing the paper.

2. **Pous, N.**; Puig, S.; Balaguer, M.D.; Colprim, J., 2015. Cathode potential and anode electron donor evaluation for a suitable treatment of nitrate-contaminated groundwater in bioelectrochemical systems. Chemical Engineering Journal 263, 151-159. DOI: 10.1016/j.cej.2014.11.002. Impact factor: 4.058. 1st quartile.

   Author's contribution: Experimental design and performance. Data monitoring and reactor operation. Writing the paper.

3. **Pous, N.**; Koch, C.; Colprim, J.; Puig, S.; Harnisch, F., 2014. Extracellular electron transfer of biocathodes: Revealing the potential for nitrate and nitrite reduction of denitrifying microbiomes dominated by *Thiobacillus* sp. Electrochemistry Communications 49, 93-97. DOI: 10.1016/j.elecom.2014.10.011. Impact factor: 4.287. 1st quartile.

   Author's contribution: Experimental design and chemical and electrochemical performance. Data monitoring and reactor operation. Writing the paper.

Chapters of this PhD thesis are ready to be submitted as journal article and the candidate PhD contribution is listed below:

4. **Pous, N.**; Koch, C.; Vilà, A.; Balaguer, M.D.; Colprim, J.; Mühlenberg, J.; Müller, S.; Harnisch, F.; Puig, S. Monitoring and engineering reactor microbiomes of denitrifying bioelectrochemical systems.

   Author's contribution: Experimental design and chemical and electrochemical performance. Data monitoring and reactor operation. Writing the paper.

5. **Pous, N.**; Puig, S.; Balaguer, M.D.; Colprim, J. Promoting high denitrification rates and disinfection in tubular denitrifying bioelectrochemical systems.

   Author's contribution: Experimental design and performance. Data monitoring and reactor operation. Writing the paper.

List of abbreviations

ARB	anode-respiring bacteria
BES	bioelectrochemical systems
CA	chronoamperometry
CE	coulombic efficiency
CEM	cation exchange membrane
COD	chemical oxygen demand
CV	cyclic voltammetry
d-BES	denitrifying bioelectrochemical system
DC	direct current
DET	direct electron transfer
DSA	Dimensionally stable anode
EET	extracellular electron transfer
FCM	flow cytometry measurement
HRT	hydraulic retention time
IC	inorganic carbon
MBR	membrane bioreactor
MEC	microbial electrolysis cell
MET	mediated electron transfer
MFC	microbial fuel cell
Mtr	metal-reducing
NAC	net anode volume
napA	nitrate reduction enzyme periplasmic
narG	nitrate reduction enzyme (G)
NCC	net cathode compartment
nirK	nitrite reduction enzyme (K)
nirS	nitrite reduction enzyme (S)
NO_3^-LR	nitrate loading rate
norB	nitric oxide reduction enzyme

nosZ	nitrous oxide reduction enzyme
OCV	open cell voltage
Ox	molecule at its oxidized state
PBS	phosphate buffer solution
PCR	polymerase chain reaction
PCR-DGGE	polymerase chain reaction-denaturing gradient gel electrophoresis
QR	quality ratio
Red	molecule at its reduced state
SEM	scanning electron microscope
SHE	standard hydrogen electrode
SP	sampling port
ST	stress-test
T-RFLP	terminal restriction fragment length polymorphism
Ti-MMO	titanium-mixed metal oxide
TOC	total organic carbon

List of figures

List of tables

Certificate of thesis direction

El Dr. Sebastià Puig Broch, la Dra. M.D. Balaguer i el Dr. Jesús Colprim Galceran, de la Universitat de Girona.

DECLAREM:

Que el treball titulat *Bioremediation of nitrate-polluted groundwater using bioelectrochemical systems*, que presenta Narcís Pous Rodriguez per a l'obtenció del títol de doctor, ha estat realitzat sota la meva direcció i que compleix els requisits per a esser publicat com a compendi de publicacions i per a poder optar a Menció Internacional.

I, perquè així consti i tingui els efectes oportuns, signo aquest document.

Dr. Sebastià Puig Broch Dr. M. Dolors Balaguer Condom Dr. Jesús Colprim Galceran

Girona,

Als meus pares, a l'Anna, a en Martí i als meus avis…

Agraïments/Acknowledgements

Finalment ha arribat el moment agrair a les diferents persones que m'han donat suport en aquest trajecte. És l'apartat més complicat, espero no deixar-me a ningú.

Primer de tot voldria agrair a en Jesús, la Marilós i en Sebastià, que hem van donar l'oportunitat d'entrar al LEQUIA ara fa 5 anys per a fer el treball experimental de la carrera de Química, que em van tornar a obrir les portes per a fer el treball de Màster, i que, al final, han acabat convertint-se en els meus directors de tesi doctoral. Vull agrair a en Sebastià la confiança que ha dipositat en mi, el fet d'apretar-me per no conformar-me amb el resultat assolit i fer-me anar un pas més enllà, el seu positivisme i el seu suport/consell tan científic com personal. Pel que fa a la Marilós, li vull agrair tot el temps que m'ha dedicat, llegint i corregint articles, ensenyant-me com re-estructurar i re-escriure els articles per facilitar-ne l'enteniment i, en general, tot el coneixement que m'ha transmès. Pel que fa a en Jesús, primer de tot voldria dir que, com dirien en castellà, "aprieta…pero no ahoga", això m'ha obligat a donar el màxim i a ser menys dubitatiu. En definitiva, moltes gràcies als tres!

Als companys del grup piles amb qui més temps he pogut compartir, a l'Anna, la Marta, la Marina i en Pau, sense els quals aquest viatge hagués estat, sense cap mena de dubte, més feixuc. Als microbiòlegs amb qui em tingut més d'una llarga discussió, en Lluís (Cacho) i l'Ariadna. També al nostre *stager* Daniele, els postdocs que s'han incorporat recentment en el grup, Erika i Fungisai, i també als altres doctorands que han volgut fer una petita estada amb nosaltres: Jorge, Krishna i Tommy.

Però per a realitzar la tesi també és necessari el suport i ajuda de la resta de companys de laboratori. A en Jordi i la Montse per la seva ajuda en els moments de redacció de la tesi i tota la burocràcia que el seu dipòsit comporta. Però també a en Tico, Xavi, Maël, Tiago, Patricia G., Helio, Elena, Alba A., Serni, Gemma R., Rafa, Ariadna C., Sara G., Teresa, Hèctor, Sara R., Patricia S., Ramón, Anna R., Marc, Alba C., Esther, Michele, Julian, Antonia, Chus, Manel G., Alexandra, Silvio.

The PhD thesis allowed me to develop research stages in Narbonne (France), Monterotondo-Roma (Italy) and Leipzig (Germany), allowing me to learn a lot from the different ways of doing research and ways of life. From my stage in Narbonne I would like to acknowledge Dr. Nicolas Bernet for allowing me to visit his team, and to Dr. Alessandro Carmona-Martínez the knowledge transmitted, the time he has spent for me and his friendship.

From Roma, I would like to thank Dr. Federico Aulenta for allowing me to work in his lab and to teach me a lot about BES. Also I would like to acknowledge Dr. Barbara Casentini for her dedication on my work in Monterotondo, and to my labmate Patricia with who I could share nice moments not only in the lab but also in the chaotic, but beautiful, Roma.

Finally, from my stage in Leipzig, I would like to thank Dr. Falk Harnisch for opening his lab to me and for allowing me to learn a lot from him. Many thanks also to Dr. Christin Koch, for being patient when teaching me microbiological knowledge and for the huge amount of time that she has spent in our work. I wouldn't like to forget of Dr. Luis Rosa, with who I had nice talks, neither of the PhD students Benny, Carla and Carolin and other people of the group: Thore, Monnie, Conny, Theresa or Anne.

Fora els murs del laboratori, voldria agrair primer de tot als meus pares per el seu suport constant i la seva total confiança en mi. A l'Anna, la meva parella, simplement gràcies per fer-me feliç, ajudar-me a decidir-me a iniciar i continuar la tesi, i per estar al meu costat. També gràcies al meu germà Martí, als avis, als meus tiets (en especial als més propers, Carme, Albert, Santi i Conxita) i als meus cosins (especialment als més propers, Roger, Eloi i Anna) que sempre han estat allà quan els he necessitat.

Finalment al grup d'amics, amb alguns dels quals he compartit pràcticament tota la meva vida i que m'han servit de vàlvula d'escapament de les preocupacions diàries. Gràcies Ricard, Mala, Iban, Cèsar, Salva i Àngel. Així com, també a les amigues químiques, la Marta i la Silvia.

Moltes gràcies a tots i totes!

This thesis was financially supported by the Catalan Government (2012 FI-B 00941, pre-doctoral grant), the University of Girona (MOB2014-ref22, mobility grant), the European Union through a COST Action ES1202 in the context of Water 2020 (COST-STSM-ECOST-STSM-ES1202-011013-035423, mobility grant) and the Spanish Government through the following projects: BEST-ENERGY (CTQ2011-23632), CONSOLIDER (CSD2007-00055). LEQUIA has been recognized as consolidated group by the Catalan Government with code 2014-SGR-1168.

Table of contents

Resum

La presència de nitrats (NO_3^-) en aigües subterrànies és una preocupació global. En certes zones geogràfiques, les concentracions de nitrat excedeixen els límits marcats per a la Organització Mundial de la Salut (OMS) per al consum humà (superiors a 50 $mgNO_3^-·L^{-1}$ (11.29 $mgN·L^{-1}$)). Actualment, les tecnologies més efectives per a eliminar el nitrat en aigües subterrànies són la osmosi inversa, la electrodiàlisi inversa o l'intercanvi iònic. Però aquestes tecnologies requereixen d'alts consums energètics i es basen en separar el nitrat i concentrar-lo en salmorra, la qual té un difícil tractament. D'altre banda, la desnitrificació biològica permet la conversió del nitrat (tòxic) en dinitrogen gas (N_2) (inert). Convencionalment, la desnitrificació es porta a terme de forma heterotròfica. Aquest procés implica la generació de biomassa en excés i requereix de l'addició de matèria orgànica, la qual s'ha d'eliminar completament per a l'ús de l'aigua pel consum humà. Per aquestes raons, els processos de desnitrificació autotròfica seria els més adients per a tractar aigua subterrània.

En biocàtodes de sistemes bioelectroquímics (BES), bactèries autotròfiques desnitrificants són capaces de reduir els nitrats a dinitrogen gas tot emprant l'elèctrode catòdic com a donador d'electrons. Aquest procés implica una baixa generació de biomassa (degut a les bactèries autotròfiques) i la utilització d'una font d'electrons segura i virtualment infinita (l'elèctrode catòdic). Degut a les seves característiques positives, aquesta tesi té com a objectiu avaluar la utilització dels sistemes BES desnitrificants per al tractament de nitrats en aigües subterrànies.

Primerament, es va demostrar que el nitrat present en aigües subterrànies es podia reduir a dinitrogen gas fent servir la tecnologia BES malgrat la baixa conductivitat de l'aigua subterrània (el qual és un factor limitant en aquesta tecnologia). A posteriori, es van avaluar diferents configuracions electroquímiques per tal de: i) assolir càrregues desnitrificants competitives, ii) incrementar la viabilitat de la tecnologia.

La operació dels sistemes bioelectroquímics es va mostrar com a un dels factors claus per tal d'obtenir altes càrregues desnitrificants sense l'acumulació de substàncies intermèdies (nitrit i òxids nitrós). En aquesta tesi, la operació del sistema a un potencial catòdic fixe en el rang de -103 a -203 mV vs SHE va permetre el tractament d'aigua subterrània contaminada per nitrats. Aquesta operació va permetre assolir els límits marcats per a aigua de consum humà en quan a nitrats i nitrits i, a més a més, va minimitzar les emissions de N_2O. Tot operant el sistema en aquestes condicions a llarg termini, es va assolir que l'aigua de sortida del reactor no contingués ni nitrats, ni nitrits, ni òxid nitrós. A més a més, es va aconseguir incrementar les càrregues d'eliminació de nitrat fins a 700 $gN \cdot m^{-3}_{NCC} \cdot d^{-1}$ quan el sistema es va operar a baixos temps de residència hidràulica i es van emprar reactors tubulars en lloc de rectangulars.

Per tal d'incrementar la viabilitat de la tecnologia, es va demostrar que l'ús d'un potencial catòdic fixe permetia el tractament de l'aigua subterrània sense la necessitat d'afegir matèria orgànica en el compartiment anòdic, ni cap mena d'agent químic extern en cap etapa del procés. En conseqüència, el tractament de l'aigua subterrània es va poder assolir a un cost d'operació competitiu. A més a més, es va estudiar la utilització d'elèctrodes anòdics de Ti-MMO per a la producció de clor lliure. Tot hi que cal optimitzar-ne el seu ús, la utilització d'ànodes de Ti-MMO permetria implementar processos de desinfecció en el compartiment anòdic.

Es va avaluar diferents estratègies per a monitoritzar les BES desnitrificants des del punt de vista microbiològic i electroquímic: i) La utilització de citometria de flux combinada amb T-RFLP va permetre elucidar la funció de les diferents subcomunitats microbianes en el biocàtode desnitrificant, tot identificant la responsabilitat de les diferents subcomunitats en els diferents passos de la desnitrificació. ii) La utilització de microcosmes va permetre caracteritzar la transferència externa d'electrons en biofilms biocatòdics. Específicament, es va descriure la termodinàmica associada a la reducció de nitrat i de nitrit en un biocàtode dominat per *Thiobacillus* sp.

Comptat i debatut, els resultats presentats en aquesta tesi demostren que els sistemes bioelectroquímics tenen el potencial per a convertir-se en una alternativa per al tractament d'aigües subterrànies contaminades per nitrats.

Summary

The presence of nitrates (NO_3^-) in groundwater is a worldwide concern. In several geographic zones, nitrate exceeds the healthy standards for drinking-water consumption (above 50 $mgNO_3^-·L^{-1}$ (11.29 $mgN·L^{-1}$)) recommended by the World Health Organization (WHO). Nowadays, reverse osmosis, reverse electrodialysis and ion exchange are considered as the most recommended technologies for dealing with nitrates in groundwater. However, these conventional technologies are energy demanding, and nitrate is concentrated in a waste brine of difficult disposal. On the contrary, biologic denitrification allows the conversion of harmful nitrate to harmless dinitrogen gas (N_2). However, conventional heterotrophic denitrification should be discarded for groundwater treatment due to excess of biomass that this process generates and the requirement of organic matter, which is not permitted in drinking-water. For these reasons, an autotrophic-based process would be desired.

In biocathodes of bioelectrochemical systems (BES), autotrophic denitrifying bacteria are able to reduce nitrates to dinitrogen gas using the cathode electrode as electron donor. This process implies low generation of sludge (autotrophic bacteria), and the use of a safe and endless source of electron donor (the cathode electrode). Because of its positive characteristics, this thesis aims to evaluate the usage of denitrifying BES for the reduction of nitrates in groundwater.

Firstly, it was demonstrated that nitrate present in groundwater could be reduced to dinitrogen gas using BES even though the low conductivity of groundwater (which is a restricting parameter of this technology). Then, different electrochemical configurations were evaluated: i) to promote competitive denitrification rates and ii) to increment the viability of the technology.

The operation of the bioelectrochemical system was seen as key factor for obtaining high denitrification rates without accumulation of intermediates (nitrite and nitrous oxide). In this PhD thesis, the operation at a poised cathode potential in a range from -103 and -203 mV vs SHE allowed successful nitrate-polluted groundwater treatment. The standards for drinking-water were accomplished in

terms of nitrates and nitrites, and N_2O emissions were minimized. At long-term operation, effluents free of nitrate, nitrite or nitrous oxide were achieved. Moreover, the operation at low hydraulic retention times and the usage of tubular reactors instead of rectangular reactors were also seen as positive for promoting higher denitrifying performances (up to nitrate consumption rates of 700 $gN \cdot m^{-3}_{NCC} \cdot d^{-1}$).

In order to increment the viability of the technology, it was demonstrated that the use of a poised cathode potential allowed a treatment free of organic carbon (no need of adding it at the anode compartment) or chemical dosages. As a consequence, a successful treatment could be reached at a competitive operational cost. Moreover, the use of Ti-MMO anodes for the production of free chlorine was also evaluated. Besides better results are needed, its optimization can bring *in situ* disinfection processes at the anode compartment.

Finally, strategies for monitoring reactor microbiomes of denitrifying BES from microbiological and electrochemical perspective were successfully evaluated. i) The use of cytometric fingerprinting using flow cytometry combined with T-RFLP allowed elucidating the structure-function relationship of a denitrifying biocathode, identifying the different subcommmunities responsible of the different denitrification steps. ii) The use of microcosms was shown as effective to characterize extracellular electron transfer of biocathodic biofilms. Concretely, the nitrate and nitrite reduction thermodynamics were described for a *Thiobacillus* sp. dominated cathode.

In conclusion, results presented in this thesis supports that bioelectrochemical systems have the potential of being an alternative for nitrate-polluted groundwater treatment.

Resumen

La presencia de nitratos (NO_3^-) en aguas subterráneas concierne a una escala global. En ciertas zonas geográficas, les concentraciones de nitrato los límites señalados por la Organización Mundial de la Salud (OMS) para consumo humano (superiores a 50 $mgNO_3^-·L^{-1}$ (11.29 $mgN·L^{-1}$)). Actualmente, las tecnologías más efectivas para la eliminación del nitrato en aguas subterráneas son la osmosis inversa, la electrodiálisis inversa o el intercambio iónico. Pero estas tecnologías requieren de un alto consumo energético, y su principio básico és la separación del nitrato y su concentración en salmuera, la cual requiere de un difícil tratamiento. En cambio, la desnitrificación biológica permite la conversión del nitrato (tóxico) en dinitrógeno gas (N_2) (inerte). De forma convencional, la desnitrificación se realiza heterotróficamente. Éste proceso implica la generación de biomasa en exceso y requiere de la adición de materia orgánica, que debe ser eliminada completamente para uso del agua para consumo humano. Por estas razones, los procesos de desnitrificación autotrófica serian los más indicados para los tratamientos de aguas subterráneas.

En biocátodos de sistemas bioelectroquímicos (BES), bacterias autotróficas desnitrificantes son capaces de reducir los nitratos a dinitrógeno gas utilizando el electrodo catódico como fuente de electrones. Éste proceso implica poca generación de biomasa (debido a las bacterias autotróficas) y la utilización de una fuente de electrones segura e infinita (el electrodo catódico). Debido a sus características positivas, esta tesis tiene como objetivo evaluar la utilización de los sistemas BES desnitrificantes para el tratamiento de nitratos en aguas subterráneas.

Primero se demostró que el nitrato presente en aguas subterráneas se podía reducir a dinitrógeno gas utilizando la tecnología BES, aunque las aguas subterráneas presentan bajas conductividades (factor limitante en la tecnología BES). Después, se evaluaron diferentes configuraciones electroquímicas con el objetivo de: i) obtener cargas desnitrificantes competitivas, ii) incrementar la viabilidad de la tecnología.

La operación de los sistemas bioelectroquímicos fue un factor determinante para obtener mayores cargas desnitrificantes sin acumulación de sustancias intermedias (nitrito y óxido nitroso). En esta tesis, la operación a un potencial catódico fijo en el rango de -103 a -203 mV vs SHE permitió cumplir los límites estipulados para agua de consumo humano en relación a nitrato y nitrito. Además, las emisiones de N_2O se minimizaron. Operando el sistema en estas condiciones a largo término, se consiguió que el agua a la salida del reactor no presentase ni nitrato, ni nitrito, ni óxido nitroso. Además, las cargas de eliminación de nitrato se incrementaron hasta 700 $gN \cdot m^{-3}_{NCC} \cdot d^{-1}$ cuando se operó el sistema a bajos tiempos de residencia hidráulica y se utilizaron reactores tubulares.

Con tal de incrementar la viabilidad de la tecnología, se demostró que el uso de un potencial catódico fijo permitía el tratamiento del agua subterránea sin la necesidad de adicionar ni materia orgánica en el compartimiento anódico, ni ningún agente químico en ninguna etapa del proceso. Como consecuencia, se obtuvo el tratamiento del agua subterránea a un coste de operación competitivo. Además, también se estudió la utilización de electrodos anódicos de Ti-MMO para la producción de cloro libre. Aunque éste proceso aún necesita de optimización, la utilización de ánodos de Ti-MMO podría permitiría implementar procesos de desinfección en el compartimiento anódico.

Se estudiaron diferentes estrategias para monitorizar las BES desnitrificantes desde el punto de vista microbiológico y electroquímico: i) La utilización de citometria de flujo combinada con T-RFLP permitió elucidar la función de las diferentes subcomunidades microbianas en el biocátodo desnitrificante, identificando qué responsabilidad tienen las diferentes subcomunidades en los diferentes pasos de desnitrificación. ii) La utilización de microcosmos permitió caracterizar la transferencia externa de electrones en biofilms biocatódicos. De forma específica, se describió la termodinámica asociada a la reducción de nitrato y nitrito en un biocátodo dominado por *Thiobacillus* sp.

En resumen, los resultados presentados en ésta tesis demuestran que los sistemas bioelectroquímicos tienen el potencial para convertirse en una alternativa para el tratamiento de aguas subterráneas contaminadas por nitratos.

Chapter 1. General introduction

1.1. Background

The presence of nitrate (NO_3^-) in groundwater is a worldwide concern because it threatens the use of groundwater as drinking-water (Menció et al., 2011; Qu and Fan, 2010; Sprague et al., 2011). Nitrate is a harmful inorganic contaminant known to cause blue-baby syndrome (Knobeloch et al., 2000) and it has been linked with cancer (van Grinsven et al., 2010; Weyer et al., 2001). The EPA only recommends reverse osmosis, electrodialysis and ion exchange as suitable treatment technologies for nitrate contaminated groundwater (EPA, 2006). However, these technologies are based on separating the contaminant, which generates waste brine that is difficult to dispose of. Moreover, these methods also require high energy demands (Twomey et al., 2010). Biological processes could allow sustainable treatment. Considering that groundwater that could be used as drinking-water does not contain organic matter, the biological removal of nitrates (i.e., denitrification (Figure 1.1)) should be carried out using an autotrophic process.

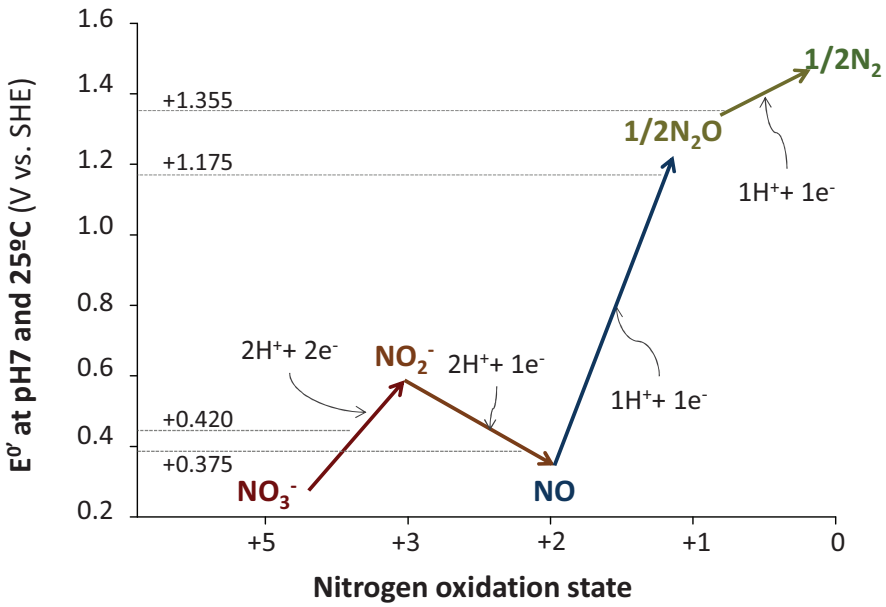

Figure 1.1. Standard redox potentials for biological denitrification at pH 7 and 25 ºC (Ferguson and Richardson, 2004).

Autotrophic denitrifying bacteria can reduce nitrates using inorganic carbon as a carbon source and inorganic compounds as electron donor. A safe electron donor with virtually unlimited availability is desirable for treatment. Thus, the use of biocathodes in bioelectrochemical systems (BES) could accomplish these requirements.

1.2. Bioelectrochemical systems (BES)

The existence of bacteria that are able to transfer electrons to an electrode was first described in 1911 (Potter, 1911). However, until 100 years later, pathways could not be identified that could enable the use of microorganisms for human devices (Schröder, 2011). The interaction between microbes and electrodes in bioelectrochemical systems remains a promising method for channeling this potential use of bacteria to human applications.

Normally, BES are composed of an anode and a cathode separated by an ion exchange membrane (Figure 1.2). In the anode compartment, oxidation reactions deliver protons to the media and electrons to the electrode. Protons diffuse to the cathode through an ion exchange membrane, while electrons are transferred by an electric connection. In the cathode, protons and electrons are consumed to carry out reduction reactions. Different applications have been found for bioelectrochemical systems depending on the reactions that occur in each compartment (Rabaey et al., 2009).

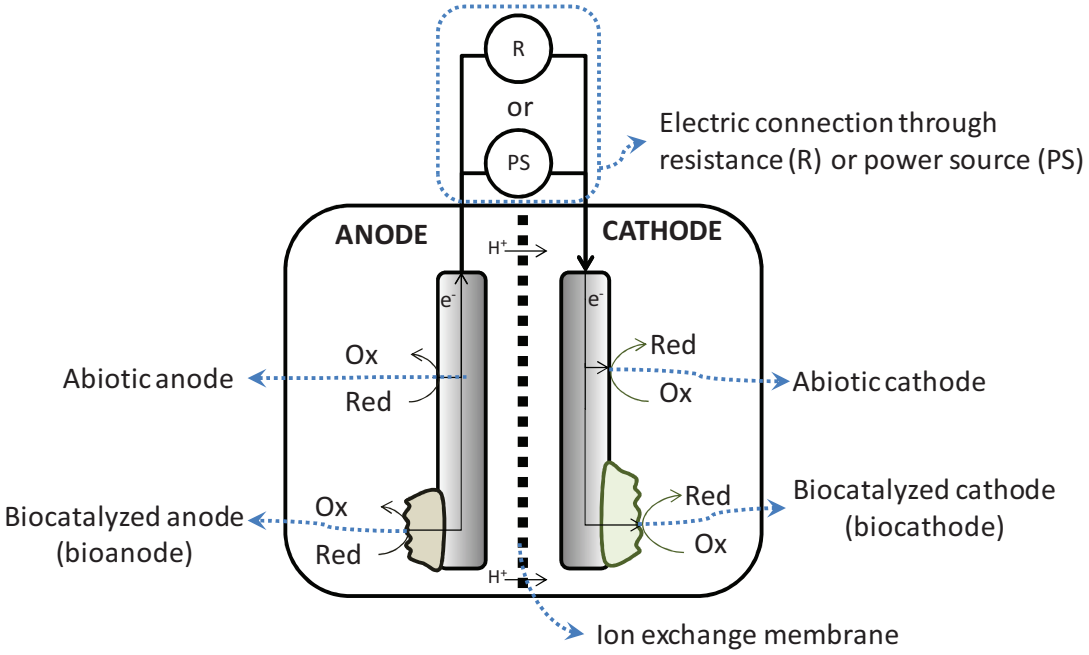

Figure 1.2. Basic schematic of a bioelectrochemical system.

As an electrochemical process, the operation of each BES is determined by the potential at which each reaction occurs. If reactions with overall positive cell potentials are coupled (equation1.1), a thermodynamically spontaneous process is produced (equation1.2) that can generate electrical current.

$$E_{cell} = E_{cathode} - E_{anode} \text{ (equation 1.1)}$$

where E_{cell} is the cell voltage (V); $E_{cathode}$ is the cathode potential (V) and E_{anode} is the anode potential (V).

$$\Delta G = -n \cdot F \cdot E_{cell} \text{ (equation 1.2)}$$

where ΔG is the Gibbs free energy (J); n represents the number of electrons involved in the overall electrochemical process; F is Faraday's constant (96485 C·mol-e^{-1}) (V) and E_{cell} is the cell voltage (V).

The first application of BES was a thermodynamically spontaneous process, the production of electricity (Min and Logan, 2004; Puig et al., 2011a; Rabaey et al., 2003). The use of BES for electricity generation began with the oxidation of organic matter at the anode and abiotic reductions at the cathode. Frequently, the abiotic

reduction of oxygen (Liu and Logan, 2004; Puig et al., 2010) or ferrocyanide was used (Aelterman et al., 2006). This configuration allows the production of energy from different types of wastewaters (Pant et al., 2010), such as urban wastewater (Liu et al., 2004; Molognoni et al., 2014; Puig et al., 2011a), swine manure (Jung et al., 2007; VIlajeliu-Pons et al., 2015) or landfill leachate (Puig et al., 2011). In contrast, if the overall cell potential is negative, a thermodynamically non-spontaneous process occurs, and energy input will be required. For example, anodic acetate oxidation with cathodic hydrogen production (Liu et al., 2005; Rozendal et al., 2008), anodic arsenite oxidation with hydrogen evolution (Pous et al., 2015a) or anodic sulfide oxidation (Dutta et al., 2010) have been explored.

The usage of cathodic abiotic reduction to sustain thermodynamically spontaneous processes requires the use of an expensive catalyst (as platinum for oxygen reduction) or contaminant chemical species (ferrocyanide). To overcome it, the use of biologic cathodes (biocathodes) started to be evaluated (He and Angenent, 2006). The use of biocathodes allows not only cathodic oxygen reduction (Chen et al., 2008; Clauwaert et al., 2007b), but the reduction of other compounds as nitrate (Gregory et al., 2004). In consequence, the coupling of organic matter oxidation at the anode with denitrification at the cathode becomes a thermodynamic spontaneous process (Clauwaert et al., 2007a; Jia et al., 2008; Virdis et al., 2008).

1.3. Biocathodes

Biocathodes are based on electroactive microorganisms that are able to obtain electrons from an electrode and perform reductive processes. The investigation of biocathodes began with oxygen reduction for a sustainable anodic organic matter treatment (Chen et al., 2008; Clauwaert et al., 2007b). Once its potential was demonstrated, two more fields of research borned: i) the production of commodity chemicals, such as hydrogen (Batlle-Vilanova et al., 2014; Jeremiasse et al., 2010; Rozendal et al., 2008), methane (Cheng et al., 2009), acetate (Batlle-Vilanova et al., 2015; Marshall et al., 2012; Nevin et al., 2010) or butyrate (Ganigué et al., 2015);

and ii) the bioremediation of pollutants, such as hexavalent uranium (Gregory and Lovley, 2005), sulfate (Coma et al., 2013), chlorinated compounds (Aulenta et al., 2008), perchlorate (Butler et al., 2010), hexavalent chromium (Xafenias et al., 2013) or nitrobenzene (Wang et al., 2011). In the group of pollutants reduced in biocathodes, nitrate could also be included (Clauwaert et al., 2007a; Gregory et al., 2004; Virdis et al., 2009b). The conversion of nitrate to dinitrogen gas in biocathodes has not been fully demonstrated, since dinitrogen gas has not been analysed in denitrifying biocathodes. The main reason is that influent mediums are usually sparged with N_2 gas in order to ensure anoxic conditions. However, the available results suggest that denitrifying biocathodes are able to convert nitrate into dinitrogen gas. The reduction of nitrate, nitrite and nitrous oxide has been described without ammonium production (Virdis et al., 2009b). It suggests that the methabolic pathway is directed to dinitrogen gas. Thus, the complete bioremediation of nitrate (nitrate conversion to dinitrogen gas) could be accomplished using biocathodes.

The removal of reducible contaminants using BES represents an alternative to conventional biologic treatments and is usually conducted using organic matter as the electron donor (i.e., heterotrophic bacteria) (Aulenta et al., 2005; Soares, 2000). Biocathodes allow autotrophic treatment, which prevents the generation of excess biomass that occurs during heterotrophic processes.

In conventional autotrophic processes for nitrate treatment, hydrogen (Lee and Rittmann, 2002), iron (Huang et al., 1998) or sulfur (Kimura et al., 2002) must be supplied. By contrast, an electrode is used as the electron donor in denitrifying BES, which results in a safe and virtually unlimited supply of electrons for the denitrification process. However, different considerations should be assessed to understand and operate denitrifying biocathodes.

For treating nitrate-polluted groundwater, the following main points should be considered: i) the nature of the reduction process (electrochemical and biological); ii) the extracellular electron transfer mechanism; iii) restrictions of the process related to water characteristics; and iv) the BES configuration.

1.4. Denitrifying biocathodes

1.4.1. Nature of the nitrate reduction process (denitrification)

Biological denitrification involves four reduction steps (Figure 1.1), from nitrate to dinitrogen gas (N_2) through nitrite (NO_2^-), nitric oxide (NO) and nitrous oxide (N_2O). In this pathway, nitrite and nitrous oxide can accumulate due to their chemical stabilities. The generation of NO_2^- or N_2O can threaten the sustainability of denitrification because nitrite is more toxic than nitrate for human health (WHO, 2011), and nitrous oxide is a greenhouse gas with 298 times more impact per unit weight than CO_2 (Forster et al., 2007). For a sustainable process, nitrate should be converted to dinitrogen gas without the accumulation of any of these intermediates.

The reduction of nitrate (Virdis et al., 2009), nitrite (Clauwaert et al., 2007a; Puig et al., 2011c; Virdis et al., 2008) and nitrous oxide (Desloover et al., 2011; Virdis et al., 2009b) in biocathodes have been demonstrated. It suggests that, from the engineering point of view, denitrification takes place in biocathodes, and thus the nitrate can be successfully converted to dinitrogen gas. However, from the author's best knowledge, dinitrogen gas production in denitrifying biocathodes has not been evaluated yet.

From the microbiological perspective, genes encoding for nitrate reductases (narG and napA), nitrite reductases (nirK and nirS), nitric oxide reductase (norB) and nitrous oxide reductase (nosZ) have been amplified in denitrifying biocathodes (Van Doan et al., 2013; Vilar-Sanz et al., 2013). The amplification of these genes supports the biological reduction of nitrate to dinitrogen gas in the cathode.

Analyses of the microbial community present in denitrifying biocathodes for wastewater treatment have been performed. The enrichment of different species in the Proteobacteria phylum has been observed in different studies (Chen et al., 2008; Cong et al., 2013; Gregory et al., 2004; Kondaveeti and Min, 2013; Park et al., 2006; Van Doan et al., 2013; Vilar-Sanz et al., 2013; Wrighton et al., 2010),

suggesting that these species play an important role in denitrifying BES. Regarding specific microorganisms, few examples of pure cultures that can performe bioelectrochemical reduction of nitrate have been reported. Gregory and co-workers (2004) demonstrated that *Geobacter metallireducens* can use electrons from an electrode to reduce nitrate to nitrite. In addition, Kato et al. (2012) observed electrical currents in a system where a compartment fed with acetate and containing *Geobacter sulfurreducens* was connected through conductive minerals with a compartment fed with nitrate and containing *Thiobacillus denitrificans*. The results of Kato et al. (2012) suggested that *Thiobacillus denitrificans* could also catalyze bioelectrochemical nitrate reduction.

1.4.2. Extracellular electron transfer mechanism

Because biocathodes employ bacteria that can use electrons delivered from an electrode to carry out reductive processes, understanding the extracellular electron transfer (EET) mechanism is fundamental. The EETs in bioanodes have been broadly investigated. Consequently, the EET mechanisms of different known anode-respiring bacteria (ARB), such as *Geobacter sulfurreducens* (Fricke et al., 2008), *Shewanella oneidensis* (Marsili et al., 2008), *Thermincola ferriacetica* (Parameswaran et al., 2013) or *Geoalkalibacter subterraneus* (Carmona-Martínez et al., 2013), have been elucidated. However, in biocathodes, this knowledge remains untapped (Rosenbaum et al., 2011). It has been hypothesized that biocathodic EETs could be similar to known anodic extracellular electron transfer mechanisms (Rosenbaum et al., 2011). According to Rosenbaum et al. (2011), this hypothesis is based mainly based on the following two considerations:

i) Fe(III)-reducing and Fe(II)-oxidizing bacteria could use the same Mtr (metal-reducing) pathway to deliver/obtain electrons (Shi et al., 2012). This is an interesting approach for nitrate reduction. The existence of microorganisms that can reduce nitrate using Fe(II) as an electron donor is well known (Straub et al., 1996), and the above mentioned species of *Geobacter metallireducens* and *Thiobacillus denitrificans* are relevant examples (Hedrich et al., 2011).

ii) Some bioanodic biofilms can work indistinctly as biocathodic biofilms for nitrate reduction (Cheng et al., 2012), hydrogen production (Geelhoed and Stams, 2011; Jeremiasse et al., 2012) or oxygen reduction (Cheng et al., 2010). Moreover, the Mtr pathway of *Shewanella oneidensis* could be reversed for reducing fumarate (Ross et al., 2011).

In consequence, as for bioanodes (Schröder, 2007), the two main EETs that could be used in biocathodes (Rosenbaum et al., 2011) (and hence in denitrifying biocathodes) are listed below.

i) Direct electron transfer mechanism (DET): Bacteria obtain electrons directly from the electrode via outer-membrane redox proteins or self-produced microbial nanowires.
ii) Mediated electron transfer mechanism (MET): The bacteria uses mediator molecules (either natural exogenous or self-produced molecules) to transfer the electrons.

The EET mechanism determines the thermodynamics of the process, and thus the energy that the bacteria can gain from the reduction reaction (Schröder, 2007). The energy gain depends on the redox potential of the involved outer-membrane redox proteins (for a DET mechanism) or mediator molecules (for a MET mechanism). Therefore, from an engineering point of view, the cathode redox potential should allow these redox processes to occur.

1.4.3. Restrictions related to water characteristics

From an engineering perspective, the characteristics of water are remarkable and should be considered. In denitrifying BES, the two main parameters that threaten the denitrification process are pH (Cheng et al., 2012; Clauwaert et al., 2009) and conductivity (Puig et al., 2012).

The reductive process in a cathode implies the consumption of protons. If the proton transfer from the anode to the cathode is not enough, the pH of the cathode increases (Logan et al., 2006; Torres et al., 2008). The basification of the cathode

would be incremented when treating groundwater because it is characterized by its low buffering capacity (conductivities below 1600 $\mu S \cdot cm^{-1}$).

Clauwaert and co-workers (2009) demonstrated that the nitrate removal rate could be increased from 0.22 to 0.50 $kgN\text{-}NO_3^- \cdot m^{-3}_{NCC} \cdot d^{-1}$ by controlling the pH at 7 when treating synthetic wastewater. However, the addition of chemicals is not recommended for treating water that will be used as drinking-water. Thus, other strategies should be investigated. In this sense, Cheng et al. (2012) proposed using an ano-cathodophilic biofilm, where the electrode potential was switched from -100 to -600 mV vs SHE to promote anodic acetate oxidation and cathodic nitrate reduction in the same compartment. This system implies that the protons consumed during the cathodic process were delivered in the same compartment from the anodic reaction. Nevertheless, the presence of acetate and nitrate in the same chamber could result in the unwanted growth of heterotrophic denitrifiers and it also requires the addition of chemicals (acetate).

As explained above, the basification of the cathode occurs due to poor proton transport between the anode and cathode. Inefficient ion transport results from the membrane characteristics and the ionic strength of the water (conductivity) (Logan et al., 2006).

In terms of membrane characteristics, the use of different membranes can increase the power output in microbial fuel cells by allowing better proton transport through the membrane (Jung et al., 2007). However, this type of study for denitrifying BES has not been conducted.

By contrast, the effects of ionic strength in denitrifying BES have been studied. Low conductivities limit the denitrifying performance (Puig et al., 2012). Low ionic strength implies a low ion transport (protons and nitrate), which limits the overall performance. This knowledge is important for treating of nitrate-polluted groundwater, which is characterized by its low conductivity ($<1600 \mu S \cdot cm^{-1}$). Therefore, the treatment of groundwater can restrict the overall performances of BES.

1.4.4. Operation of the electrochemical process

From an electrochemical perspective, two main cells can be used to deliver electrons to the cathode and sustain denitrification, i) microbial fuel cells (MFC) and ii) microbial electrolysis cells (MEC).

1.4.4.1. Denitrifying microbial fuel cell

In a microbial fuel cell (Figure 1.3), cathodic denitrification is sustained by an anodic reaction with a lower redox potential than that of the nitrate reduction (Figure 1.1). MFCs have an overall positive cell voltage (equation 1.1 and 1.2); hence, a thermodynamically spontaneous process occurs with concomitant electricity production.

Microbial fuel cell (MFC)

$$Ecell = Ecat - Ean > 0$$
$$\Delta G < 0$$

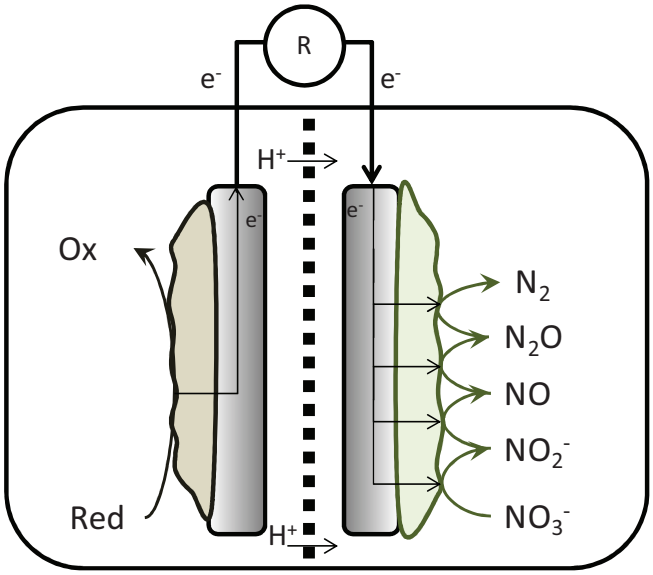

Figure 1.3. Electrochemical configuration for a denitrifying MFC.

The anode and cathode are connected with an external resistance. Although denitrifying MFCs are usually supported by the anodic oxidation of organic matter (Clauwaert et al., 2007a; Puig et al., 2012), denitrifying MFCs using sulfide oxidation at the anode compartment has also been reported (Cai and Zheng, 2013; Cai et al., 2014).

The most common configuration was first used by Clauwaert and co-workers (2007a) and was based on synthetic wastewater enriched with acetate at the anode

and nitrate at the cathode. The combination of anodic acetate oxidation (-290 mV vs SHE) and cathodic nitrate reduction (+375 mV vs SHE for NO_3^-/NO_2^-) implies an overall positive cell voltage. In this system, denitrification relies on both the anode and cathode performance.

Other configurations different from those proposed by Clauwaert et al. (2007a) have been explored. For example, the following systems have shown promising results: i) *in situ* treatment of eutrophic lakes using organic matter contained in sediments as the anode electron donor (Zhang and Angelidaki, 2012) and ii) *in situ* nitrate removal and desalination in groundwater using a submerged device with acetate dosing in the anode compartment (Zhang and Angelidaki, 2013).

For nitrate-polluted groundwater treatment methods that aim to deliver drinking-water, the different configurations explored using MFC require dosing organic matter in the anode compartment. Hence, to convince future customers that a BES operated as a MFC is suitable for groundwater bioremediation, the denitrification rates should be objectively higher than those conventional heterotrophic denitrification systems.

1.4.4.2. Denitrifying microbial electrolysis cell

In a Microbial Electrolysis Cell, external energy is supplied to the system to allow a thermodynamically non-spontaneous process to occur or to stimulate a spontaneous reaction. In a denitrifying MEC, the externally supplied energy could be used to directly empower the transfer of electrons to denitrifying bacteria, or to produce hydrogen to promote hydrogenotrophic denitrification (Sakakibara and Kuroda, 1993). The energy input can be distributed through the following two BES configurations: i) two-electrode (fixed cell voltage or fixed current) (Figure 1.4) and ii) three-electrode arrangement (fixed cathode potential) (Figure 1.5).

1.4.4.2.1. Denitrifying microbial electrolysis cell – two-electrode arrangement

In a two-electrode arrangement (Figure 1.4), a fixed cell voltage or a fixed current is used, which suggests the use of a device with low complexity. A DC power is enough to supply the energy required.

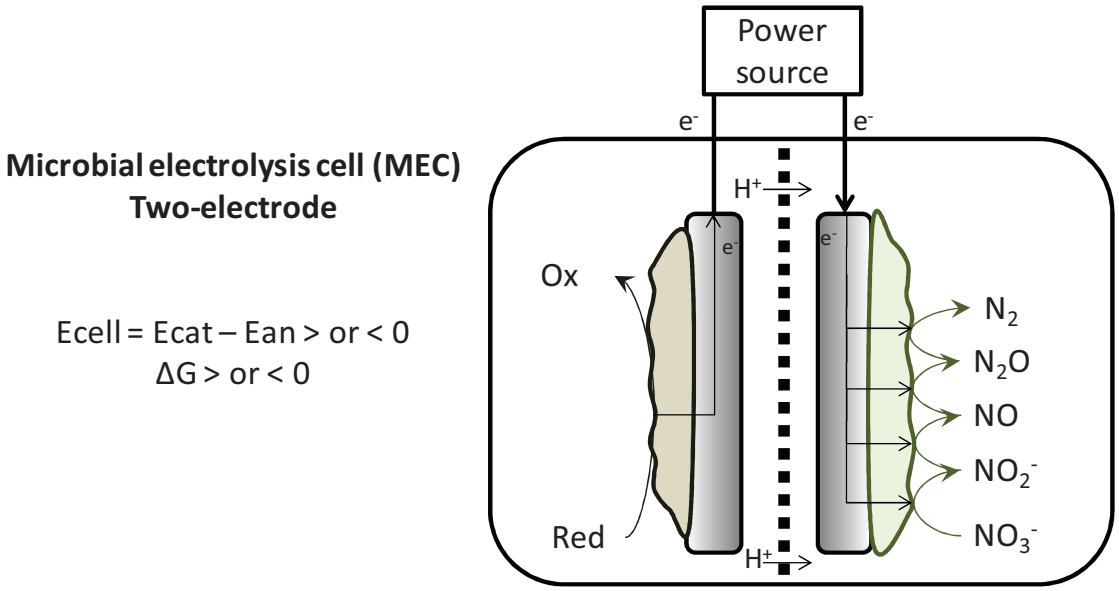

Figure 1.4. Electrochemical configuration of denitrifying MEC with two-electrode arrangement.

The first studies of denitrification using MECs did not rely on direct electron transfer between an electrode and the denitrifiers. These studies were based on the electrochemical production of hydrogen, which was further used as an electron donor for biologic denitrification (Sakakibara and Kuroda, 1993). This process was considered an alternative to conventional hydrogenotrophic denitrification (Karanasios et al., 2010), in which hydrogen gas is directly supplied to a biological reactor. But this process is limited by mass transfer due to the low solubility of hydrogen (approximately 1mM).

Sakakibara and Kuroda, (1993) demonstrated that the complete reduction of nitrate to dinitrogen gas could be accomplished by applying different currents from 0 to 40 mA. Although the authors stated that denitrification was mediated by H_2, it

cannot be discarded that denitrification using the electrode as electron donor was taking place simultaneously.

Besides the *in situ* production of hydrogen for nitrate reduction was effective, it implied a certain lack of control of the process. The hydrogen generated in the cathode may or may not be used for nitrate reduction. Hence, low energy efficiency can be expected for this type of configuration. For this reason, the use of MEC to promote the direct use of electrons for denitrifying bacteria was evaluated (Park et al., 2005b). Park et al. (2005b) investigated nitrate reduction in synthetic wastewater using electrodes as direct electron donors by applying a fixed current density. These authors observed that the rates of hydrogen production were 100-fold lower than the nitrate removal rates. Hence, H_2 was not an intermediate; nitrate was reduced directly by using the electrode as the electron donor. This system resulted in a maximum nitrate reduction rate of 435 $mgN\text{-}NO_3^-\cdot L^{-1}\cdot h^{-1}$ at a fixed current of 200 mA.

In fully autotrophic influents, the strategy of using a fixed cell voltage has been successfully demonstrated (Kondaveeti and Min, 2013; Kondaveeti et al., 2014; Lee et al., 2013). In this case, the application of a cell voltage of 0.7 V was considered as optimum for removing nitrate.

Base on the principle of applying a fixed cell current or a fixed cell voltage, other strategies for enhancing denitrification have been evaluated, such as the combination of heterotrophic and autotrophic denitrification at the cathode compartment (Cong et al., 2013; Zhao et al., 2012) or the promotion of nitrate flux into the anodic compartment to allow heterotrophic denitrification (Tong and He, 2013).

The use of external power allows thermodynamically non-spontaneous processes, such as coupling anodic oxidation of water (+820 mV vs. SHE) and cathodic nitrate reduction (Figure 1.1) (Park et al., 2005b; Sakakibara and Kuroda, 1993) that can be used for the treatment of nitrates without using organic carbon, which is ideal for groundwater treatment. Nevertheless, the use of a fixed current

or fixed voltage implies low treatment efficiency because the external energy input is continuously supplied, regardless of the denitrifying process performance.

1.4.4.2.2. Denitrifying microbial electrolysis cell – three-electrode arrangement

In a three-electrode arrangement (Figure 1.5), the system is operated at a fixed cathode potential, which implies the use of a complex apparatus, a potentiostat. In this configuration, the amount of energy supplied depends on the activity of the biocathode at the given cathode potential. By switching the cathode potential, the difference between the standard redox potential of nitrate reduction and the redox potential of the electron donor (the cathode electrode; working electrode) can be modified; thus, the energy gained by the bacteria can be switched (Schröder, 2007).

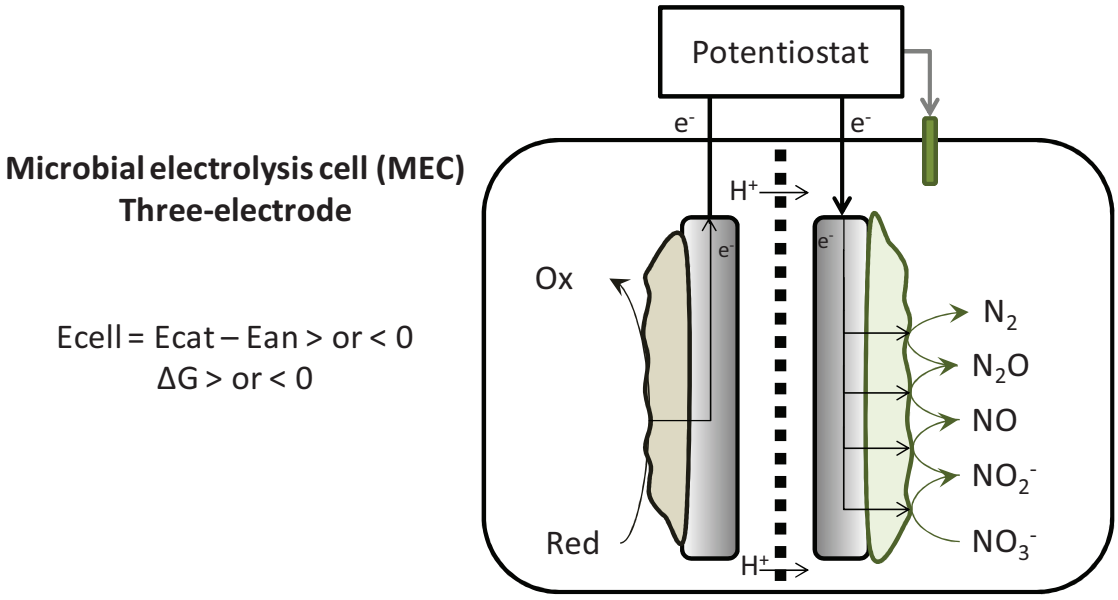

Figure 1.5. Electrochemical configuration for a denitrifying MEC with three-electrode arrangement.

In biocathodes, lower cathode potentials correspond with higher energy gains for the bacteria. Thus, higher biocatalysis can be expected. For this reason, low cathode potentials (lower than 0 mV vs SHE) are usually used in denitrifying BES. Gregory et al. (2004) used a fixed cathode potential of -303 mV vs SHE to the support bioelectrochemical reduction of nitrate to nitrite in a mixed culture enriched with Geobacteraceae. In addition, these authors demonstrated that

Geobacter metallireducens is able to reduce nitrate to nitrite at the same cathode potential by using the electrode as the electron donor.

In mixed cultures, the sole reduction of nitrate has been studied between cathode potential ranges of +100 to -200 mV vs SHE (Virdis et al., 2009) and +197 to -403 mV vs SHE (Cheng et al., 2012). In addition, the reduction of the denitrification stable intermediates (NO_2^- and N_2O) have been evaluated between +100 to -200 mV vs SHE (Virdis et al., 2009). In these two studies, the cathodic performance increased as the cathode potential was lowered when using synthetic wastewater. Because the use of a poised cathode potential can result in higher electron efficiency, the treatment of nitrate-polluted groundwater using a denitrifying biocathode operated at a poised cathode potential could be studied. In these studies, organic matter (acetate) was used as the anode electron donor. However, when treating nitrate-polluted groundwater, a process completely free of organic carbon (acetate) is desirable. Hence, using abiotic anodes instead of anodic acetate oxidation could be evaluated for treating nitrate-polluted groundwater.

Chapter 2. Objectives

The main objective of this thesis is **to assess denitrifying bioelectrochemical systems for treating nitrate-polluted groundwater for later use it as drinking-water.** The available knowledge on denitrifying BES is remarkable (Chapter 1). However, there are still knowledge gaps that need to be filled for the application of denitrifying BES to nitrate-polluted groundwater bioremediation. This PhD thesis targets different specific objectives (Figure 2.1.) to address the specific knowledge gaps.

Water characteristics are key parameters to be taken into account when using bioelectrochemical systems. In this sense, no studies evaluating the treatment of real nitrate-polluted groundwater in denitrifying bioelectrochemical systems had been reported before this thesis started. In this specific case, groundwater is characterized by relatively high pH (around pH 8) and low conductivity (< 1600µS·cm^{-1}), which limits *a priori* the cathodic denitrification. This PhD thesis contributes on evaluating denitrifying BES for treating real nitrate-polluted groundwater. For this reason, the first specific objective was to investigate the treatment of real nitrate-polluted groundwater using a denitrifying BES (A).

Linked to the restrictions related to water characteristics, it highlights the operation of the electrochemical process. Different studies have reported on the operation of denitrifying biocathodes under different electrochemical configurations. This PhD thesis contributes on investigating which electrochemical operation is more suitable for the treatment of real nitrate-polluted groundwater (B).

Moreover, engineering aspects that could prompt the real application of the technology are also addressed. The effect of using different anode electron donors and materials (C), different BES reactor designs (F) and different cathode hydraulic retention time were evaluated to improve the denitrifying BES capabilities.

Considering the nature of the denitrifying process, knowledge is lacking on the microbiome responsibility of the nitrate reducing pathway. The genetic potential for performing the whole denitrifying pathway has been proved in denitrifying

cathodes, and relevant knowledge regarding microorganisms enriched in denitrifying biocathodes have been obtained. This thesis aimed to investigate the microbial subcommunities responsible of the different denitrification steps (D). For the specific application of nitrate-polluted groundwater treatment, this thesis had the objective of identifying the microorganisms enriched in denitrifying biocathodes treating real nitrate-polluted groundwater under two different electrochemical conditions (MFC and MEC operated at a poised electrode potential).

Moving to the extracellular electron transfer mechanism, this PhD thesis highlights the existing knowledge gaps on EETs mechanisms that govern denitrifying biocathodes. This PhD thesis investigates the EET thermodynamics in a denitrifying biocathode as well as the microbiome responsible of the electrochemical signal (E).

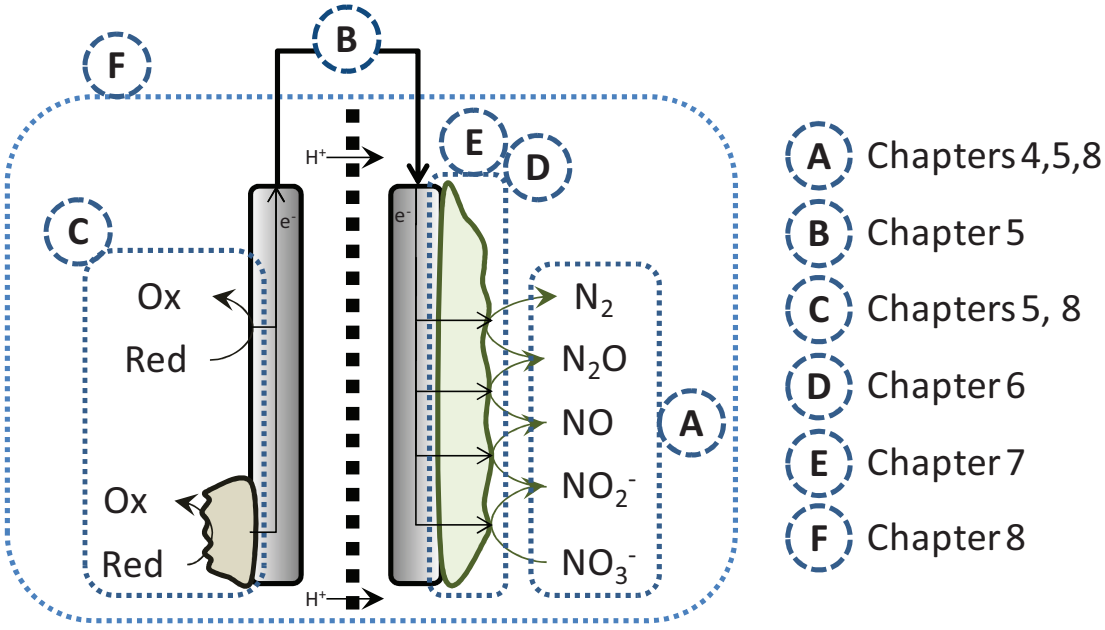

Figure 2.1. Scheme of the targets of this PhD thesis.

Chapter 3. Methodology

3.1. Denitrifying BES reactor set-up

Graphite (as conductive support and rod as electrode collector) was always used as the suitable material of the biocathode (Figure 3.1.A). On the side, different materials (graphite, stainless steel and Ti-MMO electrodes) were assessed as anode electrodes (Figure 3.1).

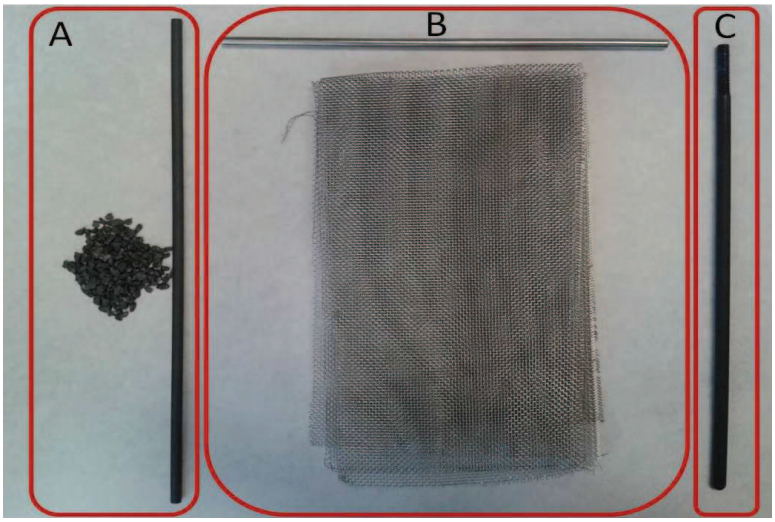

Figure 3.1. Materials used as electrodes: A) Graphite granules and graphite rod; B) Stainless steel mesh and stainless steel rods and C) Ti-MMO rod.

Three different BES designs were used during the experimental period: i) rectangular design (Figure 3.2); ii) denitrifying microcosms (Figure 3.3) and iii) tubular design (Figure 3.4).

The **rectangular BES** was used for Chapters 4-6 (Figure 3.2). It consisted on a two-chamber d-BES. It was built using two methacrylate rectangular frames (20 x 20 x 2.2 cm, Futura, Spain) separated by a cation exchange membrane (20 x 20 cm, CMI-7000, Membranes Int., USA). The cathode was filled with granular graphite (diameter 1.5 - 5 mm, EnViro-cell, Germany) and a graphite rod was used as current collector (250 x 6 mm, Mersen Ibérica, Spain) (Figure 3.1.A). Net cathode volumes (NCC) between 420 and 600 mL were observed in the different specific studies.

Two different anode materials were tested: graphite and stainless steel. For In 4 and 5, the anode compartment was filled with granular graphite (diameter 1.5 - 5 mm, EnViro-cell, Germany) and a graphite rod was used as current collector (250 x 6

mm, Mersen Ibérica, Spain) (Figure 3.1.A). A net anode volume (NAC) of 420 mL was observed. In Chapter 6, the anode contained one stainless steel rod (250 x 6 mm) and stainless steel mesh (20 x 20 cm, path: 5 x 5 mm, Mersen Ibérica, Spain) (Figure 3.1.B). This implied an increase of the NAC volume to 784 mL.

In all cases, both anode and cathode were equipped with Ag/AgCl reference electrodes (+0.197 V vs standard hydrogen electrode (SHE), model RE-5B BASi, United States). The anode and the cathode contained influent and effluent holes, as well as a recirculation loop.

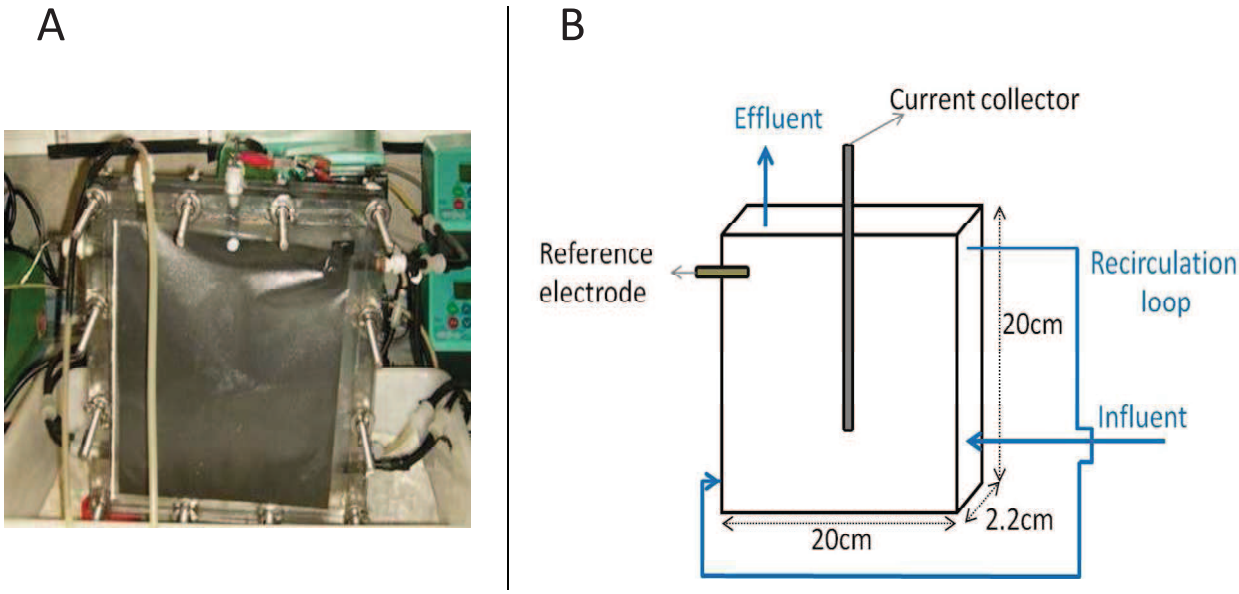

Figure 3.2. A) Rectangular BES. B) Scheme of one of the compartments of the rectangular BES.

Denitrifying microcosms were used in Chapter 7 to perform electrochemical characterization of denitrifying electroactive biofilms (Figure 3.3). Microcosms consisted on tailor-made single-chamber bioelectrochemical systems that possessed a total volume of 20 mL. Each microcosm contained two graphite rods (CP-Graphite GmbH, Germany) connected with stainless steel wire and one Ag/AgCl reference electrode (sat. KCl, SE11 Sensortechnik Meinsberg, Germany).

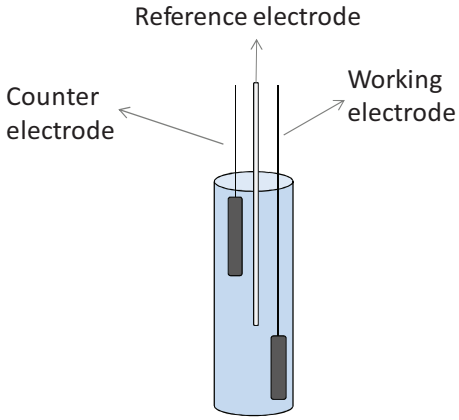

Figure 3.3. Scheme of microcosms used for electrochemical characterization (Pous et al., 2014).

In Chapter 8, a new designed **tubular BES** was used (Figure 3.4). The tubular reactor was based on a flow-through configuration. Nitrate-contaminated water was directly fed to the bottom of the cathode compartment (inner part of the reactor), and spilled from the top to the anode compartment (outer part of the reactor). A tubular cation exchange membrane surrounded the cathode (CMI-7000, Membranes Int., USA).

The cathode compartment was filled with granular graphite (diameter 1.5 - 5 mm, EnViro-cell, Germany) and a graphite rod was used as electrode collector (250 x 6 mm, Mersen Ibérica, Spain) (Figure 3.1.A). It implied a NCC of 240 mL. A Ti-MMO electrode rod was used as anode electrode (NMT electrodes, South Africa) (Figure 3.1.C). An Ag/AgCl reference electrode was introduced in the cathode compartment (+0.197 V vs standard hydrogen electrode (SHE), model RE-5B BASi, United States).

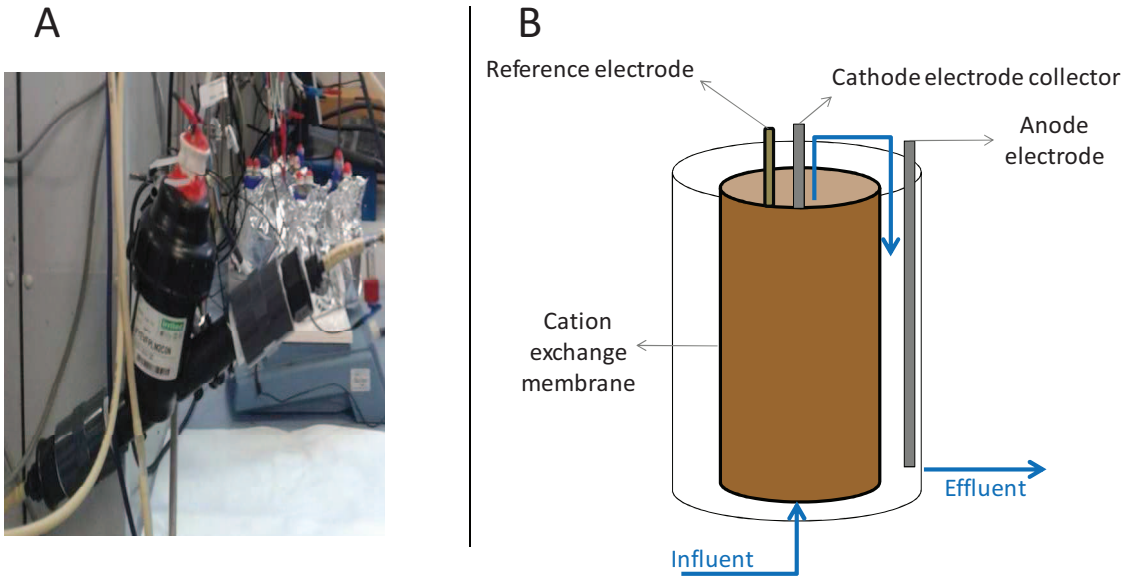

Figure 3.4. A) Tubular BES. B) Scheme of the tubular BES.

3.2. Analyses and calculations

3.2.1. Chemical analyses

Depending on the aim of the experiment, different analyses were performed. Measurements of ammonium ($N\text{-}NH_4^+$), chemical oxygen demand (COD), chloride (Cl^-), chlorine (Cl_2), inorganic carbon (IC), nitrates ($N\text{-}NO_3^-$), nitrites ($N\text{-}NO_2^-$), phosphates ($P\text{-}PO_4^{3-}$), sulfates ($S\text{-}SO_4^{2-}$) and total organic carbon (TOC) were performed according to the recommendations of the American Public Health Association (APHA) for standard wastewater (APHA, 2005).

The conductivity, the pH and the turbidity were measured with an EC-meter (EC-meter basic 30^+, Crison, Spain), a pH-meter (pH-meter basic 20^+, Crison, Spain) and a turbidimeter (Turbidimeter TN-100, Eutech instruments).

In specific experiments, the N_2O concentration at the cathode compartment was monitored online. A nitrous oxide microsensor (Unisense, Aarhus, Denmark) was collocated in the recirculation loop of the cathode compartment for the rectangular BES or at the effluent of the anode for the tubular BES (Figure 3.5). The microsensor was connected to an *in situ* amplifier that sent the collected data to a laptop, where Unisense software (sensorTrace BASIC, Unisense, Aarhus, Denmark) stored the data

every 60 seconds. The sensor was calibrated by successive additions of saturated N_2O solution, obtaining a linear calibration plot.

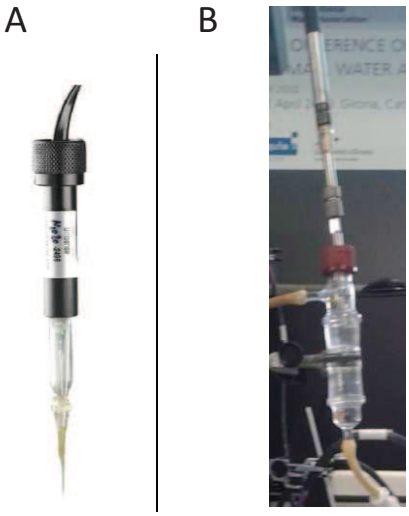

Figure 3.5. A) Nitrous oxide microsensor. B) Measurement of liquid-phase nitrous oxide in the experiments with the tubular BES.

3.2.2. Calculation of nitrous oxide concentrations

In order to calculate the total amount of N_2O in the cathode from the measured N_2O in the liquid-phase, the following steps were followed. Firstly, the amount of gas generated in the cathode was calculated from the difference between influent and effluent of nitrate (NO_3^-), nitrite (NO_2^-), and nitrous oxide in the liquid phase (N_2O_{liquid}) (equation3.1). As a result of denitrification, the gas generated is composed by nitrous oxide in the gas phase (N_2O_{gas}) and dinitrogen gas (N_2) (equation 3.1).

$$n_g = \Delta NO_3^- + \Delta NO_2^- + \Delta N_2O_{liquid} = nN_2O_{gas} + nN_2 \text{ (equation 3.1)}$$

where n_g is the amount of gas generated in the cathode per volume of groundwater treated (mol $N \cdot L_{water}^{-1}$); ΔNO_3^-, ΔNO_2^- and ΔN_2O_{liquid} are the difference between influent and effluent of the amount of nitrate, nitrite and nitrous oxide in the liquid phase (mol $N \cdot L_{water}^{-1}$); nN_2O_{gas} and nN_2 are the amount of nitrous oxide in the gas phase and dinitrogen gas produced per volume of groundwater treated (mol $N \cdot L_{water}^{-1}$). Nitric oxide production was considered negligible. The amount of N_2O in

the gas phase was calculated using equations 3.2 and 3.3. On the one hand, by assuming that the gas phase in the cathode was only composed by N_2O and N_2, the concentration of N_2O in the gas- phase is represented as shown in equation 3.2.

$$[N_2O]_{gas} = \frac{nN_2O_{gas}}{V_{gas}} = \frac{nN_2O_{gas}}{\frac{ng \cdot R \cdot T}{P}} \quad \text{(equation 3.2)}$$

where $[N_2O]_{gas}$ is the concentration of N_2O in the gas phase (mol $N \cdot m^{-3}$); V_{gas} is the volume of gas ($m^3 \cdot m_{water}^{-3}$); is the temperature (K); is the ideal gas constant (8.31451 $J \cdot K^{-1} \cdot mol^{-1}$) and is the atmospheric pressure (101325 Pa).

On the other hand, the concentration of N_2O in the gas-phase can also be calculated from the Henry's law (equation 3.3).

$$[N_2O]_{gas} = \frac{[N_2O]_{liquid}}{k_{N_2O} \cdot T \cdot R} \text{(equation 3.3)}$$

where $[N_2O]_{liquid}$ is the nitrous oxide concentration in the liquid phase (mol $N \cdot m^{-3}$) and k_{N2O} is the Henry's constant for nitrous oxide at the experimental temperature. The k_{N2O} was calculated from the Henry's constant as a function of the temperature as shown in equation 3.4.

$$k_{N_2O} = 2.47 \cdot 10^{-4} \cdot exp\left\{\frac{-19800}{R} \cdot \left(\frac{1}{T} - \frac{1}{298}\right)\right\} \text{ (equation 3.4)}$$

Finally, by coupling equations 3.2 and 3.3, the amount of nitrous oxide in the gas-phase can be calculated as presented in equation 3.5.

$$nN_2O_{gas} = \frac{[N_2O]_{liquid}}{k_{N_2O} \cdot P} \text{ (equation 3.5)}$$

In order to calculate the total amount of N_2O produced per volume of groundwater treated, equation 3.6 was used:

$$nN_2O = nN_2O_{gas} + nN_2O_{liquid} \text{ (equation 3.6)}$$

where nN_2O is the total amount of nitrous oxide produced per volume of groundwater treated (mol $N \cdot L_{water}^{-1}$). Once N_2O production was known, the amount

of N_2 produced per volume of groundwater treated was calculated by closing the nitrogen mass balance and considering negligible the presence of nitric oxide.

In Chapter 5 the nitrous oxide concentrations could not be measured and an estimation approach was used instead. The levels of N_2O production were calculated according the electron balance at the cathode following the methodology proposed by Virdis et al. (2009b) (equation 3.7) and considering that all current was related to cathodic denitrification (a coulombic efficiency of 100% was assumed).

$$5 \cdot \Delta NO_3^- - 3 \cdot \Delta NO_2^- - 2 \cdot \Delta NO - 1 \cdot \Delta N_2O - \frac{3600 \cdot j}{F \cdot V} = 0 \text{ (equation 3.7)}$$

where *j* is the current (mA); ΔNO_3^- are the nitrate consumption rate (mM-N·h^{-1}); ΔNO_2^-, ΔNO and ΔN_2O are the nitrite, nitric oxide and nitrous oxide production rate (mM-N·h^{-1}), *V* is the cathode liquid volume (L) and *F* is the Faraday's constant (96485 Coulombs per mol-e$^-$). The nitric oxide production was considered to be negligible. To close the mass balance, the level of dinitrogen gas in the effluent was calculated.

3.2.3. Calculation of quality ratio

Considering the possibility of the simultaneous presence of nitrate and nitrite in drinking-water, the WHO recommends using a quality ratio (*QR*) that involve both the concentration and the guideline value for nitrate and nitrite (WHO, 2011). The QR should not exceed a value of one (equation 3.8) to consider water as safe drinking-water in terms of nitrate and nitrite:

$$QR = \frac{C_{NO_3^-}}{11.29} + \frac{C_{NO_2^-}}{0.91} \leq 1 \quad \text{(equation 3.8)}$$

where, $C_{NO_3^-}$ is the nitrate concentration (mgN-NO_3^-·L^{-1}) and $C_{NO_2^-}$ is the nitrite concentration (mgN-NO_2^-·L^{-1}).

3.2.4. Calculation nitrate, nitrite and nitrous oxide removal rates

The performance of each reduction step from NO_3^- to N_2, the nitrate, nitrite and nitrous oxide consumption rates (ΔNO_3^-, ΔNO_2^- and ΔN_2O, respectively) were

calculated using equations 3.9 to 3.11. Nitric oxide accumulation was considered negligible (Virdis et al., 2009).

$$\Delta NO_3^- = \frac{CNO_3^-{}_{influent} - CNO_3^-{}_{effluent}}{HRT} \text{ (equation 3.9)}$$

$$\Delta NO_2^- = \Delta NO_3^- - \frac{CNO_2^-{}_{effluent}}{HRT} \text{ (equation 3.10)}$$

$$\Delta N_2O = \Delta NO_2^- - \frac{CN_2O_{effluent}}{HRT} \text{ (equation 3.11)}$$

where $CNO_3^-{}_{influent}$, $CNO_3^-{}_{effluent}$, $CNO_2^-{}_{effluent}$ and $CN_2O_{effluent}$ accounts for nitrate, nitrite and nitrous oxide concentrations at influent or effluent (either $mgN \cdot L^{-1}$ or $mmolN \cdot L^{-1}$).

3.2.5. Electrochemical analyses

In the experiments where the BES was operated as a microbial fuel cell (Chapter 5), the cell potential (V) in the MFC circuit was monitored at one-minute intervals using an on-line multimeter (Alpha-P, Ditel, Spain) with a data acquisition system (Memograph® M RSG40, Endress+Hauser, Germany).

A Bio-Logic (Bio-Logic, France) potentiostat was used to perform polarization curves, cyclic voltammetries or when the BES was operated as a microbial electrolysis cell with a three-electrode arrangement. Different models were used: A SP50 model in Chapters 4,5; VSP and VMP3 in Chapter 6 (Figure 3.6); VMP3 in Chapter 7 and VSP in Chapter 8. In Chapter 7, cyclic voltammetries (CV) were performed and three cycles were recorded from 0 to -800 mV vs Ag/AgCl at scan rate of 0.5 $mV \cdot s^{-1}$. The last cycle is reported.

Figure 3.6. Bio-Logic potentiostat model VSP.

3.2.6. Generation of Tafel plots

Tafel equations for the oxidative and reductive current are shown in equation 3.12 and 3.13, respectively (Rieger, 1994).

$$ln\, i = ln\, i_0 + \frac{\beta \cdot n \cdot F \cdot \eta}{R \cdot T} \text{ (equation 3.12)}$$

$$ln\, i = ln\, i_0 - \frac{\alpha \cdot n \cdot F \cdot \eta}{R \cdot T} \text{ (equation 3.13)}$$

where i_0 is exchange current density, i is the electrode current density ($A \cdot m^{-3}$ Net chamber), F is the Faraday constant (96485 $C \cdot mol^{-1}$ e^-), R is the ideal gas constant (8.31 $J \cdot mol^{-1} \cdot K^{-1}$), T is the absolute temperature (K), n is the number of electrons involved in the rate limiting step, η is the overpotential, which is the shift of electrode potential (E) and the equilibrium potential (E^0); and β and α are anodic and cathodic transfer coefficients, respectively. β is indicative of the oxidative kinetic activity and α for the reductive kinetic activity. Tafel equation was fitted at large overpotentials, where $|((F \cdot \eta)/(R \cdot T))| > 1$ (Bagotzky, 1993).

3.2.7. Calculation of coulombic efficiency for denitrifying biocathode

The methodology used to calculate the cathode coulombic efficiency (*CE*) was different depending on the experiment (continuous or batch mode and the nitrogen species measured).

When the system was operated under continuous-flow mode and nitrous oxide levels could not be measured, the coulombic efficiency was computed according to Virdis and co-workers (2008) (equation 3.14).

$$CE = \frac{t \cdot j}{5 \cdot \Delta NO_3^- \cdot V \cdot F}$$; (equation 3.14)

where *j* is the current (mA), *t* accounts for the time-converting factor between seconds and hours (3600); 5 is the number of electrons of electrons that are transferred during NO_3^- reduction to N_2 (mol-e^- per mol-N); ΔNO_3^- is the nitrate consumption rate (mM-N·h^{-1}), *V* is the cathode liquid volume (L) and *F* is the Faraday's constant (96485 Coulombs per mol-e^-).

When the system was operated under continuous flow-mode and nitrous oxide levels were measured, the *CE* was calculated taking into account the required current for each sequential step of nitrate reduction to dinitrogen gas. The nitric oxide accumulation was considered negligible (Virdis et al., 2009). The reduction steps considered were: the nitrate reduction to nitrite (NO_3^-/NO_2^-), nitrite to nitrous oxide (it includes NO reduction to N_2O; NO_2^-/N_2O) and nitrous oxide to dinitrogen gas (N_2O/N_2). The CE was calculated as shown in equation 3.15.

$$CE = \frac{t \cdot j}{V \cdot F \cdot \left(n_{NO_3^-/NO_2^-} \cdot \Delta NO_3^- + n_{NO_2^-/N_2O} \cdot \Delta NO_2^- + n_{N_2O/N_2} \cdot \Delta N_2O\right)}$$; (equation 3.15)

where *n* accounts for the number of electrons required for each reaction ($n_{NO_3^-/NO_2^-}$ = 2, $n_{NO_2^-/N_2O}$ = 2 and n_{N_2O/N_2} = 1); ΔNO_3^- is the nitrate consumption rate (mM-N·h^{-1}); ΔNO_2^- is the nitrite consumption rate (mM-N·h^{-1}) and ΔN_2O is the nitrous oxide consumption rate (mM-N·h^{-1}).

When the system was operated under batch mode, the coulombic efficiency for nitrate reduction to nitrite was calculated considering the consumption of two moles of electrons per mol of reduced nitrate as shown in equation 3.16.

$$CE = \frac{t \cdot C}{2 \cdot \Delta NO_3^- \cdot V \cdot F}$$; (equation 3.16)

where *C* is the accumulated coulombs (mC), 2 is the number of electrons of electrons that are transferred during NO_3^- reduction to NO_2^- (mol-e^- per mol-N); ΔNO_3^- is the nitrate consumed (mM-N).

3.2.8. Molecular analyses

Bacteria present in the cathode of denitrifying BES was analyzed using different molecular techniques: PCR-DGGE, flow cytometry and T-RFLP.

3.2.8.1. PCR-DGGE analyses

In Chapters 4 and 5, the micoorganisms attached to cathode electrodes were analyzed using PCR-DGGE. Graphite bars were immersed in 4 ml of 0.1 M of sodium pyrophosphate ($Na_4P_2O_7 \cdot 10H_2O$) and bacterial biofilms were detached by three consecutive sonication rounds for 20 seconds. The bacterial cells suspended were centrifuge at 10,000 × g for 2 minutes and the pellet was extracted using the FastDNA® SPIN Kit for soil (MP, Biomedicals) following the manufacturer's instructions.

The bacterial community composition was analyzed by PCR-DGGE approach using the 16S rRNA gene. PCR reactions were done with primers 357F (5' CTCCTACGGGAGGCAGCAG) (Turner et al., 1999) and 907R (5'CCGTCAATTCMTTTRAGTTT) (Lane, 1991). A GC-clamp was attached to the 5' end of the forward primer for DGGE analysis. PCR reactions were prepared in a total volume of 50 µL containing the following: 1× PCR buffer (Tris-HCL, KCl, 1.5 mM $MgCl_2$ and $(NH_4)_2SO_4$); 0.5 mM $MgCl_2$; 0.2 mM deoxynucleotides triphosphate; 1× Q Solution; 0.2 µM of each primer; 0.1 U of Taq polymerase. All chemicals and reagents were provided by Qiagen®. PCR amplification reactions were done in a

Gene Amp® 2700 thermal cycler (Applied Biosystems) and consisted of an initial denaturation step at 94ºC for 4 min, followed by 10 cycles of 30 sec at 94ºC, 45 sec at 52ºC and 45 sec at 72ºC and another 15 cycles only changing the annealing temperature at 50ºC. PCR products were checked by electrophoresis in agarose gels.

Approximately, 100 ng of PCR amplified DNA was loaded on loaded on 6% (v/v) acrylamide–bis-acrylamide gels with a 30–80% urea–formamide denaturing gradient. DGGE analyses were performed using an INGENY phorU® system (Ingeny, The Netherlads). Known standards consisting of PCR amplified products of the microorganisms *Micrococcus luteus*, *Pseudomonas fluorescens*, *Sulfolobus acidocaldarius*¸ *Saccharomyces cerevisiae* and *Mucor* sp. were loaded at equidistant positions and used for comparison of DGGE gels. Electrophoreses were run for 15 hours at 160 volts and 60ºC. Gels were stained with SYBR® Gold (Invitrogen, molecular Proves) for 45 minutes and visualized in a Herolab UVT-20M. Images were documented using ProgRes CapturePro 2.7 program. Bands were excised using a sterile scalpel. The DNA was recovered by elution in 35 µl Tris/HCl (pH 8.0) at 65ºC during 1 hour and re-amplified as described above. The re-amplified PCR products were purified using the QIAquick PCR purification Kit (Qiagen). The sequentiation was performed using BigDye® Terminator (Applied Biosystems) and reverse primer 907R in ABI prism TM 310 genetic analyzer (PE Applied Biosystems, California).

3.2.8.2. Flow cytometry, T-RFLP and functional genes analyses

In Chapter 6, cytometric DNA/scatter-plot distribution using flow cytometry and phylogenetic analysis (16S rDNA T-RFLP analysis and sequencing) was used to monitor the cathodic microbial community (Koch et al., 2013a, 2013b).

Directly after sampling, the cells were fixated with a 2% paraformaldehyde solution for **flow cytometry**. Fixation, washing and DAPI staining were performed according to Koch et al. (2013a). Cytometric measurements were performed following the protocol described in Koch et al. (2013b). All subcommunities of stained cells were marked with gates using a gate template and their abundance

changes followed over time. The most interesting gates were cytometrically sorted (200000 cells were separated a part) and further phylogenetically analysed (Koch et al., 2013b).

For **T-RFLP** and **functional gene analyses** performed in Chapter 6, the samples were centrifuged at 14000g and the pellet was stored at -20°C. DNA extraction, PCR amplification of 16S rDNA, T-RFLP analysis, cloning and sequencing were performed according to Koch et al. (2013a). PCR amplification of functional denitrification genes (napA, narG, nirK, nirS, nosZ) was done according to Vilar-Sanz et al. (2013).

For T-RFLP and functional gene analyses performed in Chapter 7, the electrodes were cut into four pieces and stored at -20°C at the end of the experiments. DNA was extracted according to Koch et al. (2013b). PCR amplification of 16S rDNA and functional denitrification genes was done according to Koch et al. (2013b) and Vilar-Sanz et al. (2013). Representative samples were further cloned and sequenced.

Chapter 4. Bioremediation of nitrate-polluted groundwater in a microbial fuel cell

N. Pous, S. Puig, M. Coma, M.D. Balaguer, and J. Colprim.

Laboratory of Chemical and Environmental Engineering (LEQUiA), Institute of the Environment, University of Girona, C/ Maria Aurèlia Capmany, 69, Facultat de Ciències, E-17071 Girona, Spain.

Pous, N.; Puig, S.; Coma, M.; Balaguer, M.D.; Colprim, J. “Bioremediation of nitrate-polluted groundwater in a microbial fuel cell”. Journal of Chemical Technology and Biotechnology. Vol. 88, Issue 9 (2013) : 1690-1696

http://dx.doi.org/10.1002/jctb.4020

http://onlinelibrary.wiley.com/doi/10.1002/jctb.4020/full

Issue published online: 6 AUG 2013
Article first published online: 19 FEB 2013
Accepted manuscript online: 29 DEC 2012
Manuscript Accepted: 29 DEC 2012
Manuscript Revised: 13 DEC 2012
Manuscript Received: 10 OCT 2012

BACKGROUND

Groundwater quality is threatened by nitrate accumulation in several regions around the world. Nitrate must be removed from contaminated groundwater to use it as drinking water. Microbial fuel cells (MFCs) can be used for autotrophic denitrification. Thus, the use of MFCs is a potential alternative to using traditional methods for treating nitrate-polluted groundwater.

RESULTS

The objective of this study was to evaluate the potential of MFC technology to treat nitrate-polluted groundwater (28.32 ± 6.15 mgN-NO_3^- L^{-1}). The bioanode was fed with an acetate solution that permitted electron and proton flux to the biocathode. Initially, nitrite was observed in the effluent. After 97 days of operation, the denitrifying-MFC reduced the nitrate and nitrite concentrations in the effluent (12.14 ± 3.59 mgN-NO_3^- L^{-1} and 0.14 ± 0.13 mgN-NO_2^- L^{-1}).Thus, this method improved water quality to meet World Health Organisation standards. However, nitrous oxide emissions were deduced from the electron balance, cathode coulumbic efficiency and Tafel plots. Bioelectrochemical evolution of the biocathode was related to the denitrification nature (sequential reaction steps from NO_3^- to N_2, through NO_2^- and N_2O as stable intermediates) and was supported by the Tafel plots.

CONCLUSION

The bioremediation of nitrate-polluted groundwater with a MFC biocathode is feasible. © 2012 Society of Chemical Industry

Keywords:

biocathode; bioelectrochemical systems; biological autotrophic denitrification; drinking water

Chapter 5. Cathode potential and anode electron donor evaluation for a suitable treatment of nitrate-contaminated groundwater in bioelectrochemical systems

N. Pous, S. Puig, M.D. Balaguer, and J. Colprim.

Laboratory of Chemical and Environmental Engineering (LEQUiA), Institute of the Environment, University of Girona, C/ Maria Aurèlia Capmany, 69, Facultat de Ciències, E-17071 Girona, Spain.

GRAPHICAL ABSTRACT

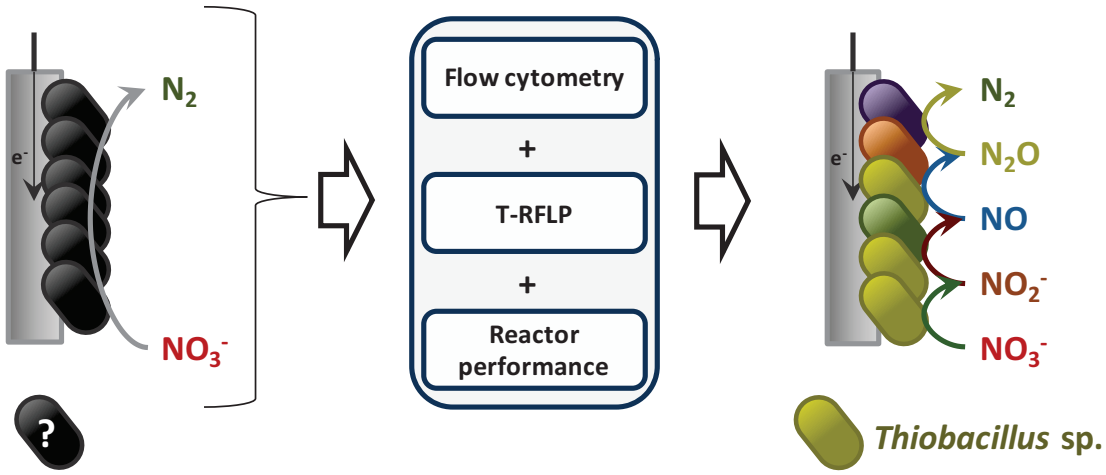

ABSTRACT

Denitrifying bioelectrochemical systems (d-BES) are a promising technology for nitrate removal. Microbial community monitoring is required to pave the way to application. In this study, for the first time flow cytometry combined with molecular biology techniques is exploited to monitor and determine the structure-function relationship of the microbiome of a denitrifying biocathode. Stable cathode performance at poised potential (-0.32 V vs Ag/AgCl) was monitored, and different stress-tests were applied (reactor leakage, nitrate concentration, buffer capacity). Stress-tests shifted the reactor microbiome and performance. The monitoring campaign covered a wide range of nitrate consumption rates (from 15 to 157 $mgN \cdot L^{-1}_{NCC} \cdot d^{-1}$), current densities (from 0 to 25 $mA \cdot L^{-1}_{NCC}$) and denitrification intermediates (nitrite and nitrous oxide consumption rates varied from 0 to 56 $mgN \cdot L^{-1}_{NCC} \cdot d^{-1}$). The reactor microbiome (composed of 21 subcommunities) was characterized and its structure-function relationship was revealed. A key role for *Thiobacillus* sp. in the bioelectrochemical reduction of nitrate is suggested, while a wider number of subcommunities were involved in NO_2^- and N_2O reduction. It was demonstrated that different bacteria catalyze each denitrification step in a biocathode. This study contributed significantly on understanding denitrifying biocathodes, paving the way for its knowledge-driven engineering.

KEYWORDS

Microbial electrochemical technology, cytometric fingerprinting, microbial flow cytometry, microbial resource management, nitrate removal, *Thiobacillus*.

1. INTRODUCTION

Nitrate (NO_3^-) is an abundant and harmful inorganic contaminant, which is present in waste water, surface water and groundwater.[1,2] Microbial electrochemical technologies (METs) are an innovative and promising technology platform which reactors are usually termed bioelectrochemical systems (BES).[3] MET allow, among other applications, the removal of inorganic contaminants,[4,5] like hexavalent uranium, arsenite or hexavalent chromium.[6-8] For BES-based nitrate removal, biological autotrophic denitrification is performed in a biocathode, where bacteria reduce nitrate using the cathode as electron donor.[9] Nitrate is reduced to dinitrogen gas (N_2) in a four-step reduction reaction, where nitrite (NO_2^-) and nitrous oxide (N_2O) are stable, environmentally even more harmful, intermediates.

Denitrifying-BES (d-BES) have evolved during the last years from the proof of concept to application in technological oriented research aiming for higher denitrification rates. The knowledge about d-BES engineering includes different reactor designs,[10,11] the effect of some key parameters (such as pH or conductivity),[12,13] or different bioelectrochemical configurations (autonomous microbial fuel cell mode[10,11] or energy demanding microbial electrolysis mode[14,15]). However, knowledge regarding the microbiome role on bioelectrochemical denitrification is scarce, limiting its further optimization.

Molecular analyses have shown so far that diverse communities are found in denitrifying biocathodes.[14,16,17] Like for anodes,[18] an electrochemically driven selection takes place at denitrifying microbial cathodes, leading usually to the enrichment of different species of Proteobacteria.[16,17]

However, which microorganisms catalyze which reduction reaction in the denitrifying process has not been elucidated, yet. Abundances variation of responsible subcommunities may clarify the successive reductive processes in d-BES. Therefore, it is essential to study the reactor performance together with the subcommunities` dynamics (i.e. cell abundances). A whole arsenal of techniques for investigating

electroactive microbial biofilms is available.[19] Whereby the combination of techniques for phylogenetic analysis (16S rDNA terminal restriction fragment length polymorphisms (T-RFLP) analysis and sequencing) and cytometric DNA/scatter-plot distributions using flow cytometry have been demonstrated to allow monitoring and deriving structure-function relationships of reactor microbiomes.[20] The use of flow cytometry is based on DNA staining for fluorescence detection, allowing the analysis of every single cell present in the sample.[21] Each cell is detected, classified in microbial subcommunities (marked as gates) and, finally, quantified within the subcommunities.

In this article, we aimed to use cytometric fingerprinting combined with 16S rDNA analysis to monitor community dynamics during denitrification at a biocathode. A d-BES was constructed, operated and monitored. Shifts on bacterial activity were provoked by the application of different stress-tests simulating events that are likely to occur in a full-scale application: a reactor leakage (loss of suspended biomass), a power shutdown (break down of bioelectrochemical nitrate reduction) and alteration of influent qualities (pH, conductivity, nitrate concentration, hydraulic retention time). Data obtained from the microbiome was evaluated together with computational fluid dynamics and reactor performance (nitrogen consumption rates, current density, coulombic efficiency) and used to reveal the microbial structure-function relationship of the denitrifying biocathode.

2. EXPERIMENTAL

2.1. Experimental set-up

A two-chamber d-BES, similar to Pous et al.,[22] was built using two methacrylate frames (200 mm x 200 mm x 22 mm) separated by cation exchange membrane (20 x 20 cm, CMI-7000, Membranes Int., USA). The cathode contained granular graphite (diameter 1.5 - 5 mm, EnViro-cell, Germany) and one graphite rod (250 mm x 6 mm, Mersen Ibérica, Spain). The anode contained one stainless steel rod (250 mm x 6 mm) and stainless steel mesh (20 x 20 cm, path 5 x 5 mm, Mersen Ibérica, Spain). Respective net anodic compartment (NAC) and net cathodic compoartment (NCC) volumes were 784 mL and 420 mL. The cathode compartment contained an Ag/AgCl reference electrode (+0.197 V vs standard hydrogen electrode (SHE), model RE-5B BASi, USA). Influents were continuously fed at 566±9 $mL \cdot d^{-1}$. An internal recirculation loop (94±4 $L \cdot d^{-1}$) was placed in each compartment (Figure 1A). Anodic and cathodic hydraulic retention times (HRT) were 1.3 and 0.7 days, respectively. Experiments were performed at room temperature (22ºC).

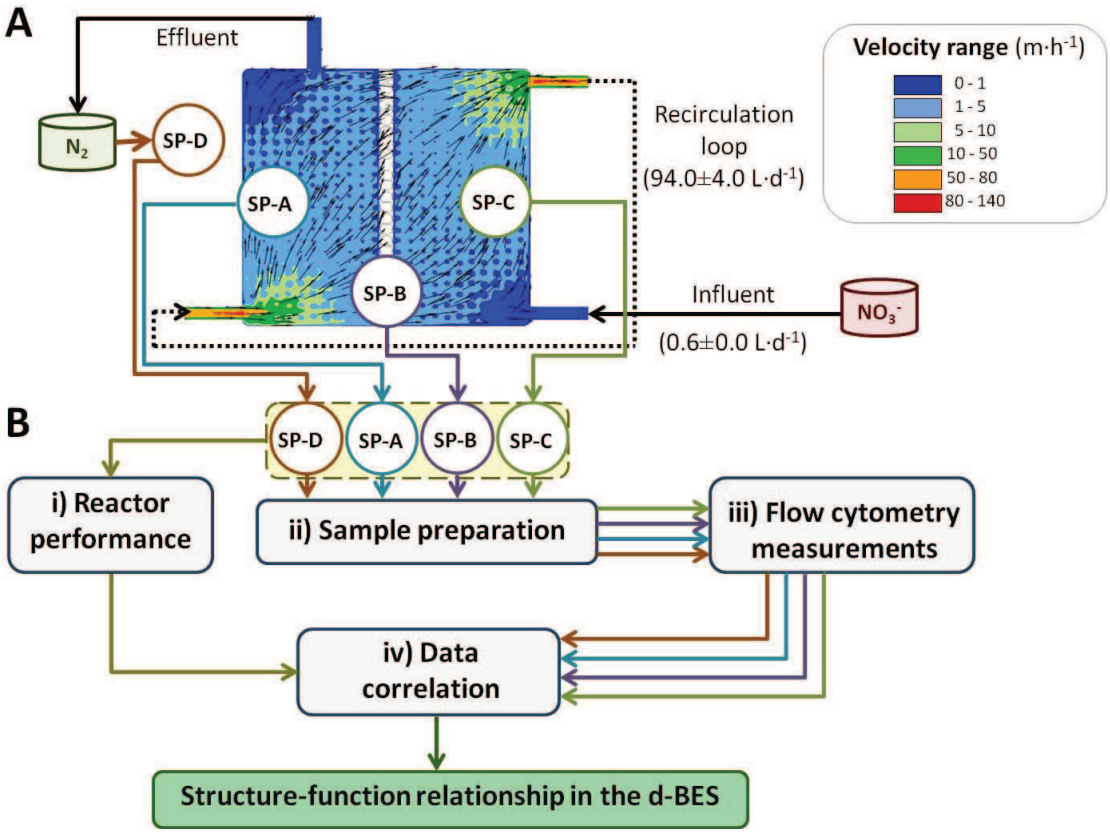

Figure 1. A) Representation of the cathode compartment showing influent/effluent and recirculation flows, the fluid dynamics (velocity and direction inside the cathode) and the positions of sampling ports (SP). B) Flow diagram for determining the structure-function relationship in the d-BES: i) Reactor performance was determined in terms of ΔNO_3^-, ΔNO_2^-, ΔN_2O, current density and *CE*; ii) Samples for microbial analysis were fixated, washed and stained with DAPI; iii) Stained samples were analysed by flow cytometry and resulting data interpreted by gating and calculating the cell abundances of each gate; iv) Cytometric and reactor performance data were correlated to elucidate the structure-function relationship of the cathode.

The cathode was fed with synthetic medium prepared with deionized water. It contained 1.21 $g \cdot L^{-1}$ $NaNO_3$ (equivalent nitrogen concentration of 200 $mgN\text{-}NO_3^- \cdot L^{-1}$); 1.00 $g \cdot L^{-1}$ $NaHCO_3$ as carbon source; 1.55 $g \cdot L^{-1}$ $Na_2HPO_4 \cdot 7H_2O$ and 0.58 $g \cdot L^{-1}$ $KH_2PO_4 \cdot H_2O$ (10 mM phosphate buffer solution (PBS)); 0.50 $g \cdot L^{-1}$ NaCl; 0.10 $g \cdot L^{-1}$ $MgSO_4 \cdot 7H_2O$; 0.02 $g \cdot L^{-1}$ $CaCl_2$; 0.02 $g \cdot L^{-1}$ NH_4Cl; 0.1 $mL \cdot L^{-1}$ trace nutrients.[23] The anode was fed with the same medium without $NaNO_3$. Respective anodic and cathodic specific conductivities were 5.3±0.1 and 4.0±0.1 $mS \cdot cm^{-1}$. Media were sparged with N_2 during 15 minutes prior feeding.

The cathode potential (i.e. working electrode) was poised at -0.32 V vs Ag/AgCl (-0.12 V vs. SHE) by a potentiostat (models SP-50 and VMP3, Bio-logic, France) based on previous studies.[24] Current was normalized to NCC and expressed as current density (*j*). The current flow was negative (cathodic process); for improved graphical representation as well as correlation analysis absolute current densities were used.

2.2. Inoculation and operation

For the cathode's inoculation, the cathode was connected in a closed-loop mode to a tank containing 2500 mL of cathode medium and 125 mL of activated sludge (Girona's WWTP, Spain). The tank's medium was replaced with fresh cathode medium when nitrate was consumed. After three medium replacements, the inoculation procedure finished (41 days), and the cathode was fed at continuous-flow mode during 15 days (in Girona) to allow complete stabilization of the microbial community. Then, the d-BES was sent to Leipzig. During the travel (4 days), the d-BES was under open circuit conditions. Then, the d-BES was operated at continuous-flow mode as well and different stress-tests (details below and Figure 2A) were applied to stimulate dynamics on denitrifying activity. Samples were taken every three days. At every new stress-test, at least three times HRT were operated before taking the first sample.

The stress-test phases, denominated as stress-test- and abbreviated as ST-, were:

ST-0) Reactor leakage; days 26 to 29. The cathode volume was withdrawn, removing the suspended biomass and exposing the cathode to oxygen.

ST-1) Activity recovery from reactor leakage (days 29 to 38).

ST-2) Stable current density after reactor leakage (days 39 to 55).

ST-3) Decrease of influent pH (days 55 to 61): Media with pH 7.6 instead of 7.1,

ST-4) Increase of influent phosphate buffer capacity (days 61 to 63, 67 to 90 and 95 to 97): Media with 20 mM PBS instead of 10 mM.

ST-5) Power shutdown (days 63 to 67): Operation at open circuit.

ST-6) Decrease of influent flow rate (days 90 to 95): From 566±0 to 283±0 $mL \cdot d^{-1}$. It decreased the nitrate loading rate ($NO_3^- LR$) from 279±5 to 140±0 $mgN\text{-}NO_3^- \cdot L^{-1} \cdot d^{-1}$.

ST-7) Decrease of influent nitrate concentration (days 97 to 104): From 205±4 to 104±2 mgN-NO_3^-·L^{-1}. It decreased the *NO_3^-LR* from 279±5 to 141±2 mgN-NO_3^-·L^{-1}·d^{-1}.

The anode was not inoculated and always fed at continuous-flow mode. Abiotic oxidations, e.g. oxygen evolution from water electrolysis, occurred at the anode .[24]

A

Stress-test	1	2	3	4	5	6	7
Influent pH	7.7±0.0	7.6±0.1	7.1±0.0	6.9±0.1	6.8±0.0	6.8±0.0	6.9±0.1
Influent PBS (mM)	10	10	10	20	20	20	20
Closed circuit?	Yes	Yes	Yes	Yes	No	Yes	Yes
HRT (days)	0.7±0.0	0.7±0.0	0.7±0.0	0.7±0.0	0.7±0.0	1.5±0.0	0.7±0.0
Influent [NO_3^-] (mgN-NO_3^-·L^{-1})	196±14	199±7	193±2	205±4	202±0	205±0	104±2
NO_3^-LR (mgN-NO_3^-·L^{-1}·d^{-1})	267±19	270±9	263±3	279±5	276±0	140±0	141±2

B

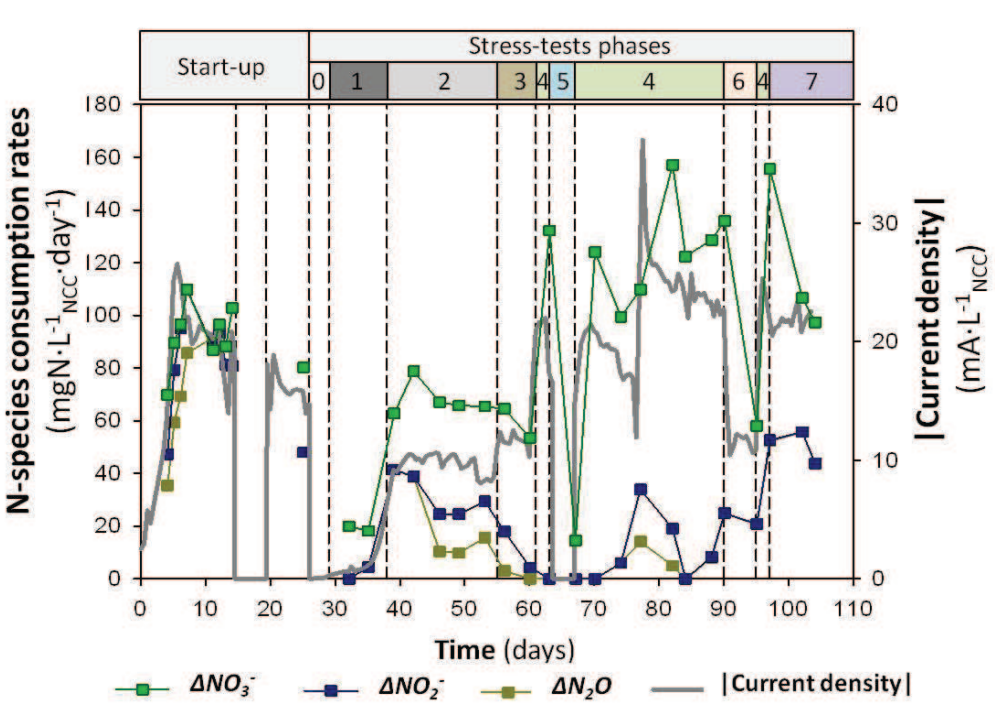

Figure 2. A) Conditions applied for each stress-test phase. B) Absolute current density and nitrate, nitrite and nitrous oxide consumption rates (*ΔNO_3^-*, *ΔNO_2^-* and *ΔN_2O*, respectively) during the continuous-flow mode operation.

2.3. Analytical methods and calculations

Nitrate and nitrite concentrations were analyzed using photometric tests (114563-NO_3^- spectroquant®, 100609-NO_2^- spectroquant®; Merck, Germany). In Girona, the N_2O

content was analyzed with a nitrous oxide microsensor (Unisense, Denmark) located at the cathode recirculation loop. In Leipzig, the N_2O content was analyzed using a gas chromatograph with headspace autosampler and electron capture detector (Agilent Technologies, USA) as explained in supporting information S1. The influent nitrate loading rate (*NO_3^-LR*) was calculated by dividing the influent nitrate concentration per HRT.

The nitrate, nitrite and nitrous oxide consumption rates (*ΔNO_3^-*, *ΔNO_2^-* and *ΔN_2O*, respectively) were calculated (equation 1 to 3). Nitric oxide accumulation was considered negligible.[15]

$$\Delta NO_3^- = \frac{CNO_3^-{}_{influent} - CNO_3^-{}_{effluent}}{HRT} \text{ (eq.1)}$$

$$\Delta NO_2^- = \Delta NO_3^- - \frac{CNO_2^-{}_{effluent}}{HRT} \text{ (eq. 2)}$$

$$\Delta N_2O = \Delta NO_2^- - \frac{CN_2O_{effluent}}{HRT} \text{ (eq. 3)}$$

where *$CNO_3^-{}_{influent}$*, *$CNO_3^-{}_{effluent}$*, *$CNO_2^-{}_{effluent}$* and *$CN_2O_{effluent}$* accounts for nitrate, nitrite and nitrous oxide concentrations at influent or effluent (either $mgN \cdot L^{-1}$ or $mmolN \cdot L^{-1}$).

The coulombic efficiency (*CE*) calculation (equation 4) was adapted from Virdis et al.,[15] considering the required number of electrons for each sequential step from NO_3^- to N_2: nitrate to nitrite (NO_3^-/NO_2^-), nitrite to nitrous oxide (NO_2^-/N_2O) and nitrous oxide to dinitrogen gas (N_2O/N_2).

$$CE = \frac{t \cdot i}{NCC \cdot F \cdot \left(n_{NO_3^-/NO_2^-} \cdot \Delta NO_3^- + n_{NO_2^-/N_2O} \cdot \Delta NO_2^- + n_{N_2O/N_2} \cdot \Delta N_2O\right)} \text{; (eq.4)}$$

where *i* is absolute current (mA); *t* is the time-converting factor between seconds and hours (3600); *NCC* is the cathode liquid volume (L); *F* is the Faraday's constant (96485 $C \cdot mol\text{-}e^{-1}$); *n* is the number of electrons required for each reaction ($n_{NO_3^-/NO_2^-} = 2$, $n_{NO_2^-/N_2O} = 2$ and $n_{N_2O/N_2} = 1$); *ΔNO_3^-*, *ΔNO_2^-* and *ΔN_2O* are the consumption rates expressed in $mmolN \cdot L^{-1}{}_{NCC} \cdot h^{-1}$.

2.4. Fluid hydrodynamics and microbiological sampling

The flows inside the cathode (Figure 1A) were calculated using computational fluid dynamics (Ansys Fluent v12.1[25]) as explained in supporting information S2. The influent flow and the recirculation loop generated heterogeneous flows, suggesting zones with different nutrients availability (Figure 1A). Accordingly, samples for microbiological analyses were taken from three sampling ports of the cathode volume (denominated as SP-A, SP-B and SP-C), and from the cathode effluent (SP-D) as shown in Figure 1. The samples were taken using a needle to scratch the graphite granules surface (electrode), drawing a total volume of 6 mL for SP-B and SP-C, and 7 mL for SP-A (lower biomass observed).

2.5. Flow cytometry: measurements and data analyses

2.5.1. Cytometric measurements

The microbiome response to the different stress-tests was monitored. We combined cytometric DNA/scatter-plot distribution using flow cytometry and phylogenetic analysis (16S rDNA T-RFLP analysis and sequencing).[20]

Directly after sampling, the cells were fixated with a 2% paraformaldehyde solution and stained with DAPI according to Koch et al.[27] Cytometric measurements were performed as described in Koch et al.[20] All subcommunities of stained cells were marked with gates using a gate template (supporting information S3) and their abundance changes followed over time.

Gate G2 of SP-C sample (day 95) was cytometrically sorted (200.000 cells) and further phylogenetically analysed.[20]

2.5.2. Cytometric data analyses

Cytometric data were statistically analyzed to elucidate the structure-function relationship of the cathode microbiome.[20,26]

To reveal electroactive subcommunities, the cell abundance of each gate was normalized to its cell abundance in open circuit conditions (ST-5) (non-bioelectrochemical control). For a better visualization of higher and lower cell abundances, a log10 transformation was applied. In this way, cell abundance increases and decreases have the same distance to the value under open circuit conditions (0,

color code grey in Figure 3). A tenfold higher cell number would be represented by 1 (dark green) and a tenfold lower cell number by -1 (dark red), respectively.

The functional relationship between cell abundances and reactor performance was investigated by generating correlation analyses. Correlations between the raw cell abundances and reactor performance (ΔNO_3^-, ΔNO_2^- and ΔN_2O, current density, *CE* and effluent pH) were calculated using a subset of data covering ST-4 and ST-5 (supporting information S7) and the whole dataset (supporting information S8).[20]

2.6. Molecular analyses

The samples were centrifuged (14.000 g) and the pellet was stored at -20 °C. DNA extraction, PCR amplification of 16S rDNA, T-RFLP analysis, cloning and sequencing were performed according to Koch et al.[27] PCR amplification of functional denitrification genes (napA, narG, nirK, nirS, nosZ) was done according to Vilar-Sanz et al.[16]

3. RESULTS AND DISCUSSION

3.1. BES start-up

The d-BES was operated under continuous-flow mode after the inoculation finished (Figure 2B, mean values and standard deviations in supporting information S4). The absolute current density and nitrogen consumption rates (ΔNO_3^-, ΔNO_2^-, ΔN_2O) rapidly increased. The current density stabilized after 7 days at 21.7±1.4 $mA \cdot L^{-1}_{NCC}$, while ΔNO_3^- was 97.7±11.5 $mgN \cdot L^{-1}_{NCC} \cdot d^{-1}$. Nitrite and nitrous oxide reductions were also promoted, ΔNO_2^- and ΔN_2O were 96.9±11.4 and 90.1±4.0 $mgN \cdot L^{-1}_{NCC} \cdot d^{-1}$, respectively. A coulombic efficiency (*CE)* of 70.7±8.1% was observed.

When re-set to a potential of -0.32 V vs Ag/AgCl (see experimental, Figure 2B days 19-26) the electroactivity of the cathode decreased in terms of current density (from 21.7±1.4 $mA \cdot L^{-1}_{NCC}$ (days 7-15) to now 14.9±1.4 $mA \cdot L^{-1}_{NCC}$). Interestingly, different affections on denitrification were observed. The ΔNO_2^- decreased significantly by 33.5% (from 90.1±4.0 to 64.4±0.0 $mgN \cdot L^{-1}_{NCC} \cdot d^{-1}$), while ΔNO_3^- decreased only by 6.4% (from 97.7±11.5 to 91.5±0.0 $mgN \cdot L^{-1}_{NCC} \cdot d^{-1}$). Therefore, a denitrifying biocathode able to reduce NO_3^- to N_2 was obtained.

3.2. Reactor performance during different stress-tests

The influence of different stress types on the system performance was tested when the current density was stable for 7 days (days 19-26). Figure 2B shows the reactor performance evolution. Mean values and standard deviations for each stress-test are reported in supporting information S4.

The reactor leakage (ST-0) led to system break-down and clearly affected the biocathode activity after re-feeding (ST-1). If activity at ST-1 is compared to the activity before the reactor leakage (start-up), it can be observed a decrease of the absolute current density (from 14.9±1.4 to 0.8±0.2 $mA \cdot L^{-1}_{NCC}$) and ΔNO_3^- (from 91.5±0.0 to 19.0±1.3 $mgN \cdot L^{-1}_{NCC} \cdot d^{-1}$). Denitrification intermediates were also affected, ΔNO_2^- and ΔN_2O decreased from 64.4±0.0 to 2.3±3.2 $mgN \cdot L^{-1}_{NCC} \cdot d^{-1}$ and from 64.4±0.0 to 2.3±3.2 $mgN \cdot L^{-1}_{NCC} \cdot d^{-1}$, respectively. Remarkably, the biocathode activity recovered quickly, without reintroducing the extracted cathode's bulk liquid or reinoculation, reaching stable current density at day 39 (ST-2 in Figure 2B) (j= 9.5±1.4 $mA \cdot L^{-1}_{NCC}$), with a ΔNO_3^- of 68.0±6.2 $mgN^- \cdot L^{-1}_{NCC} \cdot d^{-1}$. These values were 36% and 26% lower than those observed before the reactor leakage. Besides nitrate reducing activity recovered, ΔNO_2^- and ΔN_2O did not (31.7±8.0 and 23.2±3.2 $mgN \cdot L^{-1}_{NCC} \cdot d^{-1}$, respectively), leading to NO_2^- and N_2O accumulation.

On day 55, media composition was changed to investigate the influence of pH stress (ST-3) and changing buffer capacity (ST-4). During stress-test 3, the pH of the influent decreased from 7.6 to 7.1 (ST-3), and negligible differences were observed in terms of current density and denitrifying activity (Figure 2B). The decrease on influent pH was too small, and the effluent pH remained stable at high values (9.1±0.4 in ST-2 and 9.2±0.2 in ST-3), very likely limiting the reactor performance.

Increase in buffer capacity (ST-4) from 10 to 20 mM PBS, increased the biocathodic activity as expected.[13] The absolute current density (22.8±2.0 $mA \cdot L^{-1}_{NCC}$) and ΔNO_3^- (131.9±18.6 $mgN \cdot L^{-1}_{NCC} \cdot d^{-1}$) were almost doubled in comparison to ST-3. Besides promoting nitrate reduction, ΔNO_2^- remained almost stable (13.9±18.2 $mgN \cdot L^{-1}_{NCC} \cdot d^{-1}$), while ΔN_2O increased (from 1.5±2.1 to 12.0±18.2 $mgN \cdot L^{-1}_{NCC} \cdot d^{-1}$).

The simulation of a power shutdown (open circuit, ST-5) confirmed that the denitrifying activity was clearly related to electrochemical activity and thus linked to microbial electrocatalysis, as shown previously.[28] A low residual nitrate reduction was

detected (ΔNO_3^- of 14.5 $mgN \cdot L^{-1}_{NCC} \cdot d^{-1}$; 1% of the maximum rate achieved), possibly related to endogenous heterotrophic denitrification.[29]

The influence of nitrate acting as electron acceptor was assessed by decreasing the nitrate loading rate (NO_3^-LR) from 279 to 140 $mgN \cdot L^{-1}_{NCC} \cdot d^{-1}$ (ST-6 and ST-7). Two scenarios were tested: a decrease of the influent flow rate (ST-6) and a decrease of the influent nitrate concentration (ST-7).

When the influent flow rate was decreased, the absolute current density declined by 54% (from 22.8±2.0 to 10.6±0.0 $mA \cdot L^{-1}_{NCC}$), and the ΔNO_3^- by 56% (from 131.9±18.6 to 58.0±0.0 $mgN \cdot L^{-1}_{NCC} \cdot d^{-1}$). On the contrary, when the influent nitrate concentration was lowered, the absolute current density and the ΔNO_3^- increased (23.1±0.7 $mA \cdot L^{-1}_{NCC}$ and 102.0±6.6 $mgN \cdot L^{-1}_{NCC} \cdot d^{-1}$). The ΔNO_2^- was doubled (from 20.9±0.0 to 49.8±8.4 $mgN \cdot L^{-1}_{NCC} \cdot d^{-1}$) and no accumulation of N_2O was detected. Therefore, at the same NO_3^- *LR*, high HRTs decreased denitrification rates in comparison to low influent nitrate concentration, which supported denitrification rates. From the engineering perspective, it can be hypothesized that higher denitrification performances can be achieved by operating the system at lower HRTs.

The stress-tests caused variations on reactor performance. A wide range of ΔNO_3^-, ΔNO_2, ΔN_2O and current densities were detected in the same d-BES. Consequently, microbiome activity dynamics were expected as well.

3.3. Chemical-physical heterogeneity within the cathode volume

The application of computational fluid dynamics inside the cathode compartment showed flow heterogeneity (Figure 1A) and consequently, different N-species distribution (NO_3^-, NO_2^- and N_2O). The cathode's chemical-physical heterogeneity was investigated by analyzing the NO_3^- concentration and pH at each cathode volume sampling port (SP-A, -B and -C). The results obtained at each port were normalized to the value measured at the effluent (SP-D).

SP-C presented the highest relative availability of nitrate (1.05±0.01), while SP-A had the lowest (0.98±0.02). The pH was more homogeneous. The lowest relative pH ratio was at SP-C (0.99±0.00), while at SP-A and SP-B the same ratio (1.01±0.00) was presented. Thus, chemical-physical heterogeneity was observed, being SP-C the most favorable zone for nitrate reducing bacteria to grow.

3.4. Monitoring biocathode microbiome using flow cytometry

The stress-tests provoked dynamics on reactor performance (Figure 2B). Consequently, microbiome dynamics were also expected, and monitoring using flow cytometry and phylogenetic analysis was performed.[20]

For cytometric analysis a gate template was constructed consisting of 21 subcommunities (supporting information S3). The cell abundances of each gate during the whole study can be found in supporting information S5 (dataset) and S6 (box plot). Three subcommunities were predominant in all sampling ports (gates 2, 6 and 9 (G2, G6 and G9); with mean values of 18, 13 and 15%, respectively). Additionally, G1 was also abundant in SP-D (11%). In the following sections the cytometric data was used to elucidate the structure-function relationship in this d-BES.

3.4.1. Dynamics of cell abundances

The cell abundance dynamics are shown in Figure 3 and the evolution of cytometric measurements can be visualized in video 1. From a first sight it can be clearly seen that cell abundances of subcommunities changed in response to the different stress-tests (ST-1 to ST-7) as did the performance parameters (Figure 2B).

Some subcommunities presented higher cell abundance (shades of green) when the electrical circuit was closed (all phases except SP-5), while some did not (shades of red). Hence, in closed circuit conditions, some subcommunities benefited from the applied potential, and their cell abundance increased (e.g. G2_B, G5_C), while other subcommunities increased their relative cell abundance under open circuit conditions (ST-5) (e.g. G17_C, G18_B, G19_C). It suggests that only a portion of the microbial community was directly involved in the bioelectrochemical process.

Especially the cell abundance in G2 (G2 of all sampling ports evolved similar and grouped closely together) follows the course of ΔNO_3^- and current density over the different stress-test phases. During the recovery phase (ST-1) the cell abundance is comparable to ST-5 (power shutdown) while it increases over the other stress phases with highest abundances in ST-4 (cell abundance of G2 in all SPs of 21.1±6.0). As the dynamics of the highly abundant subcommunity G2 seem to follow the performance

regarding nitrate reduction and current density, a relevant role of G2 for the bioelectrochemical nitrate reduction is indicated.

3.4.2. Correlating cell abundance with reactor performance

For a deeper understanding of subcommunities` dynamics, the correlation between the cell abundances and reactor performance was investigated.[27] To avoid overlapping effects of the different stress-tests, the specific case of recovery after a power shutdown is considered first. This case covers phases ST-4 and ST-5 (days 61 to 90) and, therewith, also the development during the longest stress with more data points enabling meaningful statistical analysis. Figure 4 visualizes the correlation of the three most abundant gates (G2, G6 and G9 of all sampling ports) with the reactor performance including nine time points. The results of all gates and respective correlation values can be found in supporting information S7. The following gate correlations for this case are discussed: i) nitrate consumption rate (ΔNO_3^-); ii) reduction of denitrification intermediates (ΔNO_2^- and ΔN_2O); and iii) absolute current density and *CE*. Correlations higher than moderate positives correlations according to Dancey and Reidy[30] were considered (> 0.4).

Correlation analyses (Figure 4 and supporting information S7) shows a moderate to high correlation of subcommunity G2 to ΔNO_3^- for all sampling ports (0.5 – 0.7). Other subcommunities also presented at least moderate correlation to ΔNO_3^- (G6_B, G9_B, G5_C, G8_C and G21_C), but this behaviour was not homogeneous in all sampling ports (e.g. G6_A and G9_A showed no correlation to ΔNO_3^- (-0.1)).

For complete denitrification, NO_2^- and N_2O reduction have to be considered, as these are environmentally harmful. ΔNO_2^- and ΔN_2O increased in ST-4 in comparison to the power shutdown (ST-5), but the consumption rates were in range of the other stress-test. None of the gates showed positive correlations in all sampling ports for ΔNO_2^- or ΔN_2O suggesting heterogeneities of NO_2^- and N_2O concentration in the d-BES, which is in accordance with the flow heterogeneity discussed in 3.3. Twelve gates presented correlations higher than moderate positive with ΔNO_2^- and eleven with ΔN_2O (supporting information S7) with the highest positive correlations for G21_C with ΔNO_2^- (0.8) and with ΔN_2O (0.9).

The correlation of microbiome dynamics to absolute current density and *CE* should also be considered in a BES. The current density presented strong positive correlation to ΔNO_3^- (0.9), thus only subcommunities previously correlated to ΔNO_3^- presented at least moderate positive correlations to current density (G2 at all sampling ports, G6_B, G9_B). Again, G2 presented the highest correlation to current density (0.5 - 0.7) and also to *CE* (G2_B 0.6 and G2_C 0.7). Since G2 was the most abundant gate, it suggested that the cells in this subcommunity played a relevant role for the bioelectrochemical nitrate reduction.

Considering all stress-tests (ST-1 to ST-7) for correlation analysis (supporting information S8), the increase of G2 cell abundance with the increase of ΔNO_3^- and absolute current density (Figure 3, ST-2 to ST-4, ST-6 and ST-7) is also confirmed (correlation values between 0.6 and 0.7 for ΔNO_3^- and 0.6 to 0.8 for current density depending on the SP). A small number of gates showed also at least moderate positive correlation to ΔNO_3^-, ΔNO_2^- or ΔN_2O without a general trend over all sampling ports (supporting information S8).

Based on the above described dynamics and correlations, it can be concluded that in this d-BES, nitrate was mainly reduced by subcommunity G2, while a wider group of subcommunities were responsible for NO_2^- and N_2O reduction. These cytometric results were supported by conventional functional gene analysis performed on microbial community samples.[16] Denitrifying functional genes napA, narG, nirS and nosZ were successfully amplified, but not nirK. The amplified genes were sequenced, a high diversity was found for every single gene and *Thiobacillus* sp. was identified as contributor to nitrate reduction by narG gene.

3.4.3. Identifying key subcommunity

As a consequence of correlation results, the cells in subcommunity G2 were further investigated on a representative sample (day 95 at SP-C). The molecular analysis showed a predominance of the betaproteobacterium *Thiobacillus* sp. in G2. *Thiobacillus* sp. contributes to the geochemical iron cycling, performing Fe(II)-dependent nitrate-reduction.[31] Electric currents through natural conductive minerals have been demonstrated between *Geobacter sulfurreducens* and *Thiobacillus denitrificans*, suggesting electrotroph capability for *Thiobacillus*.[32] Furthermore, we

took samples from the d-BES to inoculate 18 mL-microcosms, which demonstrated that a biofilm predominantly covered by *Thiobacillus* sp. was able to reduce nitrate to nitrite using the electrode as electron donor at a mid-point potential of -0.30V vs. Ag/AgCl.[28]

The relevance of *Thiobacillus* sp. was also supported by molecular analyses of microbial community samples taken within the cathode compartment (supporting information S10). T-RFLP analyses showed an enrichment of *Thiobacillus* sp. from 0% (below the detection limit) in all sampling ports (day 31), to values between 25 and 33% (day 83).

Taking together all results, in the evaluated d-BES, nitrite and nitrous oxide reduction were catalyzed by a number of subcommunities, while nitrate reduction was mainly performed by a single, *Thiobacillus* sp. dominated subcommunity.

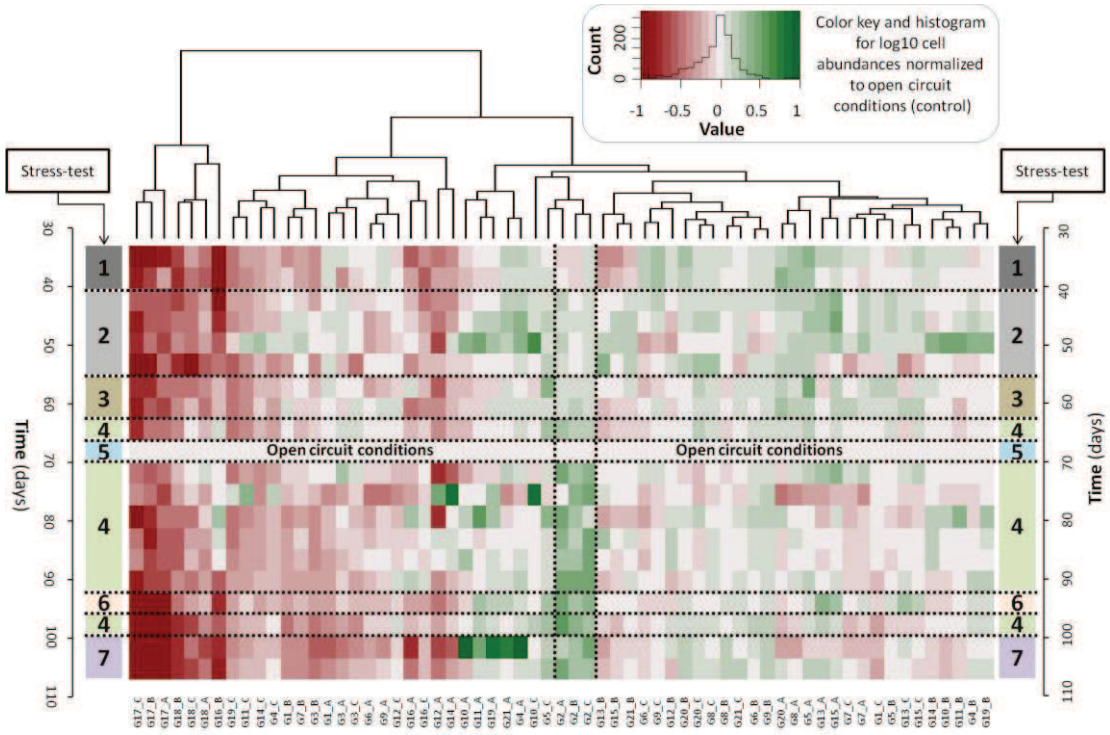

Figure 3. Microbiome dynamics during the different stress-test phases (from ST-1 to ST-7). The CyBar visualizes the cell abundance of individual subcommunities. Gates are labeled as G*X*_*Y*, where: *X* = gate number, and *Y* = sampling port. For a better visualization of higher and lower cell abundances, a log10 transformation was applied. Cell abundance increases and decreases have the same distance to the value under open circuit conditions (0, color code grey). A tenfold higher cell number is represented by 1 (color code dark green) and a tenfold lower cell number by -1 (color code dark red), respectively.

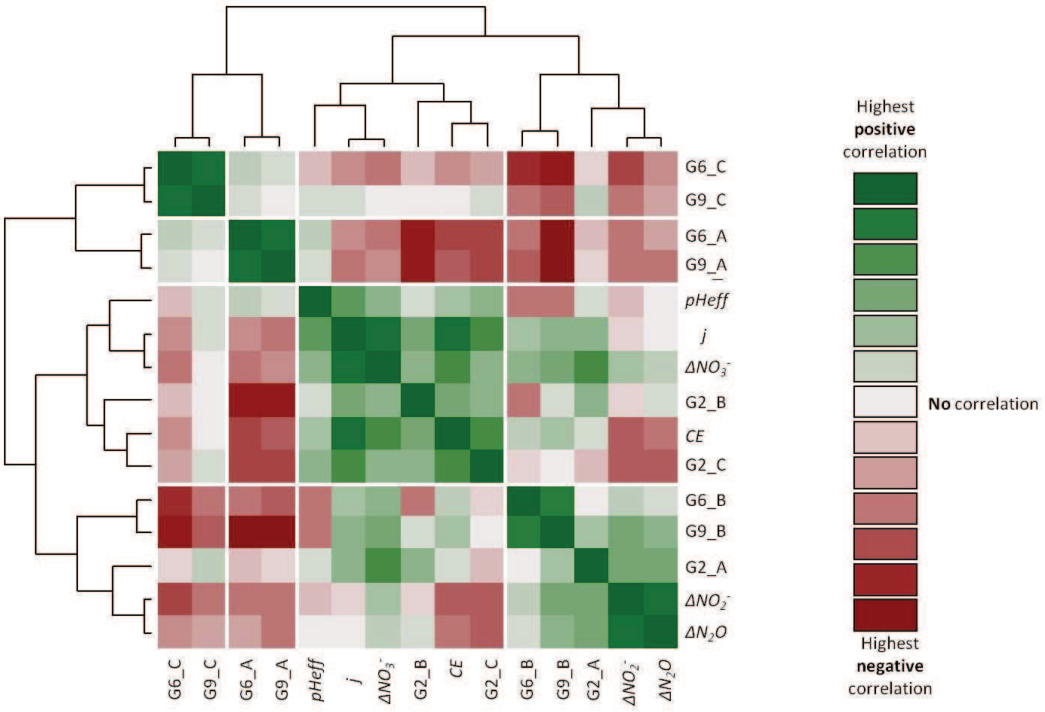

Figure 4. Correlation of the most abundant subcommunities G2, G6 and G9 with reactor performance using Spearman's rank correlation in ST-4 and ST-5 phases. Strong positive correlation is indicated by color code dark green. Strong negative correlation is indicated by color code dark red. The different gates have been labeled as G*X*_*Y*, where: *X* = gate number and *Y* = sampling port. Reactor performance included: pH at cathode effluent (*pHeff*), absolute current density (*j*), coulombic efficiency (*CE*) and nitrate, nitrite and nitrous oxide consumption rates (ΔNO_3^-, ΔNO_2^- and ΔN_2O, respectively).

3.5. Perspectives for engineering and monitoring denitrifying-BES

Engineering and monitoring are key factors for full-scale applications of denitrifying-BES. In this study, we aimed to use cytometric fingerprinting combined with 16S rDNA analysis and sequencing to monitor a denitrifying biocathode and to derive structure-function relationships of its microbiome.

Different stress-tests were applied simulating events that could occur in full-scale denitrifying-BES. Stress-tests provoked shifts in reactor performance. Among other operational strategies, the stress-tests suggested that the operation at low influent nitrate concentration and low HRT promotes higher denitrification rates.

As a result of the reactor performance variations, dynamics on the biocathodic microbiome were expected, which were fast and effectively monitored using flow

cytometry. The monitoring campaign revealed functional relevant subcommunities, which were further confirmed with phylogenetic analysis. A microbial subcommunity mainly composed of *Thiobacillus* sp. was the major contributor to the bioelectrochemical reduction of nitrate to nitrite. While the reduction of NO_2^- and N_2O was performed by a wide number of microbial subcommunities. The further characterization of different bacteria catalyzing each reaction as well as the interplay of these species will contribute to improve nitrate treatment in BES by understanding their specific requirements and behavior under different operational conditions (e.g. cathode potential, or medium composition).

The workflow followed in this study allowed not only investigating the microbiome dynamics, but also enabled to find relevant microbial subcommunities that were catalyzing the individual denitrification steps. Further on, the followed strategy can serve as role model for future analysis of BES microbiomes.

Acknowledgements

This work was supported by the Spanish Government (CTQ2011-23632, CTQ2014-SGR-1168) and the Helmholtz-Association within the Research Programme Terrestrial Environment. F.H. acknowledges support by the BMBF (Research Award "Next generation biotechnological processes – Biotechnology 2020+") and the Helmholtz-Association (Young Investigators Group). N.P. was supported by the Catalan Government (2012FI-B00941) and the University of Girona (MOB2014-ref22).

REFERENCES

(1) Seitzinger, S.P.; Styles, R.V.; Boyer, E.W.; Alexander, R.B.; Billen, G.; Howarth, R.W.; Mayer, B.; Van Breemen, N. Nitrogen retention in rivers: Model development and application to watersheds in the northeastern U.S.A. *Biogeochemistry* **2002,** 57-58, 199–237; DOI: 10.1023/A:1015745629794.

(2) Nolan, B.T.; Ruddy, B.C.; Hitt, K.J.; Helsel, D.R. Risk of nitrate in groundwaters of the United States - A national perspective. *Environ. Sci. Technol.* **1997**, 31(8), 2229–2236; DOI: 10.1021/es960818d.

(3)Schröder, U.; Harnisch, F.; Angenent, L.T. Microbial electrochemistry and technology: terminology and classification. *Energ. Environ. Sci.* **2015**, 8, 513-519; DOI: 10.1039/C4EE03359K.

(4) He, Z.; Angenent, L.T. Application of bacterial biocathodes in microbial fuel cells. *Electroanal*. **2006**, 18 (19-20), 2009–2015; DOI: 10.1002/elan.200603628.

(5) Rosenbaum, M.; Aulenta, F.; Villano, M.; Angenent, L.T. Cathode as electron donors for microbial metabolism: Which extracellular electron transfer mechanisms are involved? *Bioresour. Technol.* **2011**, 102 (1), 324-333; DOI: 10.1016/j.biortech.2010.07.008.

(6) Gregory, K.B.; Lovley, D.R. Remediation and recovery of uranium from contaminated subsurface environments with electrodes. *Environ. Sci. Technol.* **2005**, 39 (22), 8943-8947; DOI: 10.1021/es050457e.

(7) Pous, N.; Casentini, B.; Rossetti, S.; Fazi, S.; Puig, S.; Aulenta, F. Anaerobic arsenite oxidation with an electrode serving as the sole electron acceptor: A novel approach to the bioremediation of arsenic-polluted groundwater. *J. Hazard Mater.* **2015**, 283, 617-622; DOI: 10.1016/j.jhazmat.2014.10.014.

(8) Huang, L.; Chai, X.; Chen, G.; Logan, B.E. Effect of set potential on hexavalent chromium reduction and electricity generation from biocathode microbial fuel cells. *Environ. Sci. Technol.* **2011**, 45 (11), 5025-5031; DOI: 10.1021/es103875d.

(9) Gregory, K.B.; Bond, D.R.; Lovley, D.R. Graphite electrodes as electron donors for anaerobic respiration. *Environ. Microbiol.* **2004**, 6 (6), 596–604; DOI: 10.1111/j.1462-2920.2004.00593.x.

(10) Clauwaert, P.; Rabaey, K.; Aelterman, P.; De Schamphelaire, L.; Pham, T.H.; Boeckx, P.; Boon, N.; Verstraete, W. Biological denitrification in microbial fuel cells. *Environ. Sci. Technol.* **2007**, 41 (9), 3354–3360; DOI: 10.1021/es062580r.

(11) Zhang, Y.; Angelidaki, I. A new method for in situ nitrate removal from groundwater using submerged microbial desalination-denitrification cell (SMDDC). *Water Res.* **2013**, 47 (5), 1827–1836; DOI: 10.1016/j.watres.2013.01.005.

(12) Clauwaert, P.; Aelterman, P.; Pham, T.H.; De Schamphelaire, L.; Carballa, M.; Rabaey, K.; Verstraete, W. Minimizing losses in bio-electrochemical systems: the road to applications. *Appl. Microbiol. Biotechnol.* **2008**, 79 (6), 901–913; DOI: 10.1007/s00253-008-1522-2.

(13) Puig, S.; Coma, M.; Desloover, J.; Boon, N.; Colprim, J.; Balaguer, M.D. Autotrophic denitrification in microbial fuel cells treating low ionic strength waters. *Environ. Sci. Technol.* **2012**, 46 (4), 2309–2315; DOI: 10.1021/es2030609.

(14) Van Doan, T.; Lee, T.K.; Shukla, S.K.; Tiedje, J.M.; Park, J. Increased nitrous oxide accumulation by bioelectrochemical denitrification under autotrophic conditions: Kinetics and expression of denitrification pathway genes. *Water Res.* **2013**, 47 (19), 7087–7097; DOI: 10.1016/j.watres.2013.08.041.

(15) Virdis, B.; Rabaey, K.; Yuan, Z.; Rozendal, R.A.; Keller, J. Electron fluxes in a microbial fuel cell performing carbon and nitrogen removal. *Environ. Sci. Technol.* **2009**, 43 (13), 5144–5149; DOI: 10.1021/es8036302.

(16) Vilar-Sanz, A.; Puig, S.; García-Lledó, A.; Trias, R.; Balaguer, M.D.; Colprim, J.; Bañeras, L. Denitrifying bacterial communities affect current production and nitrous oxide accumulation in a microbial fuel cell. *PLoS One* **2013**, 8 (5), e63460; DOI: 10.1371/journal.pone.0063460.

(17) Wrighton, K.C.; Virdis, B.; Clauwaert, P.; Read, S.T.; Daly, R.A.; Boon, N.; Piceno, Y.; Andersen, G. L.; Coates, J. D.; Rabaey, K. Bacterial community structure corresponds to performance during cathodic nitrate reduction. *ISME J.* **2010**, 4 (11), 1443–1455; DOI: 10.1038/ismej.2010.66.

(18) Harnisch, F.; Koch, C.; Patil, S.; Hübschmann, T.; Müller, S.; Schröder, U. Revealing the electrochemically driven selection in natural community derived microbial biofilms using flow-cytometry. *Energy Environ. Sci.* **2011**, 4 (4), 1265-1267; DOI: 10.1039/c0ee00605j.

(19) Harnisch, F.; Rabaey, K. The diversity of techniques to study electrochemically active biofilms highlights the need for standardization. *ChemSusChem*, **2012**, 5 (6), 1012-1019; DOI: 10.1002/cssc.201100732.

(20) Koch, C.; Günther, S.; Desta, A.F.; Hübschmann, T.; Müller, S. Cytometric fingerprinting for analyzing microbial intracommunity structure variation and identifying subcommunity function. *Nat. Protoc.* **2013**, 8 (1), 190–202; DOI: 10.1038/nprot.2012.149.

(21) Müller, S.; Nebe-Von-Caron, G. Functional single-cell analyses: Flow cytometry and cell sorting of microbial populations and communities. *FEMS Microbiol. Rev.* **2010**, 34 (4), 554–587; DOI: 10.1111/j.1574-6976.2010.00214.x.

(22) Pous, N.; Puig, S.; Coma, M.; Balaguer, M.D.; Colprim, J. Bioremediation of nitrate-polluted groundwater in a microbial fuel cell. *J. Chem. Technol. Biot.* **2013**, 88 (9), 1690-1696; DOI: 10.1002/jctb.4020.

(23) Rabaey, K.; Ossieur, W.; Verhaege, M.; Verstraete, W. Continuous microbial fuel cells convert carbohydrates to electricity. *Water Sci. Technol.* **2005**, 52 (1-2), 515–523.

(24) Pous, N.; Puig, S.; Balaguer, M.D.; Colprim, J. Cathode potential and anode electron donor for a suitable treatment of nitrate-contaminated groundwater in bioelectrochemical systems. *Chem. Eng. J.* **2015**, 263, 151-159; DOI: 10.1016/j.cej.2014.11.002.

(25) Ansys. Ansys fluent theory guide. Inc Northbrook IL**, 2009**, 49–53.

(26) Schumann, J.; Koch, C.; Günther, S.; Fetzer, I.; Müller, S. FlowCyBar: Analyze flow cytometric data using gate information. **2014**. R package version 1.2.1.

(27) Koch, C.; Fetzer, I.; Schmidt, T.; Harms, H.; Müller, S. Monitoring functions in managed microbial systems by cytometric bar coding. *Environ. Sci. Technol.* **2013**, 47 (3), 1753–1760; DOI: 10.1021/es3041048.

(28) Pous, N.; Koch, C.; Colprim, J.; Puig, S.; Harnisch, F. Extracellular electron transfer of biocathodes: Revealing the potentials for nitrate and nitrite reduction of denitrifying microbiomes dominated by *Thiobacillus* sp. *Electrochem. Commun.* **2014**, 49, 93-97; DOI: 10.1016/j.elecom.2014.10.011.

(29) Xiao, Y.; Zheng, Y.; Wu, S.; Yang, Z.H.; Zhao, F. Bacterial community structure of autotrophic denitrification biocathode by 454 pyrosequencing of the 16S rRNA gene. *Microb. Ecol.* **2014**, in press; DOI: 10.1007/s00248-014-0492-4.

(30) Dancey, C.; Reidy, J. Statistics without maths for psychology: using SPSS for Windows, London, Prentice Hall, 2004.

(31) Straub, K.L.; Benz, M.; Schink, B.; Widdel, F. Anaerobic, nitrate-dependent microbial oxidation of ferrous iron. *Appl. Environ. Microbiol.* **1996**, 62 (4), 1458–1460.

(32) Kato, S.; Hashimoto, K.; Watanabe, K. Microbial interspecies electron transfer via electric currents through conductive minerals. *Proc. Natl. Acad. Sci. U. S. A.* **2012**, 109 (25), 10042–10046; DOI: 10.1073/pnas.1117592109.

Supporting information for manuscript

Cathode potential and anode electron donor evaluation for a suitable treatment of nitrate-contaminated groundwater in bioelectrochemical systems

Narcis Pous, Sebastià Puig*, M. Dolors Balaguer and Jesús Colprim

Laboratory of Chemical and Environmental Engineering (LEQUiA), Institute of the Environment, University of Girona, Campus Montilivi, s/n, Facultat de Ciències, E-17071 Girona, Spain.

* Corresponding author:

E-mail address: sebastia@lequia.udg.cat (S. Puig)

LEQUiA, Institute of the Environment, University of Girona, Campus Montilivi, s/n, Facultat de Ciències, E-17071 Girona, Spain.

Tel: +34972418182; Fax: +34972418150

Summary:

S1: Calculation of nitrous oxide (N_2O) in the gas phase from N_2O measured in de liquid- phase.

In order to calculate the total amount of N_2O in the cathode from the measured N_2O in the liquid- phase, the following steps were followed.

Firstly, the amount of gas generated in the cathode was calculated from the difference between influent and effluent of nitrate (NO_3^-), nitrite (NO_2^-), and nitrous oxide in the liquid phase (N_2O_{liquid}) (eq.S1). As a result of denitrification, the gas generated is composed by nitrous oxide in the gas phase (N_2O_{gas}) and dinitrogen gas (N_2) (eq. S1).

$$n_g = \Delta NO_3^- + \Delta NO_2^- + \Delta N_2O_{liquid} = nN_2O_{gas} + nN_2 \text{ (eq. S1)}$$

Where n_g is the amount of gas generated in the cathode per volume of groundwater treated (mole $N \cdot L_{groundwater}^{-1}$); ΔNO_3^-, ΔNO_2^- and ΔN_2O_{liquid} are the difference between influent and effluent of the amount of nitrate, nitrite and nitrous oxide in the liquid phase (mole $N \cdot L_{groundwater}^{-1}$); nN_2O_{gas} and nN_2 are the amount of nitrous oxide in the gas phase and dinitrogen gas produced per volume of groundwater treated (mole $N \cdot L_{groundwater}^{-1}$). Nitric oxide production was considered negligible.

In order to calculate the amount of N_2O in the gas phase, two different equations must be taken into account (eq. S2 and eq.S3). On the one hand, by assuming that the gas phase in the cathode was only composed by N_2O and N_2, the concentration of N_2O in the gas- phase is represented as shown in equation S2.

$$[N_2O]_{gas} = \frac{nN_2O_{gas}}{V_{gas}} = \frac{nN_2O_{gas}}{\frac{n_g \cdot R \cdot T}{P}} \text{ (eq. S2)}$$

Where $[N_2O]_{gas}$is the concentration of N_2O in the gas phase (mole $N \cdot m^{-3}$); V_{gas} is the volume of gas ($m^3 \cdot m_{groundwater}^{-3}$); T is the temperature (K); R is the ideal gas constant (8.31451 $J \cdot K^{-1} \cdot mole^{-1}$) and P is the atmospheric pressure (101325 Pa).

On the other hand, the concentration of N_2O in the gas- phase can also be calculated from the Henry's law (equation S3).

$$[N_2O]_{gas} = \frac{[N_2O]_{liquid}}{k_{N_2O} \cdot T \cdot R} \text{(eq.S3)}$$

Where $[N_2O]_{liquid}$ is the nitrous oxide concentration in the liquid phase (mole $N \cdot m^{-3}$) and k_{N2O} is the Henry's constant for nitrous oxide at the experimental temperature. The k_{N2O} was calculated from the Henry's constant as a function of the temperature as shown in equation S4.

$$k_{N_2O} = 2.47 \cdot 10^{-4} \cdot exp\left\{\frac{-19800}{R} \cdot \left(\frac{1}{T} - \frac{1}{298}\right)\right\} \text{ (eq.S4)}$$

Finally, by coupling equation S2 and equation S3, the amount of nitrous oxide in the gas- phase can be calculated as presented in equation S5.

$$nN_2O_{gas} = \frac{[N_2O]_{liquid}}{k_{N_2O} \cdot P} \text{ (eq.S5)}$$

In order to calculate the total amount of N_2O produced per volume of groundwater treated, equation S6 was used:

$$nN_2O = nN_2O_{gas} + nN_2O_{liquid} \text{(eq. S6)}$$

Where nN_2O is the total amount of nitrous oxide produced per volume of groundwater treated (mole $N \cdot L_{groundwater}^{-1}$). Once N_2O production was known, the amount of N_2 produced per volume of groundwater treated was calculated by closing the nitrogen mass balance and considering negligible the presence of nitric oxide (NO).

S2: Results obtained from the tests where acetate was fed at the anode (tests 1 to 7).

Table S1. Nitrate removal rate, nitrogen concentrations at the effluent, nitrate removal efficiency and current when acetate was fed at the anode (tests 1 to 7).

Experiment	Cathode potential (mV vs SHE)	NO_3^- removal rate (mg N-NO_3^- L^{-1}_{NCC} h^{-1})	Nitrogen concentrations at the effluent (mgN L^{-1})		NO_3^- removal efficiency (%)	Current (mA)
			NO_3^-	NO_2^-		
Test 1 (Free)	-13±9	1.98±0.12	12.14±3.59	0.14±0.13	64±8	4.5±0.8
Test 2	+597	1.05±0.06	19.56±0.64	1.31±0.25	38±2	1.2±0.3
Test 3	+397	1.47±0.04	18.15±0.65	1.65±0.17	47±2	0.5±0.2
Test 4	+196	1.64±0.03	18.30±0.36	1.46±0.17	49±1	0.3±0.1
Test 5	+21	2.01±0.06	13.76±0.67	1.24±0.05	61±2	1.6±0.1
Test 6	-103	2.12±0.08	5.68±0.86	0.13±0.23	80±3	9.4±1.0
Test 7 (OCV)	+279	0.23±0.01	23.64±0.64	0.00±0.00	10±0	0.0±0.0

Table S2. Nitrogen speciation at the effluent and percentage of nitrite accumulation in respect to nitrate removed when acetate was fed at the anode (tests 1 to 7).

Experiment	Cathode potential (mV vs SHE)	Nitrogen speciation at the effluent (%)		NO_2^-/ $NO_3^-{}_{removed}$ (%)
		NO_3^-	NO_2^-	
Test 1 (Free)	-13±9	35.7±8.2	0.4±0.4	0.6±0.6
Test 2	+597	61.6±2.0	4.1±0.8	11.1±2.5
Test 3	+397	52.2±1.5	4.7±0.5	10.1±1.1
Test 4	+196	50.6±1.0	4.0±0.5	8.2±0.8
Test 5	+21	38.8±1.9	3.5±0.1	5.7±0.1
Test 6	-103	19.8±3.0	0.4±0.8	0.6±1.0
Test 7 (OCV)	+279	89.8±0.0	0.0±0.0	0.0±0.0

S3: Results obtained from the tests where water was fed at the anode (tests 8th to 18th).

Table S3. Nitrate removal rate, nitrogen concentrations at the effluent, nitrate removal efficiency and current when water was fed at the anode (tests 8 to 18).

Experiment	Cathode potential (mV vs SHE)	NO_3^- removal rate (mg N-NO_3^- L^{-1}_{NCC} h^{-1})	Nitrogen concentrations at the effluent (mgN L^{-1})				NO_3^- removal efficiency (%)	Current (mA)
			NO_3^-	NO_2^-	N_2O	N_2 + N assimilated		
Test 8	+97	0.96 ±0.04	21.40±0.39	0.61±0.06	1.17±0.18	8.31±1.31	32±1	1.5±0.0
Test 9	-3	1.17±0.03	20.97±0.26	0.58±0.02	1.89±0.54	9.50±2.71	37±1	2.7±0.0
Test 10	-53	1.47±0.02	17.10±0.23	0.00±0.00	1.64±0.47	14.44±4.13	48±1	4.2±0.0
Test 11	-102	2.16±0.05	9.77±0.48	0.00±0.00	1.62±0.47	20.39±5.94	69±2	6.7±0.0
Test 12	-123	2.76±0.04	3.46±0.45	0.00±0.00	1.82±0.32	27.89±4.89	90±1	8.0±0.0
Test 13	-203	2.53±0.04	4.59±0.45	0.00±0.00	6.29±1.46	22.65±5.27	86±1	12.6±0.0
Test 14	-303	3.62±0.04	4.10±0.29	13.92±1.19	5.94±1.08	8.32±1.51	87±1	15.8±0.0
Test 15	-403	5.44±0.09	4.61±0.47	13.25±0.75	4.29±0.49	11.81±1.36	86±1	17.6±0.0
Test 16	-503	5.46±0.07	6.86±0.18	11.28±0.93	3.26±0.43	14.03±1.86	81±1	19.5±0.0
Test 17	-603	6.15±0.03	3.31±0.15	14.35±0.51	2.57±0.13	16.14±0.81	91±0	22.0±0.0
Test 18	-703	6.16±0.05	0.48±0.29	16.87±0.28	4.10±0.32	12.63±0.99	99±1	23.5±0.0

Table S4. Nitrogen speciation at the effluent and nitrate reduction end- products when water was fed at the anode (tests 8 to 18).

Experiment	Cathode potential (mV vs SHE)	Nitrogen speciation at the effluent (%)				Nitrate reduction end- products (%)		
		NO_3^-	NO_2^-	N_2O	N_2 + N assimilated	NO_2^-	N_2O	N_2 + N assimilated
Test 8	+97	68.2±1.2	1.9±0.2	3.7±0.6	26.5±4.2	6.1±0.6	11.8±1.9	83.4±13.1
Test 9	-3	63.2±0.8	1.7±0.1	5.7±1.6	28.6±8.2	4.7±0.2	15.5±4.4	77.9±22.3
Test 10	-53	51.5±0.7	0.0±0.0	5.0±1.4	43.5±12.4	0.0±0.0	10.2±2.9	89.8±25.6
Test 11	-102	30.7±1.5	0.0±0.0	5.1±1.5	64.1±18.7	0.0±0.0	7.4±2.1	92.6±27.0
Test 12	-123	10.4±1.3	0.0±0.0	5.5±1.0	84.1±14.8	0.0±0.0	6.1±1.1	93.9±16.5
Test 13	-203	13.7±1.3	0.0±0.0	18.8±4.4	67.5±15.7	0.0±0.0	21.7±5.1	78.3±18.2
Test 14	-303	12.7±0.9	43.2±3.7	18.4±3.3	25.8±4.7	49.5±4.2	21.1±3.8	29.6±5.4
Test 15	-403	13.6±1.4	39.0±2.2	12.6±1.5	34.8±4.0	45.2±2.6	14.6±1.7	40.3±4.6
Test 16	-503	19.4±0.5	31.9±2.6	9.2±1.2	39.7±5.3	39.5±3.3	11.4±1.5	49.2±6.5
Test 17	-603	9.1±0.4	39.5±1.4	7.1±0.4	44.4±2.2	43.4±1.5	7.8±0.4	48.8±2.5
Test 18	-703	1.4±0.9	49.5±0.8	12.0±0.9	37.1±2.9	50.2±0.8	12.2±1.0	37.6±3.0

Chapter 6. Monitoring and engineering reactor microbiomes of denitrifying bioelectrochemical systems

N. Pous [a], C. Koch [b], A. Vilà [a], M.D. Balaguer [a], J. Colprim [a], J. Mühlenberg [c], S. Müller [b], F. Harnisch [b], and S. Puig [a].

[a] Laboratory of Chemical and Environmental Engineering (LEQUiA), Institute of the Environment, University of Girona, C/ Maria Aurèlia Capmany, 69, Facultat de Ciències, E-17071 Girona, Spain.

[b] Helmholtz Centre for Environmental Research - UFZ, Department of Environmental Microbiology, Permoserstraße 15 I 04318 Leipzig, Germany.

[c] DBFZ Deutsches Biomasseforschungszentrum gemeinnützige GmbH, Torgauer Straße 116, 04347 Leipzig, Germany.

Supporting information for the manuscript:

Monitoring and engineering reactor microbiomes of denitrifying bioelectrochemical systems

Authors: Pous, N.; Koch, C.; Vilà, A.; Balaguer, M.D.; Colprim, J.; Mühlenberg, J.; Müller, S.; Harnisch, F.; Puig, S.

Summary:

S1: Analyses of N_2O using gas chromatography.

Instrumental:

The analyses of N_2O were performed on an Agilent 7890A GC/µECD system with an Agilent G1888 headspace autosampler.

Gas chromatograph

The injection mode was split 1:10. The injector temperature was kept at 250 °C. For the separation a HP-Plot/Q column (30 m x 0.53 mm x 40 µm; Agilent Technologies) was used. The gas chromatography system was operating at programmed-temperature-mode as follows: initial temperature 40 °C hold for 4 min, linear ramp 30 °C·min^{-1} till 220 °C and hold for 1 min. A µECD (electron capture detector) heated at 250 °C was used for data acquisition.

Headspace-sampler

Table S1. Instrumental settings of the headspace-sampler.

Temperatures		**Timing**		**Pressures**	
Oven	90 °C	Vial equilibration	0.5 min	Carrier	7.0 psi
Loop (1 ml)	150 °C	Pressurization	0.5 min	Vial	7.2 psi
Transfer line	180 °C	Loop fill	0.4 min		
		Loop equilibration	0.1 min		
		Inject	0.4 min		

Sample preparation:

For the analysis 3 mL of sample were placed in a 20-mL headspace vial and tightly closed with an aluminium crimp cap with PTFE/silicone septum using a hand crimper. Samples have to be carefully transferred from experimental equipment to the 20 mL vial, to prevent loss of nitrous oxide by shaking or outgassing.

Calibration was done by analyzing different dilutions of a saturated N_2O-solution. Water has been filled into a 100 mL volumetric flask and the nitrous oxide was passed

through a filter with 300 $mL \cdot min^{-1}$ for 3 min at room temperature and atmospheric pressure. The solubility of nitrous oxide at 20 °C and atmospheric pressure is 1200 $mg \cdot L^{-1}$.[1] Calibration levels were between 2.4 and 600 $mg \cdot L^{-1}$. The detection limit is 2.4 mgL^{-1} .

S2: Computational fluid dynamics calculation

The velocities generated inside the cathode were calculated using a computational fluid dynamics program (Ansys Fluent v12.1 [2]). To do this, both mass and momentum equations are solved. The mass conservation is shown in equation S1.

$$\frac{d\rho}{dt} + \nabla \cdot (\rho \vec{v}) = S_m \text{ (eq. S1)}$$

Where □ is the fluid density, *v* represents the velocity vector, and Sm is a source term (by chemical reaction, phases mass exchanges, among others).

The equation of momentum conservation in an inertial (non-accelerating) reference frame is described as shown in equation S2.

$$\frac{d}{dt}(\rho \vec{v}) + \nabla \cdot (\rho \vec{v} \vec{v}) = -\nabla p + \nabla \cdot (\bar{\tau}) + \rho \vec{g} + \vec{F} \text{ (eq. S2)}$$

From which p is the static pressure, □g and F are gravitational and external body forces, and □ is the stress tensor, which is calculated using equation S3.

$$\vec{\tau} = \mu \left[(\nabla \vec{v} + \nabla \vec{v}^T) - \frac{2}{3} \nabla \cdot \vec{v} I \right] \text{(eq. S3)}$$

Steady state simulations were developed considering single water based phase. To close the solution of the different solutions, velocity inlet boundary conditions for the influent/outflow streams, as well as for both recirculation streams were defined, taking in account the fluxes specified in experimental section. The inlet recirculation streams values were formulated based on the values from the outflow recirculation stream. Wall boundary conditions were developed for the methacrylate walls of the reactor as well as for the rod graphite surface. The simulations were performed at a constant temperature of 22ºC and atmospheric pressure. The influent flow and the recirculation loop generated heterogeneous flows inside this chamber, which suggested zones with different nitrate availability.

S3: Gate template used for flow cytometry data analyses.

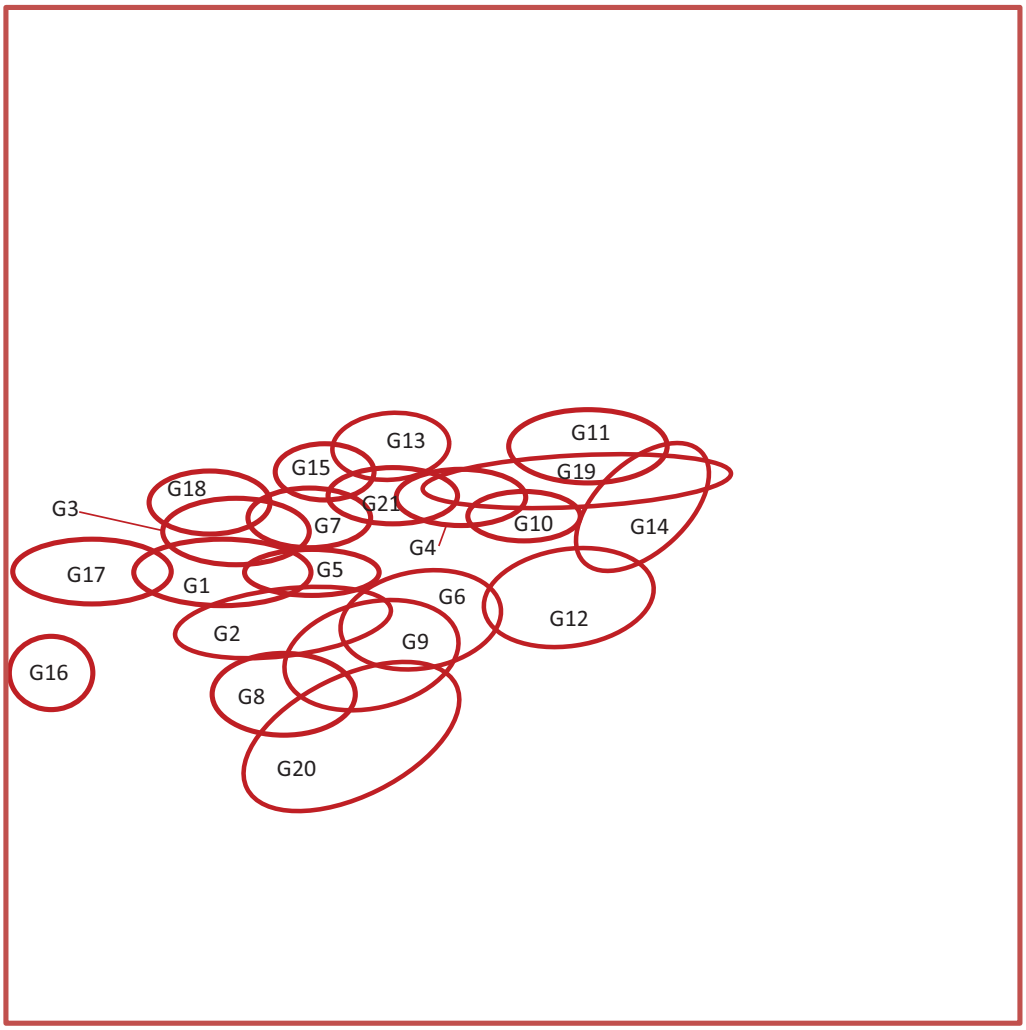

Figure S1. Gate template used for flow cytometry data analyses.

S4: Absolute current density and nitrate, nitrite and nitrous oxide consumption rates at the different stress-tests.

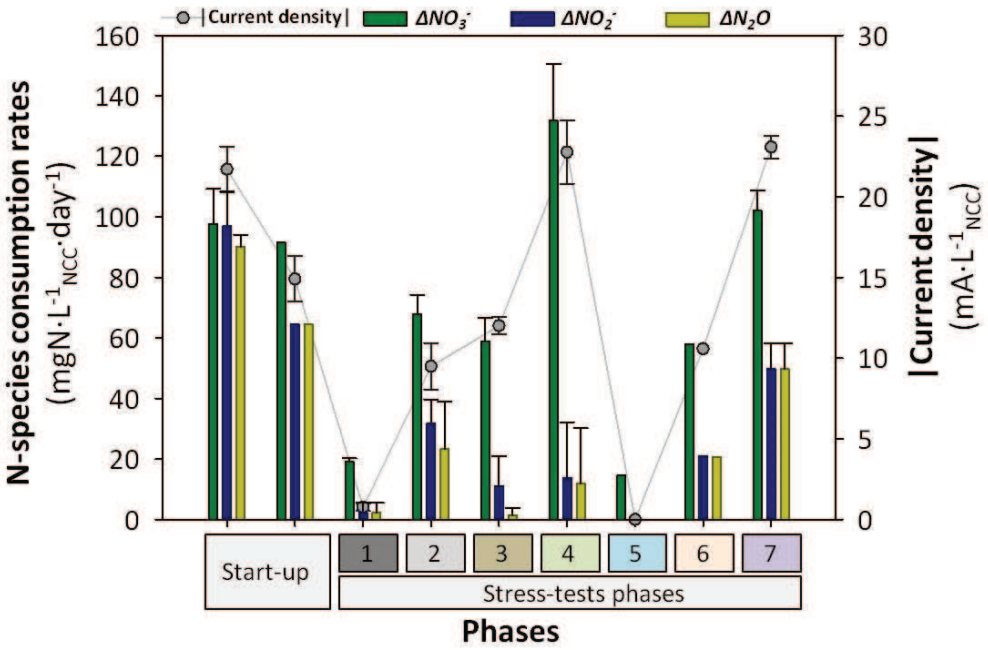

Figure S2. Current density expressed in absolute values, and nitrate, nitrite and nitrous oxide consumption rates at the phases. Error bars represent the standard deviation of the different stress-tests.

Table S2. Mean value and standard deviation of current density (in absolute value) and nitrate, nitrite and nitrous oxide consumption rates at the different phases.

Phases		*j* ($mA \cdot L^{-1}_{NCC}$)	ΔNO_3^- ($mgN \cdot L^{-1}_{NCC} \cdot day^{-1}$)	ΔNO_2^- ($mgN \cdot L^{-1}_{NCC} \cdot day^{-1}$)	ΔN_2O ($mgN \cdot L^{-1}_{NCC} \cdot day^{-1}$)
Start-up		21.7±1.4	97.7±11.5	96.9±11.4	90.1±4.0
		14.9±1.4	91.5±0.0	64.4±0.0	64.4±0.0
Stress-tests	**ST-1**	0.8±0.2	19.0±1.3	2.3±3.2	2.3±3.2
	ST-2	9.5±1.4	68.0±6.2	31.7±8.0	23.2±15.6
	ST-3	12.0±0.6	58.9±7.8	11.1±9.7	1.5±2.1
	ST-4	22.8±2.0	131.9±18.6	13.9±18.2	12.0±18.2
	ST-5	0.0±0.0	14.5±0.0	0.0±0.0	0.0±0.0
	ST-6	10.6±0.0	58.0±0	20.9±0.0	20.6±0.0
	ST-7	23.1±0.7	102.0±6.6	49.8±8.4	49.6±8.6

S5: Cell abundance of each gate during the whole experimental study at the different SP.

Table S3. Cell abundance of each gate at SP-A at each sampling day.

Day	G1_A	G2_A	G3_A	G4_A	G5_A	G6_A	G7_A	G8_A	G9_A	G10_A	G11_A	G12_A	G13_A	G14_A	G15_A	G16_A	G17_A	G18_A	G19_A	G20_A	G21_A
32	10.70	8.00	6.28	3.48	7.94	16.10	4.22	8.66	20.60	1.53	1.61	4.42	2.01	1.63	1.66	0.20	0.78	0.92	3.46	8.94	3.37
38	9.83	9.19	2.17	2.81	5.45	16.70	2.44	9.22	24.50	1.16	1.38	5.91	1.29	1.68	1.17	0.40	3.15	0.78	3.27	11.90	2.89
42	7.72	13.90	5.64	3.45	4.34	15.30	5.31	7.69	19.50	1.34	1.68	5.11	2.45	1.55	2.46	0.45	1.71	1.57	3.46	7.80	3.84
46	9.23	12.10	6.42	4.78	6.16	9.32	5.23	6.17	11.60	1.59	2.40	3.70	2.77	1.96	2.78	0.58	1.64	1.92	5.57	6.88	4.83
49	7.43	15.40	5.80	4.98	4.80	8.28	5.44	6.47	11.30	4.23	4.50	2.69	2.06	3.99	1.86	0.65	1.39	1.51	7.83	6.31	3.99
53	8.75	11.70	3.06	2.43	4.86	15.70	2.69	7.60	20.20	1.50	1.55	7.73	1.10	2.62	0.98	0.32	1.99	0.85	3.75	8.03	2.27
56	10.00	12.10	4.70	2.13	8.41	9.79	3.92	6.30	12.50	1.08	1.19	3.48	1.10	2.39	1.41	0.80	2.03	1.39	3.13	9.14	2.68
60	7.26	12.60	4.20	2.63	5.17	16.10	3.96	7.46	21.00	1.28	1.22	5.44	1.37	2.34	1.38	0.25	1.39	1.12	4.40	9.63	2.88
63	7.87	18.30	5.38	2.46	5.13	16.90	3.07	5.52	18.90	1.17	1.46	4.81	1.21	2.27	1.25	0.50	2.11	1.86	3.66	7.01	2.59
67	7.82	9.32	4.74	2.17	2.99	17.50	3.10	4.65	18.20	1.74	1.54	12.20	1.29	3.53	0.98	0.70	6.23	3.08	3.67	5.45	2.35
70	8.16	26.80	8.43	2.72	4.82	12.90	5.10	5.35	15.20	0.81	1.34	2.00	2.38	0.89	2.31	0.50	2.25	4.23	2.78	4.04	3.51
74	3.08	10.10	2.44	1.36	1.42	5.83	1.32	1.83	6.76	1.90	1.68	36.90	0.61	24.80	0.65	0.33	1.25	1.43	6.49	1.80	0.91
77	4.95	26.10	4.31	2.28	3.18	9.44	2.31	4.93	14.40	2.88	5.31	2.22	0.92	3.51	1.16	1.36	2.29	2.65	7.54	7.97	1.80
82	4.99	22.50	3.65	2.30	3.22	12.40	2.66	5.69	15.50	1.87	1.31	14.40	1.21	4.01	1.08	0.58	1.57	1.45	3.60	4.34	2.33
84	3.93	19.00	2.84	2.70	2.83	16.40	2.33	5.00	17.10	3.14	1.70	12.50	1.15	4.56	0.94	0.64	1.53	1.17	4.97	4.83	2.26
88	4.19	27.30	3.42	3.45	4.19	12.00	2.57	6.40	15.20	1.29	1.54	4.84	1.33	2.08	1.35	1.02	1.21	1.44	4.68	5.85	3.25
95	4.05	25.20	3.48	2.97	3.91	10.90	3.70	4.93	11.20	1.35	2.84	3.72	3.37	1.96	1.82	0.39	0.60	2.07	5.17	4.70	3.30
97	3.18	31.60	2.41	2.53	3.93	15.10	2.46	3.71	14.30	1.65	2.31	6.16	2.11	2.60	1.30	0.50	0.51	1.31	4.68	3.77	2.39
102	2.17	13.30	1.43	34.60	2.43	8.15	2.12	2.46	7.35	21.00	4.48	2.37	0.99	1.03	0.79	0.11	0.17	0.60	23.70	2.59	14.30
104	3.38	27.90	2.48	2.57	4.50	11.90	2.41	4.66	13.50	1.04	1.81	4.35	1.93	1.96	1.33	0.22	0.56	1.11	4.27	6.36	2.62

Table S4. Cell abundance of each gate at SP-B at each sampling day.

Day	G1_B	G2_B	G3_B	G4_B	G5_B	G6_B	G7_B	G8_B	G9_B	G10_B	G11_B	G12_B	G13_B	G14_B	G15_B	G16_B	G17_B	G18_B	G19_B	G20_B	G21_B
32	2.74	8.18	2.42	1.75	3.70	13.40	2.34	7.11	14.40	1.51	1.75	8.05	0.84	3.09	0.66	0.07	0.25	0.99	3.01	13.70	1.69
38	5.48	8.38	2.39	2.11	4.56	15.20	2.36	6.01	16.10	1.39	1.47	8.48	0.98	2.90	0.98	0.21	1.35	0.76	3.09	10.10	2.24
42	7.51	10.10	3.61	2.83	6.05	13.00	3.71	6.88	16.30	1.39	1.51	6.97	1.73	2.28	1.60	0.27	1.43	0.88	3.18	9.36	3.46
46	9.51	12.50	5.77	3.64	7.34	10.10	5.19	6.53	12.60	1.42	1.63	4.20	2.04	1.92	2.52	0.43	1.57	1.51	4.16	8.17	4.40
49	8.97	11.10	6.80	5.00	5.24	7.58	6.73	5.67	9.02	4.10	4.08	3.43	2.65	5.44	2.22	0.71	1.90	1.80	7.97	6.31	4.33
53	3.74	10.30	2.52	1.82	5.22	14.80	5.01	5.85	15.20	1.35	1.18	8.90	4.78	2.68	1.54	0.86	0.48	0.79	2.80	9.95	3.82
56	6.21	14.10	3.95	2.33	6.29	13.30	4.49	5.47	14.40	1.48	1.41	6.81	1.83	2.91	1.39	1.55	1.11	1.49	3.37	7.62	3.32
60	8.11	17.20	4.98	2.02	5.98	12.40	3.66	6.65	15.10	1.24	1.00	5.44	1.11	2.50	1.27	1.86	1.75	1.75	2.99	7.63	2.26
63	7.07	16.10	4.69	2.06	5.31	16.00	3.00	4.97	16.20	1.24	1.28	7.05	1.17	2.50	1.16	3.44	1.96	1.98	3.02	6.90	2.30
67	7.06	10.20	6.35	2.15	4.35	11.60	4.58	6.14	12.30	1.33	1.44	6.41	1.85	2.52	1.46	2.68	5.85	4.29	3.05	6.88	2.67
70	5.90	21.30	5.75	1.99	4.56	15.60	3.81	5.23	16.90	1.21	1.50	6.35	1.72	2.70	1.57	2.43	1.55	2.89	2.99	5.38	2.44
74	4.40	23.40	4.18	1.88	3.98	15.90	3.60	5.58	18.60	1.11	1.21	5.80	2.19	2.36	1.41	2.97	1.83	2.27	2.80	6.17	2.62
77	3.21	17.80	2.47	1.86	3.81	16.20	2.19	6.15	18.40	2.22	3.38	7.43	0.99	3.64	0.87	5.08	1.09	1.43	5.41	7.84	1.63
82	3.53	16.20	2.55	2.02	4.27	15.80	3.74	6.19	16.40	1.42	1.40	10.20	3.28	3.89	1.47	3.41	0.87	1.19	3.51	6.37	3.24
84	3.35	18.60	2.54	2.06	3.88	15.80	2.77	6.85	16.50	1.39	1.44	9.75	1.82	3.63	1.09	2.75	1.29	1.24	3.37	6.77	2.62
88	4.07	30.50	3.60	3.05	4.03	10.90	2.48	6.09	14.50	1.17	1.45	4.33	1.20	2.12	1.29	0.76	1.35	1.61	4.30	5.55	3.03
95	3.88	19.30	3.06	2.63	5.55	12.20	2.93	8.31	15.90	1.03	1.51	4.64	1.83	1.92	1.55	0.49	0.55	1.30	3.92	9.02	2.82
97	2.63	22.00	2.01	2.60	3.86	16.30	2.53	6.67	19.00	1.28	1.52	7.79	1.57	2.64	1.05	0.69	0.51	0.82	4.11	7.73	2.72
102	2.96	19.70	1.76	2.10	4.21	13.80	1.85	8.76	18.10	0.95	1.10	8.46	1.04	1.96	1.06	0.51	0.35	0.69	3.25	9.61	2.03
104	2.74	20.30	1.93	2.92	4.19	12.50	2.01	8.90	18.30	0.95	1.21	4.60	1.25	1.90	1.13	0.38	0.59	0.68	3.93	10.00	2.91

Table S5. Cell abundance of each gate at SP-C at each sampling day.

Day	G1_C	G2_C	G3_C	G4_C	G5_C	G6_C	G7_C	G8_C	G9_C	G10_C	G11_C	G12_C	G13_C	G14_C	G15_C	G16_C	G17_C	G18_C	G19_C	G20_C	G21_C
32	6.40	11.30	6.85	3.26	3.70	22.80	4.76	7.00	29.30	1.29	1.47	3.64	1.86	1.52	2.05	0.26	0.77	2.18	3.53	7.95	3.23
38	6.36	11.50	5.39	3.01	4.08	24.30	4.19	7.40	31.70	1.28	1.37	3.93	1.58	1.58	1.67	0.18	1.15	1.51	3.35	8.22	3.21
42	8.38	11.50	5.71	3.85	4.34	20.30	4.17	6.26	23.40	1.52	1.75	4.18	1.76	2.24	1.89	0.21	1.90	1.51	4.56	7.97	3.75
46	7.48	10.40	6.08	3.11	5.06	14.70	4.48	7.95	18.50	1.29	1.60	3.96	1.68	1.93	2.16	0.33	1.15	1.57	3.85	9.72	3.57
49	7.90	11.70	6.20	5.30	4.83	8.17	5.80	5.68	10.30	4.88	4.63	3.21	1.94	5.67	1.91	0.41	1.35	1.55	8.56	6.80	4.09
53	5.09	9.59	2.10	2.09	5.47	11.10	2.20	9.50	15.10	1.05	1.17	4.38	0.62	2.05	0.84	0.39	0.50	0.42	2.71	13.80	2.14
56	9.54	11.00	6.17	2.78	8.11	10.20	4.70	7.34	13.40	0.97	1.26	3.25	1.27	1.86	1.86	0.46	1.24	1.55	3.02	10.20	3.60
60	7.28	10.60	8.85	2.57	4.05	13.90	6.20	7.29	17.40	1.23	1.35	5.47	2.28	2.40	2.48	0.28	1.13	2.56	3.39	8.58	3.62
63	6.37	11.90	7.74	2.46	7.47	11.70	4.27	7.07	14.00	1.01	1.31	3.97	1.22	2.09	1.86	0.49	1.29	4.45	3.16	9.06	3.19
67	6.17	8.51	6.62	4.68	3.60	14.80	4.24	5.33	15.20	1.10	3.04	4.37	1.44	3.14	1.44	0.68	7.49	4.35	9.64	6.45	3.13
70	6.68	21.60	7.89	2.61	4.81	17.90	4.91	5.10	19.40	0.80	1.64	3.05	1.96	1.27	2.07	0.63	2.32	4.39	3.54	4.55	3.07
74	6.26	24.10	5.84	7.43	3.13	9.88	2.72	3.91	13.30	8.48	6.95	1.91	1.23	1.19	1.25	0.60	3.14	3.35	11.30	4.05	2.74
77	6.23	10.30	3.90	2.92	8.33	8.48	2.93	5.83	11.70	1.18	1.15	2.99	0.91	1.48	1.18	0.94	0.78	1.43	3.15	9.55	3.53
82	6.78	26.30	5.32	2.79	4.96	11.90	3.57	6.82	16.40	0.99	1.43	3.33	1.53	1.56	1.59	0.65	2.55	2.43	3.53	5.58	3.24
84	6.16	27.50	5.38	2.78	4.47	10.60	3.77	6.01	13.90	1.04	1.44	3.57	1.58	1.80	1.58	0.59	3.25	2.72	3.70	4.89	3.19
88	4.40	22.90	3.56	3.24	4.58	13.40	3.33	5.99	16.10	1.20	1.56	5.94	1.85	2.24	1.59	0.92	1.06	1.56	4.74	6.27	3.54
95	4.88	21.50	3.98	3.32	6.34	10.80	3.91	5.46	12.50	1.13	2.25	3.62	2.77	1.74	2.08	0.37	0.59	2.11	4.90	6.42	3.97
97	3.50	14.90	2.88	4.72	6.86	12.90	3.03	6.60	16.00	1.64	1.91	5.76	1.18	2.24	1.22	0.58	0.48	0.98	5.45	8.84	4.32
102	4.22	25.20	2.95	3.14	5.77	11.80	2.59	5.51	15.20	1.11	1.69	3.83	1.65	1.86	1.47	0.41	0.37	1.43	4.29	7.51	3.46
104	3.54	15.10	3.94	4.75	6.47	11.70	4.22	5.98	14.60	1.46	1.78	4.42	1.42	1.88	1.21	0.47	0.55	1.02	5.32	8.47	4.50

Table S6. Cell abundance of each gate at SP-D at each sampling day.

Day	G1_D	G2_D	G3_D	G4_D	G5_D	G6_D	G7_D	G8_D	G9_D	G10_D	G11_D	G12_D	G13_D	G14_D	G15_D	G16_D	G17_D	G18_D	G19_D	G20_D	G21_D
38	5.41	8.54	3.15	22.10	2.19	10.00	4.50	3.16	11.10	13.40	0.93	1.47	1.01	0.67	0.92	0.33	1.87	0.93	8.87	19.10	14.60
42	16.90	15.50	9.50	3.60	6.70	11.00	5.88	5.30	14.50	1.19	2.05	2.23	3.12	1.08	2.66	0.40	2.85	1.83	3.41	4.95	4.36
46	10.00	14.00	5.77	5.18	6.02	9.00	4.33	5.91	12.20	1.87	2.83	3.56	2.54	2.03	2.29	0.71	1.78	1.25	6.01	6.39	4.73
49	12.30	13.90	5.26	4.48	6.86	7.23	5.00	6.55	10.60	1.82	2.59	2.91	2.03	2.11	1.74	0.83	2.22	1.36	5.44	6.45	4.24
53	12.70	12.50	6.27	3.08	6.21	8.93	4.40	6.05	11.00	1.53	1.90	4.17	1.59	2.19	1.75	0.67	2.87	1.90	4.18	6.48	3.01
56	13.30	14.20	7.15	2.83	6.84	9.21	5.03	4.75	11.40	1.39	1.93	3.45	1.62	2.10	1.92	0.76	2.59	2.06	4.02	6.35	3.04
60	11.30	18.30	5.97	3.27	6.08	9.02	4.48	5.68	12.10	1.72	1.83	2.71	1.54	1.75	1.91	0.47	2.50	1.73	4.51	5.36	3.03
63	9.74	14.50	6.85	2.51	5.69	11.50	3.75	5.22	12.30	1.54	1.85	4.41	1.71	2.09	1.76	0.58	2.08	2.46	4.01	5.82	2.70
67	26.40	9.91	8.49	16.20	8.94	5.17	2.57	2.21	5.65	12.10	3.09	1.77	0.81	0.82	1.05	0.23	6.02	1.90	9.98	1.73	5.99
70	10.80	25.50	11.30	2.51	4.54	11.40	5.70	4.91	13.40	0.96	1.77	1.53	2.31	0.98	2.30	0.51	2.37	4.41	2.93	3.53	3.18
74	9.14	33.20	6.66	1.99	4.25	10.40	3.20	4.23	13.50	0.80	1.59	1.65	1.45	1.52	1.42	0.86	3.90	3.04	2.94	3.93	2.26
77	7.10	30.80	3.44	1.67	3.55	10.80	1.94	3.90	14.80	1.13	2.82	2.25	0.99	2.74	0.90	1.54	2.96	1.72	4.52	7.15	1.58
82	32.10	16.70	14.50	2.32	11.10	7.84	3.29	3.47	10.20	0.81	1.87	1.83	1.36	1.24	1.46	0.44	4.88	2.49	3.61	2.61	2.61
84	6.56	29.40	4.56	2.73	4.10	10.40	3.00	5.72	13.80	1.18	1.74	3.11	1.33	1.60	1.20	0.78	3.33	1.98	3.68	4.35	2.68
88	4.46	27.70	2.98	3.56	4.20	11.80	2.26	4.97	14.10	1.57	2.07	4.75	1.28	2.64	1.07	1.31	1.42	1.23	5.23	4.94	3.08
95	4.31	21.40	2.89	4.26	4.04	11.40	2.96	6.77	14.70	1.77	2.92	4.03	2.14	2.44	1.34	0.47	0.73	1.11	6.49	5.38	3.66
97	3.80	33.30	2.56	2.59	4.18	14.80	2.34	3.44	14.30	1.54	2.41	5.50	1.98	2.34	1.14	0.46	0.74	1.29	4.64	3.03	2.39
102	2.17	21.10	1.44	20.30	2.66	7.06	1.74	2.47	8.58	20.90	7.13	1.80	1.09	1.90	0.63	0.15	0.27	0.71	21.70	2.28	6.10

S6: Box plot for cell abundances of each gate during the whole experimental study.

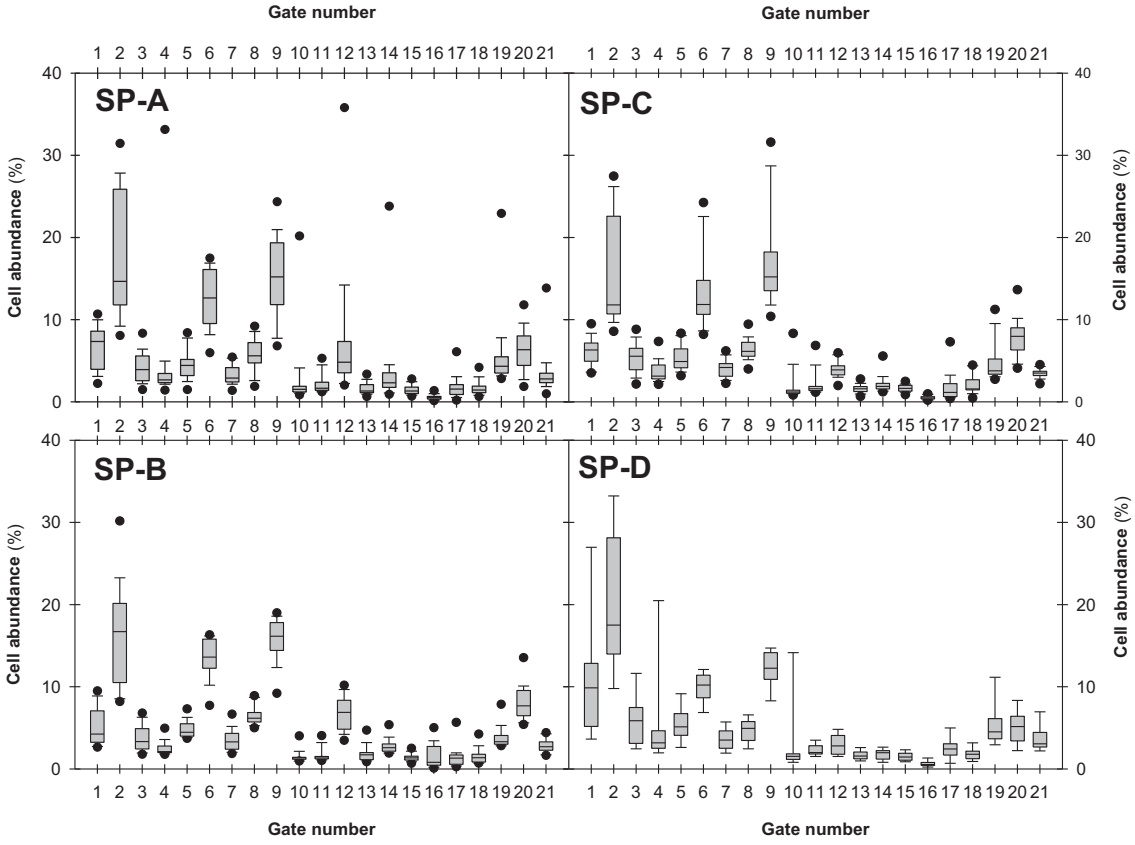

Figure S3. The box plot shows the relative cell abundance of each gate (numbered as gate number) at each sampling port (SP-A, –B, -C and –D) during the whole experimental study. The box plot allows an easy visualization of which gates are the most abundant at each sampling port. In this study, gates 2, 6 and 9 were the most abundant in sampling ports SP-A, -B and -C, while gates 1, 2, 6 and 9 were the most abundant in sampling port SP-D.

S7: Correlation data between gate cell abundances and reactor performance using data of ST-4 and ST-5 phases.

Table S7. Correlation of SP-A gates with reactor performance using data of ST-4 and ST-5 phases. The different gates have been labeled as G*X*_*Y*, where: *X* = gate number and *Y* = sampling port. Reactor performance data included: pH at cathode effluent (pHeff), current density (Current_den), coulombic efficiency (*CE*) and nitrate, nitrite and nitrous oxide consumption rates (ΔNO_3^-, ΔNO_2^- and ΔN_2O, respectively). Green colored indicates positive correlations higher than 0.4.

	Current_den	ΔNO_3^-	ΔNO_2^-	ΔN_2O	*CE*
Current_den	1.0	0.9	0.1	0.2	0.9
ΔNO_3^-	0.9	1.0	0.4	0.4	0.7
ΔNO_2^-	0.1	0.4	1.0	0.9	-0.2
ΔN_2O	0.2	0.4	0.9	1.0	-0.2
CE	0.9	0.7	-0.2	-0.2	1.0
pHeff	0.7	0.5	0.1	0.2	0.4
G1_A	-0.4	-0.4	-0.5	-0.5	-0.3
G2_A	0.5	0.7	0.6	0.6	0.3
G3_A	-0.2	-0.1	-0.4	-0.4	0.0
G4_A	0.3	0.3	0.0	0.0	0.2
G5_A	0.3	0.4	0.0	0.0	0.2
G6_A	-0.1	-0.1	-0.2	0.0	-0.3
G7_A	0.0	0.0	-0.3	-0.2	0.0
G8_A	0.2	0.2	-0.2	-0.3	0.1
G9_A	-0.1	-0.1	-0.2	-0.2	-0.3
G10_A	-0.1	-0.1	0.2	0.0	-0.2
G11_A	-0.3	0.0	0.6	0.3	-0.3
G12_A	0.0	-0.2	-0.2	-0.2	0.1
G13_A	0.2	0.3	0.2	0.4	0.0
G14_A	0.0	-0.2	-0.1	-0.1	0.2
G15_A	0.2	0.3	0.0	0.0	0.2
G16_A	-0.3	-0.1	0.3	0.0	-0.3
G17_A	-0.9	-0.9	-0.4	-0.4	-0.8
G18_A	-0.5	-0.4	-0.3	-0.3	-0.3
G19_A	-0.1	0.0	0.4	0.2	-0.1
G20_A	-0.3	-0.1	0.0	-0.2	-0.3
G21_A	0.2	0.2	-0.2	-0.1	0.2

Table S8. Correlation of SP-B gates with reactor performance using data of ST-4 and ST-5 phases. The different gates have been labeled as G*X*_*Y*, where: *X* = gate number and *Y* = sampling port. Reactor performance data included: pH at cathode effluent (pHeff), current density (Current_den), coulombic efficiency (*CE*) and nitrate, nitrite and nitrous oxide consumption rates (ΔNO_3^-, ΔNO_2^- and ΔN_2O, respectively). Green colored indicates positive correlations higher than 0.4.

	Current_den	ΔNO_3^-	ΔNO_2^-	ΔN_2O	*CE*
Current_den	1.0	0.9	0.1	0.2	0.9
ΔNO_3^-	0.9	1.0	0.4	0.4	0.7
ΔNO_2^-	0.1	0.4	1.0	0.9	-0.2
ΔN_2O	0.2	0.4	0.9	1.0	-0.2
CE	0.9	0.7	-0.2	-0.2	1.0
pHeff	0.7	0.5	0.1	0.2	0.4
G1_B	-0.5	-0.6	-0.7	-0.6	-0.2
G2_B	0.6	0.5	0.1	0.3	0.6
G3_B	-0.5	-0.7	-0.7	-0.6	-0.3
G4_B	0.2	0.2	0.2	0.4	0.1
G5_B	0.0	0.0	-0.5	-0.4	0.2
G6_B	0.4	0.5	0.3	0.3	0.3
G7_B	-0.5	-0.6	-0.5	-0.5	-0.3
G8_B	0.0	0.0	0.5	0.5	-0.3
G9_B	0.5	0.6	0.6	0.5	0.4
G10_B	-0.3	0.0	0.4	0.1	-0.4
G11_B	-0.3	0.0	0.5	0.2	-0.3
G12_B	0.3	0.3	0.2	0.1	0.0
G13_B	0.2	0.1	-0.1	-0.2	0.1
G14_B	0.1	0.3	0.2	-0.1	0.0
G15_B	-0.1	-0.2	-0.6	-0.5	0.1
G16_B	-0.3	-0.2	-0.1	-0.4	-0.2
G17_B	-0.9	-0.9	-0.5	-0.4	-0.7
G18_B	-0.8	-0.9	-0.6	-0.5	-0.5
G19_B	0.0	0.2	0.7	0.4	-0.2
G20_B	-0.3	0.0	0.7	0.5	-0.5
G21_B	0.4	0.2	-0.1	0.0	0.2

Table S9. Correlation of SP-C gates with reactor performance using data of ST-4 and ST-5 phases. The different gates have been labeled as G*X*_*Y*, where: *X* = gate number and *Y* = sampling port. Reactor performance data included: pH at cathode effluent (pHeff), current density (Current_den), coulombic efficiency (*CE*) and nitrate, nitrite and nitrous oxide consumption rates (ΔNO_3^-, ΔNO_2^- and ΔN_2O, respectively). Green colored indicates positive correlations higher than 0.4.

	Current_den	ΔNO_3^-	ΔNO_2^-	ΔN_2O	*CE*
Current_den	1.0	0.9	0.1	0.2	0.9
ΔNO_3^-	0.9	1.0	0.4	0.4	0.7
ΔNO_2^-	0.1	0.4	1.0	0.9	-0.2
ΔN_2O	0.2	0.4	0.9	1.0	-0.2
CE	0.9	0.7	-0.2	-0.2	1.0
pHeff	0.7	0.5	0.1	0.2	0.4
G1_C	-0.2	-0.3	-0.6	-0.8	0.1
G2_C	0.7	0.5	-0.2	-0.2	0.7
G3_C	-0.2	-0.3	-0.8	-0.7	0.1
G4_C	-0.3	-0.4	0.1	0.2	-0.2
G5_C	0.1	0.4	0.6	0.4	-0.1
G6_C	-0.1	-0.2	-0.3	-0.1	-0.1
G7_C	-0.1	-0.2	-0.6	-0.5	0.0
G8_C	0.4	0.5	0.3	0.3	0.1
G9_C	0.3	0.2	-0.1	0.0	0.2
G10_C	0.0	-0.1	-0.1	0.0	0.2
G11_C	-0.2	-0.4	-0.2	-0.1	0.0
G12_C	0.1	0.1	0.3	0.5	-0.2
G13_C	0.3	0.1	-0.5	-0.4	0.4
G14_C	-0.5	-0.5	0.0	0.1	-0.7
G15_C	0.3	0.2	-0.6	-0.6	0.5
G16_C	-0.3	-0.1	0.2	0.0	-0.2
G17_C	-0.7	-0.9	-0.5	-0.5	-0.6
G18_C	-0.3	-0.5	-0.8	-0.7	0.0
G19_C	-0.5	-0.6	-0.2	0.0	-0.4
G20_C	-0.2	0.1	0.6	0.5	-0.4
G21_C	0.2	0.4	0.8	0.9	-0.2

S8: Correlation data between gate cell abundances and reactor performance using the whole dataset.

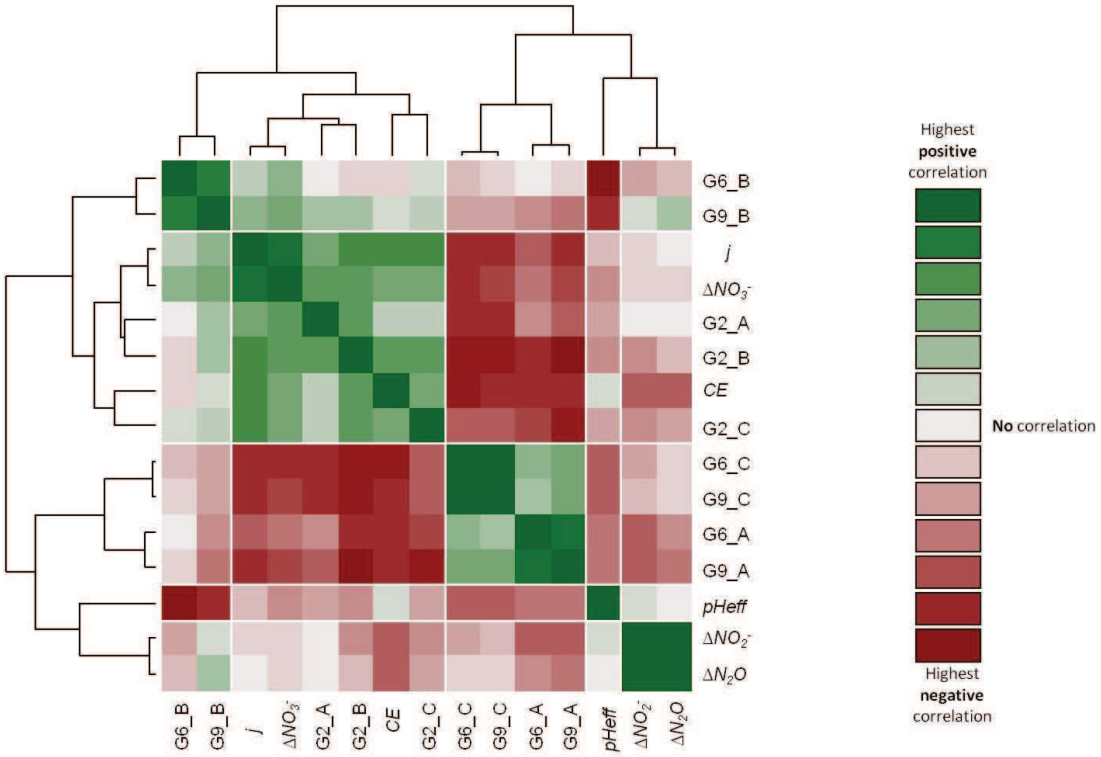

Figure S4. Correlation of the most abundant subcommunities G2, G6 and G9 with reactor performance using Spearman's rank correlation in the whole monitored period. Strong positive correlation is indicated by color red. Strong negative correlation is indicated by blue. The different gates have been labeled as G*X*_*Y*, where: *X* = gate number and *Y* = sampling port. Reactor performance included: pH at cathode effluent (*pHeff*), current density (*j*), coulombic efficiency (*CE*) and nitrate, nitrite and nitrous oxide consumption rates (ΔNO_3^-, ΔNO_2^- and ΔN_2O, respectively).

Table S10. Correlation of SP-A gates with reactor performance using the whole dataset. The different gates have been labeled as G*X*_*Y*, where: *X* = gate number and *Y* = sampling port. Reactor performance data included: pH at cathode effluent (pHeff), current density (Current_den), coulombic efficiency (*CE*) and nitrate, nitrite and nitrous oxide consumption rates (ΔNO_3^-, ΔNO_2^- and ΔN_2O, respectively). Green colored indicates positive correlations higher than 0.4.

	Current_den	ΔNO_3^-	ΔNO_2^-	ΔN_2O	*CE*
Current_den	1.0	0.9	0.2	0.2	0.8
ΔNO_3^-	0.9	1.0	0.2	0.2	0.6
ΔNO_2^-	0.2	0.2	1.0	0.9	-0.2
ΔN_2O	0.2	0.2	0.9	1.0	-0.2
CE	0.8	0.6	-0.2	-0.2	1.0
pHeff	0.1	0.0	0.3	0.2	0.3
G1_A	-0.7	-0.6	-0.3	-0.4	-0.4
G2_A	0.6	0.7	0.2	0.2	0.4
G3_A	-0.3	-0.2	-0.5	-0.6	-0.1
G4_A	0.2	0.1	0.4	0.5	0.0
G5_A	-0.4	-0.4	-0.2	-0.2	-0.1
G6_A	-0.2	-0.2	-0.2	-0.1	-0.3
G7_A	-0.4	-0.4	-0.2	-0.2	-0.1
G8_A	-0.5	-0.4	-0.1	-0.2	-0.3
G9_A	-0.4	-0.3	-0.2	-0.2	-0.4
G10_A	0.2	0.1	0.4	0.4	0.0
G11_A	0.0	0.1	0.5	0.3	-0.2
G12_A	0.1	0.1	-0.3	-0.2	0.1
G13_A	-0.2	-0.2	0.1	0.1	-0.1
G14_A	0.1	0.1	-0.2	-0.2	0.2
G15_A	-0.2	-0.2	0.0	-0.1	0.0
G16_A	0.0	0.2	-0.1	-0.3	-0.1
G17_A	-0.5	-0.4	-0.3	-0.3	-0.6
G18_A	-0.1	0.0	-0.4	-0.4	-0.1
G19_A	0.2	0.1	0.5	0.5	0.1
G20_A	-0.6	-0.5	0.0	-0.1	-0.3
G21_A	0.2	0.0	0.4	0.5	0.0

Table S11. Correlation of SP-B gates with reactor performance using the whole dataset. The different gates have been labeled as G*X_Y,* where: *X* = gate number and *Y* = sampling port. Reactor performance data included: pH at cathode effluent (pHeff), current density (Current_den), coulombic efficiency (*CE*) and nitrate, nitrite and nitrous oxide consumption rates (ΔNO_3^-, ΔNO_2^- and ΔN_2O, respectively). Green colored indicates positive correlations higher than 0.4.

	Current_den	ΔNO_3^-	ΔNO_2^-	ΔN_2O	*CE*
G1_B	-0.4	-0.4	-0.2	-0.3	0.0
G2_B	0.8	0.7	0.0	0.1	0.7
G3_B	-0.3	-0.3	-0.5	-0.5	0.0
G4_B	0.0	-0.1	0.2	0.1	0.0
G5_B	-0.3	-0.3	0.0	-0.1	0.1
G6_B	0.4	0.5	0.0	0.1	0.1
G7_B	-0.4	-0.3	-0.2	-0.4	-0.1
G8_B	0.1	-0.1	0.5	0.6	-0.1
G9_B	0.5	0.6	0.3	0.5	0.3
G10_B	-0.3	-0.1	0.0	-0.2	-0.2
G11_B	-0.2	-0.1	0.1	-0.1	-0.2
G12_B	0.1	0.3	0.1	0.1	-0.2
G13_B	-0.1	0.0	0.0	-0.2	0.0
G14_B	-0.1	0.1	-0.1	-0.3	-0.1
G15_B	-0.1	-0.1	0.0	-0.2	0.1
G16_B	0.2	0.4	-0.4	-0.5	0.2
G17_B	-0.4	-0.4	-0.4	-0.4	-0.4
G18_B	-0.2	-0.2	-0.6	-0.6	-0.1
G19_B	0.0	0.1	0.2	0.0	0.0
G20_B	-0.5	-0.5	0.3	0.3	-0.5
G21_B	-0.1	-0.1	0.1	0.0	0.0

Table S12. Correlation of SP-C gates with reactor performance using the whole dataset. The different gates have been labeled as G*X*_*Y*, where: *X* = gate number and *Y* = sampling port. Reactor performance data included: pH at cathode effluent (pHeff), current density (Current_den), coulombic efficiency (*CE*) and nitrate, nitrite and nitrous oxide consumption rates (ΔNO_3^-, ΔNO_2^- and ΔN_2O, respectively). Green colored indicates positive correlations higher than 0.4.

	Current_den	ΔNO_3^-	ΔNO_2^-	ΔN_2O	*CE*
G1_C	-0.4	-0.3	-0.3	-0.5	0.0
G2_C	0.7	0.6	-0.1	0.0	0.6
G3_C	-0.2	-0.3	-0.7	-0.6	0.2
G4_C	0.0	-0.1	0.1	0.2	-0.1
G5_C	0.3	0.3	0.4	0.2	0.2
G6_C	-0.4	-0.3	-0.1	0.1	-0.4
G7_C	-0.3	-0.4	-0.4	-0.4	0.1
G8_C	-0.3	-0.2	0.1	0.0	-0.2
G9_C	-0.4	-0.3	0.0	0.1	-0.4
G10_C	0.0	0.0	-0.1	-0.1	0.2
G11_C	0.0	-0.1	-0.1	-0.1	0.1
G12_C	0.1	0.1	0.2	0.3	-0.1
G13_C	-0.1	-0.3	-0.2	-0.1	0.2
G14_C	-0.2	-0.3	0.0	0.0	-0.2
G15_C	-0.2	-0.3	-0.4	-0.4	0.2
G16_C	0.4	0.5	-0.2	-0.2	0.2
G17_C	-0.2	-0.2	-0.5	-0.4	-0.3
G18_C	0.0	0.0	-0.7	-0.6	0.1
G19_C	-0.1	-0.2	-0.1	0.0	-0.2
G20_C	-0.3	-0.2	0.4	0.2	-0.3
G21_C	0.2	0.1	0.4	0.4	0.1

Table S13. Gates with positive correlations higher than 0.4 to reactor performance using the whole dataset. The different gates have been labeled as G*X*_*Y*, where: *X* = gate number and *Y* = sampling port. Reactor performance data included: current density (Current_den), coulombic efficiency (*CE*) and nitrate, nitrite and nitrous oxide consumption rates (ΔNO_3^-, ΔNO_2^- and ΔN_2O, respectively).

Current_den		ΔNO_3^-		ΔNO_2^-		ΔN_2O		*CE*	
G2_A	0.6	G2_A	0.7	G4_A	0.4	G4_A	0.5	G2_A	0.4
G2_B	0.8	G2_B	0.7	G10_A	0.4	G10_A	0.4	G2_B	0.7
G6_B	0.4	G6_B	0.5	G11_A	0.5	G19_A	0.5	G2_C	0.6
G9_B	0.5	G9_B	0.6	G19_A	0.5	G21_A	0.5		
G2_C	0.7	G16_B	0.4	G21_A	0.4	G8_B	0.6		
G16_C	0.4	G2_C	0.6	G8_B	0.5	G9_B	0.5		
		G16_C	0.5	G5_C	0.4	G21_C	0.4		
				G20_C	0.4				
				G21_C	0.4				

S9: Dynamics on G2 cell abundance organized through nitrate consumption rate.

Table S14. G2 cell abundance dynamics at SP-A, SP-B and SP-C organized through nitrate consumption rate. Other parameters of reactor performance are also shown organized through nitrate consumption rate.

ΔNO_3^-	G2 cell abundance (%)			Sampling day	Current density	ΔNO_2^-	ΔN_2O
($mgN \cdot L^{-1}_{NCC} \cdot d^{-1}$)	SP-A	SP-B	SP-C	(day)	($mA \cdot L^{-1}_{NCC}$)	($mgN \cdot L^{-1}_{NCC} \cdot d^{-1}$)	($mgN \cdot L^{-1}_{NCC} \cdot d^{-1}$)
14.5	9.32	10.20	8.51	67	0.00	0.0	0.0
19.9	8.00	8.18	11.30	32	0.59	0.0	0.0
53.4	12.60	17.20	10.60	60	11.61	4.2	0.0
58.0	25.20	19.30	21.50	95	10.58	20.9	20.6
62.8	9.19	8.38	11.50	38	7.77	41.4	41.4
64.4	12.10	14.10	11.00	56	12.40	18.0	3.0
65.4	11.70	10.30	9.59	53	8.06	29.3	15.6
65.8	15.40	11.10	11.70	49	10.45	24.5	9.8
67.1	12.10	12.50	10.40	46	10.64	24.5	10.4
78.8	13.90	10.10	11.50	42	10.53	38.7	38.7
97.3	27.90	20.30	15.10	104	22.58	43.8	43.6
99.5	10.10	23.40	24.10	74	19.17	6.0	6.0
106.7	13.30	19.70	25.20	102	23.56	55.7	55.7
109.8	26.10	17.80	10.30	77	11.90	33.9	14.1
122.4	19.00	18.60	27.50	84	25.02	0.0	0.0
124.2	26.80	21.30	21.60	70	21.47	0.0	0.0
128.7	27.30	30.50	22.90	88	23.31	8.3	8.0
132.2	18.30	16.10	11.90	63	22.01	0.0	0.0
155.5	31.60	22.00	14.90	97	23.80	52.7	52.2
157.1	22.50	16.20	26.30	82	25.04	19.0	5.0

S10: Contribution of *Thiobacillus* sp. according to T-RFLP analysis of the samples taken directly from the cathode volume.

Table S15. Contribution of the terminal restriction fragment affiliated to *Thiobacillus* sp. in the complete community based on T-RFLP. Data shown in percentage (%).

Stress-test	Day	SP-A	SP-B	SP-C
ST-1	**31**	0	0	0
ST-2	**45**	23	6	4
ST-3	**59**	15	23	10
ST-4	**62**	15	19	11
ST-5	**66**	5	3	2
ST-4	**69**	26	23	12
ST-4	**83**	30	33	25
ST-6	**95**	30	10	15
ST-7	**104**	54	10	14

References

(1) Thieme Chemistry (Hrsg.): *RÖMPP Online - Version 3.5*. Georg Thieme Verlag KG. Stuttgart **2009**.

(2) Ansys. Ansys fluent theory guide. Inc Northbrook IL**. 2009**. 49–53.

Chapter 7. Extracellular electron transfer of biocathodes: Revealing the potentials for nitrate and nitrite reduction of denitrifying microbiomes dominated by *Thiobacillus* sp.

N. Pous [a], C. Koch [b], J. Colprim [a], S. Puig [a], and F. Harnisch [b].

[a] Laboratory of Chemical and Environmental Engineering (LEQUiA), Institute of the Environment, University of Girona, C/ Maria Aurèlia Capmany, 69, Facultat de Ciències, E-17071 Girona, Spain.

[b] Helmholtz Centre for Environmental Research - UFZ, Department of Environmental Microbiology, Permoserstraße 15 I 04318 Leipzig, Germany.

Pous, N.; Koch, C.; Colprim, J.; Puig, S.; Harnisch, F. “Extracellular electron transfer of biocathodes: Revealing the potential for nitrate and nitrite reduction of denitrifying microbiomes dominated by Thiobacillus sp.” *Electrochemistry Communications*. Vol. 49 (Dec. 2014) : 93-97

http://dx.doi.org/10.1016/j.elecom.2014.10.011

http://www.sciencedirect.com/science/article/pii/S1388248114003294

Received 25 September 2014
Received in revised form 21 October 2014
Accepted 21 October 2014
Available online 29 October 2014

Abstract

The use of biocathodes in bioelectrochemical systems (BES) for the removal of nitrate in wastewater has become a vital field of research. However, the elucidation of the underlying extracellular electron transfer (EET) fundamentals of denitrifying biocathodes is still lacking, but required for a deeper BES understanding and engineering. This study reports for the first time on the thermodynamics of microbial cathodes for nitrate and nitrite reductions using microbial microcosms isolated from a running denitrifying BES. Cyclic voltammetry showed that nitrate and nitrite reduction proceed at − 0.30 V, and − 0.70 V vs. Ag/AgCl, respectively, by surface associated EET sites. The biocathodes were predominantly covered by *Thiobacillus* sp. contributing with a nitrate reductase (narG) to the major function of the microcosms. In conclusion, the EET characteristics of denitrifying biocathodes are demonstrated for the first time.

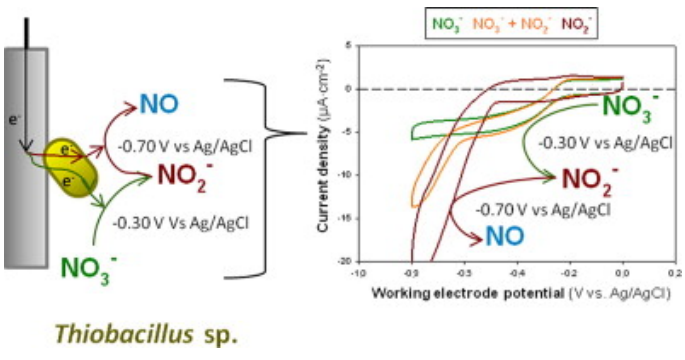

Keywords

Autotrophic biological denitrification; Bioelectrochemical system; Cyclic voltammetry; Microbial electrochemical technology; Nitrate reductase; Nitrogen removal

Chapter 8. Promoting high denitrification rates and disinfection in tubular denitrifying bioelectrochemical systems

N. Pous, S. Puig, M.D. Balaguer, and J. Colprim.

Laboratory of Chemical and Environmental Engineering (LEQUiA), Institute of the Environment, University of Girona, C/ Maria Aurèlia Capmany, 69, Facultat de Ciències, E-17071 Girona, Spain.

ABSTRACT

Denitrifying bioelectrochemical systems (BES) allows safe nitrate polluted groundwater treatment without chemicals requirements and at a competitive cost. However, the technology should be improved in terms of removal rate before scaling-up. In this study, we assessed a novel tubular design d-BES for short-time nitrate reduction and pre-disinfection of nitrate polluted groundwater. A nitrate consumption rate up to 700 $gN \cdot m^{-3}_{NCC} \cdot day^{-1}$ was reached without accumulation of nitrites at HRT of 36 minutes. Ti-MMO electrodes promoted hypochlorite in batch experiments, but negligible hypochlorite concentrations were detected under continuous-flow mode. Therefore, this study presents an innovative design for nitrate removal and pre-disinfection of water using denitrifying BES.

KEYWORDS

Biocathode, bioremediation, denitrification, microbial fuel cell, nitrogen.

1. INTRODUCTION

The presence of nitrate in different kinds of water (groundwater, surface water and wastewater) highlights the investigation of innovative technologies for its removal (Ghafari et al., 2008). Denitrifying bioelectrochemical systems (d-BES) could emerge as alternative for nitrate treatment (Clauwaert et al., 2007; Virdis et al., 2009), especially in waters with low organic carbon content as groundwater (Puig et al., 2012; Zhang and Angelidaki, 2013).

In d-BES, autotrophic denitrifying bacteria reduces nitrate using an electrode as the sole electron donor (Gregory et al., 2004; Pous et al., 2014).Denitrifying BES were usually operated feeding organic matter at the anode to serve as anodic electron donor (Clauwaert et al., 2007; Virdis et al., 2009). But nitrate-polluted groundwater can be treated at a competitive cost using water as anode electron donor and controlling the cathode potential (Pous et al., 2015). This converts d-BES into an organic-carbon-free technology to treat nitrates. Nevertheless, nitrate reduction rates obtained in d-BES should still be increased.

Our previous study suggested that denitrification performance could be promoted by operating the d-BES at low influent nitrate concentrations but at high flows (low hydraulic retention time (HRT)) (Pous et al., in preparation). The operation at low HRT

diminishes the reactor size, making the technology stronger. Moreover, the increase of water flux inside the BES compartments could improve the proton transport inside the BES. It would avoid the basification usually observed in cathodes of denitrifying BES and, consequently, increase the denitrifying performances (Cheng et al., 2012; Clauwaert et al., 2009).

Not only cathode performances needs to be improved, but also research on anode compartment is needed to increment the positive aspects of d-BES technology. In the anode, when a d-BES driven by external energy input is implemented, alternative oxidation processes could be investigated. In a biological process, a post-disinfection treatment would be desired for specific applications (e.g. for the usage of treated water as drinking-water). In this sense, the use of hypochlorite-evolving anodes could promote hypochlorite (and thus free chlorine) from chloride oxidation (equation 1). The *in situ* generated free chlorine could be used to disinfect the effluent water of the cathode compartment.

$$Cl^- + H_2O \xrightarrow{E^{o\prime}=+1.35V} 2H^+ + 2e^- + ClO^- \leftrightarrow 1/2Cl_2 + H_2O \text{ (eq. 1)}$$

In this work, we aimed to use a novel tubular d-BES for obtaining high nitrate reduction rates with *in situ* pre-disinfection. The cathodic nitrate reduction was coupled with a pre-disinfection process at the anode compartment, based on promoting chlorine through electrochemical hypochlorite evolution.

Chapter 9. Discussion

9.1. Denitrifying BES for nitrate-polluted groundwater treatment

The principal objective of applying denitrifying bioelectrochemical systems (d-BES) for nitrate-polluted groundwater was to obtain an effluent that accomplishes the standards of nitrates and nitrites (11.29 and 0.91 $mgN \cdot L^{-1}$, respectively (WHO, 2011)). Denitrifying BES are based on autotrophic denitrification, where microorganisms are able to use the electrode as an electron donor (Gregory et al., 2004; Park et al., 2005b). Before this thesis started, denitrifying BES was used for treating nitrate, nitrite and nitrous oxide in synthetic wastewater (Clauwaert et al., 2007a; Desloover et al., 2011; Puig et al., 2011c; Virdis et al., 2008). However, the application of denitrifying BES for nitrate-polluted groundwater had not yet been attempted.

Groundwater is characterized by its low ionic strength, which has a negative impact on BES performance (Logan et al., 2006). A lower conductivity implies a lower ion-transport, which raises the related overpotentials (membrane transport, ohmic and pH gradients), ending-up with lower overall performances. In a preliminary study carried out in LEQUiA, it was demonstrated that water with low ionic strength limited the denitrifying performance in a denitrifying bioelectrochemical system operated as MFC (Puig et al., 2012). By decreasing the conductivity from 4303 to 1277 $\mu S \cdot cm^{-1}$, the overpotentials related to ion-transport grew up to 80%. Consequently, the nitrate removed decreased by 44%. Hence, the treatment of nitrate-polluted groundwater using denitrifying BES was challenging. Nevertheless, the possibility of a biologic treatment, able to remove nitrates using an electrode as the sole electron donor, was exciting.

This PhD thesis assessed the use of denitrifying bioelectrochemical systems for nitrate-polluted groundwater treatment. It evaluated the electrochemical operation of the d-BES (MFC or MEC), the anode electron donor (and electrode material), the effect of the hydraulic retention time and new tools for monitoring reactor microbiomes of denitrifying BES (from the microbiological and electrochemical perspective).

9.1.1. Electrochemical operation for reaching a high effluent quality (NO_3^- and NO_2^-)

Two different electrochemical configurations were studied to treat nitrate-polluted groundwater:

i) Microbial fuel cell (MFC). It was the typical operation used for treating nitrates in BES (Clauwaert et al., 2007a; Virdis et al., 2008).

ii) Microbial electrolysis cell (MEC) using a three-electrode arrangement. It allowed the research to focus on one compartment without being limited by the anode performance (Cheng et al., 2012; Virdis et al., 2009).

Table 9.1 summarizes the results obtained. The d-BES operation, using MFC to treat nitrate-polluted groundwater, was evaluated in a 97-day study (Chapter 4, (Pous et al., 2013)). Acetate was used at the anode compartment as an electron donor and the denitrifying cathode was operated at an HRT of 11.9 h. Nitrate contained in groundwater was reduced at a maximum nitrate consumption rate of 47.6±2.4 $gN \cdot m^{-3}_{NCC} \cdot d^{-1}$. However, the nitrate content at the effluent (12.1±3.60 $mgN \cdot L^{-1}$) did not always meet the standards required for drinking-water (11.29 $mgN \cdot L^{-1}$) (WHO, 2011). Although the standards for nitrite were met (0.14±0.13 $mgN \cdot L^{-1}$), the electron balances suggested that high nitrous oxide emissions were produced (around 50% of nitrate reduced). Therefore, suitable treatment of nitrate-polluted groundwater could not be reached operating the d-BES as an MFC.

In a denitrifying MFC, the success of the treatment relies not only on the biocathodic performance, but also on the bioanode. In wastewaters containing both organic matter and nitrate, it is valuable to enhance both the organic matter anodic oxidation and nitrate cathodic reduction for concomitant electricity production. However, organic matter is scarce in nitrate-polluted groundwater. For this reason, the MEC was evaluated at a poised cathode potential (three-electrode arrangement). In this configuration, the nitrate treatment depends only on the biocathodic activity.

Firstly, different cathode potentials were studied to find a cathode potential that allow a suitable treatment of nitrate-polluted groundwater (i.e., meeting the drinking-water standards for nitrate and nitrite, meanwhile minimizing N_2O emissions) (Chapter 5, (Pous et al., 2015b)). A cathode potential range from +597 to -703 mV vs SHE was tested. An increase in nitrate consumption rate was observed at lower cathode potentials. The nitrate consumption rate increased from +597 to -403 mV vs SHE, where it stabilized. Moreover, the standards for nitrate were met below a cathode potential of -103 mV vs SHE. Destabilization of nitrite and nitrous oxide accumulations (denitrification intermediates) were seen at low cathode potentials. It was observed that nitrite and nitrous oxide were reduced at a lower rate than nitrate at low cathode potentials, ending-up with nitrite and nitrous oxide accumulations at cathode potentials lower than -303 and -203 mV vs SHE, respectively. Hence, a range of cathode potentials between -103 and -203 were considered as suitable for nitrate-polluted groundwater treatment (Patent WO/2014/082989 (Colprim et al., 2014)). At -123 mV vs SHE, the highest nitrate conversion (93.9%) to N_2 was found at a nitrate consumption rate of 66.4±1.0 $gN \cdot m^{-3}_{NCC} \cdot d^{-1}$, without accumulation of nitrites and a low N_2O emission of 6.1±1.1% of removed nitrate.

Previously, two articles had reported the effect of the cathode potential on nitrate consumption performance using synthetic wastewater (Cheng et al., 2012; Virdis et al., 2009). Both showed an increase in denitrifying performance as the cathode potential was lowered, until a minimum cathode potential of -200 mV vs SHE (Virdis et al., 2009) and -400 mV vs SHE (Cheng et al., 2012). The outcome obtained in this PhD thesis revealed: i) the suitable cathode potentials for treating real nitrate-polluted groundwater; ii) a larger range of cathode potentials (from +597 to -703 mV vs SHE) and iii) the effect of the cathode potential not only on nitrate consumption, but also nitrite and nitrous oxide reduction (i.e., the entire denitrifying pathway).

The technologies that would compete with denitrifying BES for treating nitrate-polluted groundwater are based on the separation principle or on the nitrate

conversion to dinitrogen gas. It has to be mention that, up to now, only the separation-based technologies reverse osmosis, electrodialysis and ion exchange are considered as suitable treatment technologies for nitrate contaminated groundwater (EPA, 2006). In order to evaluate the d-BES technology and compare its performance with the existing technologies, an energetic analysis was performed considering the operational energy demand of the system (Table 9.1.). The operational cost related to energy demand was calculated from the Gibbs free energy and the specific power consumption (Ali et al., 2010). For these calculations, the measured cell voltage and current were used. At a poised cathode potential of -123 mV vs SHE (test 12 of Chapter 5), the estimated energy demand of the d-BES was between 0.38 and 0.20 $kWh \cdot m^{-3}_{treated}$ ($0.68 \cdot 10^{-2}$ and $1.27 \cdot 10^{-2}$ $kWh \cdot gN_{removed}^{-1}$).

The electricity demand of the d-BES is similar to the values reported for separation-based technologies, such as electrodialysis (between 0.04 and 1.32 $kWh \cdot m^{-3}_{treated}$ (El Midaoui et al., 2002; Twomey et al., 2010) or reverse osmosis (between 1.03 and 2.09 $kWh \cdot m^{-3}_{treated}$ (Twomey et al., 2010)). Positively, with similar energy requirements, the denitrifying BES was able to diminish the nitrate content in groundwater below to its guideline value (WHO, 2011) without producing toxic products (NO_2^- and NH_4^+) and with low emission as N_2O (6.1±1.1% of removed nitrate). Therefore, in the d-BES nitrate is most probably converted to dinitrogen gas or assimilated by bacteria.

When considering technologies able to biologically reduce NO_3^- to N_2, two groups can be distinguished: i) without chemical electron donor dosing (biofilm-electrode reactor (BER) (Sakakibara et al., 2001)) or ii) with chemical electron donor dosing (organic matter- or sulfur- based denitrification (McAdam et al., 2008; Wan et al., 2009; Zhao et al., 2011; Zhou et al., 2007).

In the BER presented by Sakakibara and co-workers (2001), an external power input was used to control the cell voltage to produce hydrogen in the cathode, which was subsequently used by bacteria to reduce nitrates. Although a power input is also applied in the denitrifying BES operated at a poised cathode potential, no H_2 production was detected at -123 mV vs SHE. Hence, biologic reduction of

nitrate at -123 mV vs SHE was not mediated through hydrogen oxidation. According to results, the difference on the controlling system (control of the cathode potential or of the cell voltage) implied a control on nitrate reduction end-products and a lower energy consumption in the d-BES (0.68·10-2 and 1.27·10-2 kWh $gN\text{-}NO_3^-{}_{removed}^{-1}$) with respect to the BER (7.00·10-2 kWh $gN\text{-}NO_3^-{}_{removed}^{-1}$ (Sakakibara et al., 2001)).

When comparing the technologies where chemical electron donors as sulfur (Wan et al., 2009) or organic matter (McAdam et al., 2008; Zhao et al., 2011; Zhou et al., 2007) are supplemented, the denitrifying BES operated at a poised cathode potential was also competitive. Despite the dose of chemical electron donors, similar/lower energy consumption was observed in all cases, with the only exception of the system proposed by Zhao and co-workers (2011), which presented a significantly low energy demand. Nevertheless, this system implied a dose of methanol, which would have to be completely removed before introducing the groundwater into the drinking-water supply system.

It is worth to mention that technologies able to abiotically reduce nitrates are also under investigation, such as zero valent iron (Fu et al., 2014) or electrocatalytic nitrate reduction (Duca et al., 2012). These technologies present the advantage of allowing nitrate reduction without the external care required for biological systems and could sustain nitrate treatment in those waters where life is restricted, as in nuclear wastes (Duca et al., 2012). Nevertheless, they present some challenges. In the case of zero valent iron, nitrate is normally converted to NH_4^+, which needs a post-treatment. It also requires the dose of Fe(0), which is released as Fe(II) or Fe(III) due to the oxidation process (such iron release needs to be controlled as well) (Fu et al., 2014). On the contrary, d-BES allows nitrate conversion without generating toxic products as nitrite or ammonium and no dosing of external chemicals is required since the electron donor is the cathode electrode itself.

In the case of electrocatalytic nitrate reduction, expensive catalysts are required as rhodium or platinum (Duca et al., 2012) while d-BES uses microorganisms, which can be considered as a cheap and self-regenerating catalyst. Moreover, different

nitrate reducing pathways can be observed depending on electrode material; being preferent the conversion to ammonium or nitrous oxide. Nitrous oxide is usually not reduced in electrocatalytic processes since few catalysts are able to catalyse N_2O conversion to N_2 before nitrous oxide desorbs from the electrode surface (Duca et al., 2012), while nitrous oxide can be correctly reduced in a denitrifying biocathode (Desloover et al., 2011; Pous et al., 2015b; Virdis et al., 2009b).

Table 9.1. Comparison of energy consumption and characteristics for nitrate- polluted groundwater treatment for denitrifying BES (Chapter 5 - test 12), conventional treatments and other technologies found in the bibliography (adapted from Chapter 5, Table 3). In references where energy consumption was not directly mentioned, it was calculated from Gibbs free energy and Specific power consumption. Legend: Not mentioned (n.m.).

Reference	Energy consumption (kWh $gN\text{-}NO_3^-{}_{removed}{}^{-1}$)		Energy consumption (kWh $m^{-3}{}_{treated}$)		Nitrate removal pathway	Addition of chemicals?
	From Gibbs free energy	Specific power consumption (Ali et al., 2010)	From Gibbs free energy	Specific power consumption (Ali et al., 2010)		
Denitrifying BES (test 12 of Chapter 5)	$1.27 \cdot 10^{-2}$	$0.68 \cdot 10^{-2}$	0.38	0.20	Reduction to N_2	No
3D electrode biofilm reactor (Zhou et al., 2007)	$3.35 \cdot 10^{-2}$	$1.46 \cdot 10^{-2}$	1.01	0.44	Reduction to N_2	Yes, ethanol
Biofilm-electrode reactor (Zhao et al., 2011)	$0.16 \cdot 10^{-2}$		0.08		Reduction to N_2	Yes, methanol
Biofilm electrode reactor + sulfur denitrification (Wan et al., 2009)	$4.79 \cdot 10^{-2}$	$1.50 \cdot 10^{-2}$	1.00	0.31	Reduction to N_2	Yes, sulphur and anthracite granules
Biofilm- electrode reactor (Sakakibara et al., 2001)	$7.00 \cdot 10^{-2}$		1.12		Reduction to N_2	No
Membrane Bioreactor (McAdam et al., 2008)	$2.04 \cdot 10^{-2}$		0.30		Reduction to N_2	Yes, organic matter source
Electrodialysis (Ortiz et al., 2008)	$4.95 \cdot 10^{-2} – 1.01 \cdot 10^{-2}$		0.92 – 1.69		Separation in a waste brine	No
Electrodialysis (El Midaoui et al., 2002)	$0.40 \cdot 10^{-2} – 0.80 \cdot 10^{-2}$		0.04 – 0.11		Separation in a waste brine	No
Electrodialysis (Twomey et al., 2010)	n.m.		0.69 – 1.32		Separation in a waste brine	No
Reverse Osmosis (Twomey et al., 2010)	n.m.		1.03 – 2.09		Separation in a waste brine	No

As a consequence of both denitrifying performance and competitive cost, the operation at a poised cathode potential of -123 mV vs SHE was chosen for further studies.

The cathode potential of -123 mV vs SHE was imposed during a 96 day treatment of nitrate-polluted groundwater with an influent nitrate concentration of 33.11±2.55 $mgN \cdot L^{-1}$ and conductivity of 918±31 $\mu S \cdot cm^{-1}$ (Chapter 5, (Pous et al., 2015b)). Two cathodic HRT (11 h and 5 h) were assessed. Nearly complete removal of influent nitrate (96.5±1.7 %) was reached at a nitrate consumption rate of 65.4±4.9 $gN \cdot m^{-3}_{NCC} \cdot d^{-1}$, without accumulation of NO_2^- or N_2O at an HRT of 11 h. At a cathodic HRT of 5 h, a nitrate consumption rate of 112.9±8.0 $gN \cdot m^{-3}_{NCC} \cdot d^{-1}$ was reached. The nitrate and nitrite standards were met and N_2O emissions of 6.4±8.2 % were detected. Hence, long-term experiments confirmed that a poised cathode potential of -123 mV vs SHE can suitably treat nitrate-polluted groundwater.

In order to compare the denitrifying performances with published results, synthetic wastewater was also used in certain studies (Chapters 6 and 8).

Using the rectangular BES, the cathode was also fed with synthetic wastewater with a conductivity of 5293±155 $\mu S \cdot cm^{-1}$, influent nitrate concentration of 200 $mgN \cdot L^{-1}$ and HRT of 16.8 h (Chapter 6). The best stable denitrifying performance was a nitrate consumption rate of 97.4±9.4 $gN \cdot m^{-3}_{NCC} \cdot d^{-1}$ with 1.2±1.6 % of reduced nitrate accumulated as NO_2^- and 13.4±13.8 % of N_2O emissions (chapter 6). In this case, denitrifying activities higher than those when using real nitrate-polluted groundwater were not observed.

The application of computational fluid dynamics to the rectangular reactor revealed heterogeneity (Chapter 6). It could imply the presence of zones of low activity inside the cathode compartment, lowering the overall removal capacity. For this reason, the BES was modified to a new tubular design. This configuration reached the highest nitrate consumption rate at an HRT of 0.6 h (the lowest studied), with a mean value of 699.8±7.0 $gN \cdot m^{-3}_{NCC} \cdot d^{-1}$. Nitrite was not accumulated and N_2O emissions of 33.3±9.5 % were detected. By lowering the HRT, the N_2O

emission was lowered from 77.0±10.6 % to 33.3±9.5 %. Therefore, the use of a tubular BES and operating at low HRT increased the nitrate consumption rates roughly 600 %, without observing nitrite accumulation.

Table 9.2. Denitrification stable performances at different conditions. Legend: * = estimated value.

Electrochemical configuration	**MFC**	**MEC with poised cathode potential at -123 mV vs SHE**		
BES geometry	Rectangular	Rectangular	Rectangular	Tubular
Water	Real groundwater		Synthetic wastewater	
Conductivity ($\mu S \cdot cm^{-1}$)	955±121	918±31	5293±155	4199±282
HRT (h)	11.9	5.0	16.8	0.6
NO_3^- consumption rate ($gN \cdot m^{-3}_{NCC} \cdot d^{-1}$)	47.6±2.4	112.9±8.0	97.4±9.4	699.8±7.0
NO_2^- accumulation (% reduced NO_3^-)	0.6±0.6	0.0±0.0	1.2±1.6	0.0±0.0
N_2O emissions (% reduced NO_3^-)	50*	6.4±8.2	13.4±13.8	33.3±9.5
Reference	Chapter 4 (Pous et al., 2013)	Chapter 5 (Pous et al., 2015b)	Chapter 6	Chapter 8

Table 9.3 summarizes denitrifying performances reported for denitrifying BES and for biologic-based technologies that are also being developed for nitrate-polluted treatment.

Different nitrate-consumption rates have been observed:

i) MFC procedure: Clauwaert et al. (2009) reached 500 $gN \cdot m^{-3}_{NCC} \cdot d^{-1}$ using a pH control at the cathode compartment and Zhang and Angelidaki (2013) reached 483 $gN \cdot m^{-3}_{NCC} \cdot d^{-1}$.

ii) MEC with a poised cathode potential: At a cathode potential of -100 mV vs SHE, Virdis et al. (2009) reported 163 $gN \cdot m^{-3}_{NCC} \cdot d^{-1}$.

iii) MEC with a fixed current: Van Doan et al. (2013) observed a 39.6 $gN \cdot m^{-3}_{NCC} \cdot d^{-1}$ and Park et al. (2005b) an impressive 7608 $gN \cdot m^{-3}_{NCC} \cdot d^{-1}$.

Therefore, nitrate consumption rates observed in this thesis were on the level of the highest previously reported in denitrifying BES (when a tubular reactor operated at an HRT of 0.6 h and a poised cathode potential of -123 mV vs SHE).

Other biologic-based technologies are being developed for nitrate-polluted groundwater treatment. The heterotrophic removal of nitrates in groundwater using membrane bioreactors has also been evaluated. Wasik et al. (2001) reported a value of 1700 $gN \cdot m^{-3} \cdot d^{-1}$. Hydrogenotrophic denitrification presents a wide range of efficiencies when H_2 is supplied. Zhang et al., (2009) reported 404 $gN \cdot m^{-3} \cdot d^{-1}$, while Ergas and Reuss (2001) found 770 $gN \cdot m^{-3} \cdot d^{-1}$. When H_2 is electrochemically produced inside the reactor, Prosnansky et al. (2002) achieved a rate of 394 $gN \cdot m^{-3} \cdot d^{-1}$. Additionally, sulfur based denitrification have presented rates of 100 $gN \cdot m^{-3} \cdot d^{-1}$ (Darbi et al., 2003). Hence, the reported values in denitrifying bioelectrochemical systems are remarkable compared to competing biologic-based technologies. The use of an electrode as an electron donor for nitrate reduction can achieve nitrate consumption rates similar to those using inorganic compounds as an electron donor (as H_2 or sulfur).

Overall, it can be stated that the electrochemical configuration of the denitrifying BES was demonstrated to be a key factor in the successful treatment of nitrate-polluted groundwater. By improving the electrochemical configuration, the standards, in terms of nitrates and nitrites, can be met with low nitrous oxide emissions.

Table 9.3. Denitrifying performance using different operational modes of denitrifying BES or competing technologies. Legend: n.m. = not mentioned.

Reference	Operation mode		Water	Max. nitrate consumption rate ($gN \cdot m^{-3} \cdot d^{-1}$)	NO_2^- accumulation (%)	N_2O emission (%)
Zhang and Angelidaki (2012)	MFC		Water in eutrophic lake	3.9	0	15.3-18.2
Zhang and Angelidaki (2013)	MFC		Real groundwater	483	0	n.m.
Clauwaert et al. (2007a)	MFC		Synthetic wastewater	146	0	Negligible
Clauwaert et al. (2009)	MFC with pH control		Synthetic wastewater	503	0	n.m.
Virdis et al. (2009)	Poised cathode potential	-100 mV vs SHE	Synthetic wastewater	163	0	29.1
		-200 mV vs SHE	Synthetic wastewater	142	0	17.0
Cheng et al. (2012)	Poised cathode potential (-600 mV vs SHE)		Synthetic wastewater	151	n.m.	n.m.
Van Doan et al. (2013)	Fixed current		Synthetic wastewater	40	0	70
Park et al. (2005b)	Fixed current		Synthetic wastewater	7608	0	n.m.
Wan et al. (2009)	Fixed current + sulfur based denitrification		Real groundwater	240	0	n.m.
Zhao et al. (2011)	Fixed current + heterotrophic denitrification with methanol		Synthetic groundwater with methanol	146	0	n.m.
Prosnansky et al. (2002)	Hydrogenotrophic by electrochemical production of H_2		Synthetic groundwater	394	0	n.m.
Zhang et al. (2009)	Hydrogenotrophic by H_2 supply		Synthetic groundwater	414	0	n.m.
Ergas and Reuss (2001)	Hydrogenotrophic by H_2 supply		Real groundwater	770	0	n.m.
Darbi et al. (2003)	Sulfur based denitrification		Synthetic groundwater	100	< 2.4	n.m.
Wasik et al. (2001)	Heterotrophic denitrification in MBR		Synthetic groundwater	1700	<0.9	n.m.

9.1.2. Electrochemical operation for decreasing N_2O emissions

Although nitrous oxide is not regulated in drinking-water, its emissions in the denitrifying process should be avoided due to its potential as a greenhouse gas (Forster et al., 2007). In the field of denitrifying bioelectrochemical systems, nitrous oxide emissions have been a matter of inconsistency (Table 9.3). Desloover et al. (2011) demonstrated the bioelectrochemical reduction of N_2O to N_2 in a biocathode at a poised cathode potential. Cathode potentials between -200 and 0 mV vs SHE were considered to be optimum, and high nitrous oxide consumption rates (between 760 and 1830 $gN \cdot m^{-3}_{NCC} \cdot d^{-1}$) were achieved. Hence, N_2O can also be reduced bioelectrochemically. In the present thesis, different N_2O emissions have been observed, dependent upon the electrochemical configuration of the denitrifying BES.

When the d-BES was operated as MFC (Chapter 4, (Pous et al., 2013)), it was estimated that nitrous oxide emissions of reduced nitrate were 50%. In denitrifying BES operated as MFC, lower N_2O emissions have been reported. Puig et al. (2012) estimated a nitrous oxide emission of reduced nitrate of 4% at a conductivity of 4303 $\mu S \cdot cm^{-1}$ and a maximum of 22% at 1768 $\mu S \cdot cm^{-1}$. Zhang and Angelidaki (2012) estimated N_2O emissions between 15.3 and 18.2% when treating water from a eutrophic lake. The difference relies on the performance of the anode compartment and the medium characteristics.

On the contrary, when a poised cathode potential was used, the N_2O emissions could be controlled (Chapter 5, (Pous et al., 2015b)). Different nitrous oxide emissions were observed at the different cathode potentials. By lowering the cathode potential from +597 to -203 mV vs SHE, N_2O emissions decreased. But at cathode potentials lower than -203 mV vs SHE, N_2O emissions increased. A minimum emission of 6.1 % was observed at a cathode potential of -123 mV vs SHE, and N_2O concentrations at the effluent could be lowered below the detection limit when the cathode potential was poised for a longer period of time (48 days). This thesis evaluated a wider range of cathode potentials when compared to previous

works (Virdis et al., 2009). Virdis et al. (2009) observed that N_2O emissions decreased from 52.9 to 17.0 % by decreasing the cathode potential from +100 to -200 mV vs SHE when treating synthetic wastewater.

On the other hand, by operating a denitrifying BES at a fixed current, Van Doan et al. (2013) described nitrous oxide emissions up to 70 % using synthetic wastewater.

Hence, electrochemical operation of a denitrifying BES influences nitrous oxide emissions. The use of a poised cathode potential allows the control of N_2O emissions. Two hypotheses can be formulated to explain the better performance compared to the operation as MFC or the operation as MEC under fixed current: i) electron competition and ii) bacterial energy gain.

In a denitrifying process, four reduction steps are involved, and thus, four different enzymes. The electron competition between denitrifying enzymes has been demonstrated in conventional heterotrophic denitrification processes, resulting in higher nitrous oxide emissions (Lu and Chandran, 2010; Pan et al., 2013). When operating as a MEC at a fixed current, a limited number of electrons are continuously delivered to the cathode. While under MFC operation, the electron flux to the cathode is limited by the bioanodic activity. Thus, in both cases, a limited amount of electrons are available for cathodic denitrifying bacteria, which could promote electron competition. On the contrary, when operating with a poised cathode potential, an unlimited amount of electrons are available for biocathodic denitrifying bacteria. In consequence, the reductive process is not limited and lower N_2O emissions are observed.

However, shifts in N_2O emissions were detected at different cathode potentials, indicating that thermodynamics are also playing a key role. Here is where the bacterial energy gain becomes important. At high cathode potentials, low energy gain is available for bacteria (Schröder, 2007). At cathode potentials higher than 0 mV vs SHE, Desloover et al. (2011) observed lower nitrous oxide removal rates and higher N_2O emissions. This is in agreement with the results presented in this thesis

(Pous et al., 2015b). While at cathode potentials between 0 and -200 mV vs SHE, the energy gain is enlarged, N_2O is reduced at higher rates (Desloover et al., 2011) and less N_2O is emitted in denitrifying BES (Pous et al., 2015b; Virdis et al., 2009). In this scenario, operating in MFC mode can also be threatened, since it requires high cathodic potential to drive the process.

Therefore, the use of a poised cathode potential has been observed as being a key parameter for controlling N_2O emissions in a denitrifying BES.

9.1.3. Anode electron donor and anode material

Throughout thesis, a plethora of anode electron donors (acetate, water and chloride) and anode materials (granular graphite, stainless steel and titanium) were evaluated (Table 9.4). The objective was to investigate how the anode compartment can improve the viability of d-BES for nitrate-polluted groundwater treatment.

Table 9.4. Anode electron donors used along this PhD thesis.

Electron donor	Oxidation reaction (redox potential at pH 7)	Electrode material	Catalysis	Reference
Acetate	E0' = -290 mV vs SHE	Graphite	Biotic	Chapters 4 and 5 (Pous et al., 2015b, 2013)
Water	E0' = +840 mV vs SHE	Graphite	Abiotic	Chapter 5 (Pous et al., 2015b)
		Stainless steel	Abiotic	Chapter 6
Chloride	E0' = +890 mV vs SHE	Ti-MMO	Abiotic	Chapter 8

In denitrifying BES, organic matter is commonly used as anode electron donor, usually in form of acetate (Clauwaert et al., 2007a; Virdis et al., 2009). Acetate is oxidized by anode-respiring bacteria, thereby delivering electrons to the anode electrode.

In this study, the use of acetate was evaluated for MFC (Chapter 4 (Pous et al., 2013)) and for MEC at a poised cathode potential (Chapter 5 (Pous et al., 2015b)). An excess of acetate was dosed at the anode compartment (three times the

stoichiometric requirements of acetate) to avoid limiting the cathodic denitrification.

Coulombic efficiencies below 20% were observed in the anode compartment regardless of the electrochemical configuration used (MFC or MEC with poised cathode potential). Either because of the excess of acetate (three times higher than the stoichiometric value to avoid limitations on denitrifying performance), or the low conductivity of groundwater, the coulombic efficiencies were lower than other values reported in literature for denitrifying BES. Zhang and Angelidaki (2013) observed anodic coulombic efficiencies of 59-70% by operating the d-BES as MFC for nitrate removal and desalination of groundwater. Virdis et al. (2009) observed *CEs* between 45.6 and 46.7% in an MEC operated at a poised cathode potential, but treating synthetic wastewater.

The low *CE*s indicated that a low percentage of the acetate consumed at the anode was used for transferring electrons to the cathode. Since groundwater does not contain organic matter, the treatment of nitrate-polluted groundwater would require an external dose of organic matter to the anode. Hence, the low coulombic efficiencies were directly related to a low economic viability of the process. When the d-BES is operated as MFC, the biological oxidation of acetate is essential for the overall performance, since it is a spontaneous process.

On the other side, when the BES is operated at a poised cathode potential, the performance of acetate oxidation does not affect the cathodic process, since it is supported by the external energy supply. If the anodic acetate oxidation does not fulfill the cathodic requirements of the current, the anode process switches to a more efficient oxidation.

In this thesis, when the d-BES was operated at a poised cathode potential and high currents were demanded, the anode catalysis switched from acetate to water oxidation (Chapter 5 (Pous et al., 2015b)). Under experimental conditions, the standard redox potential for acetate to carbon dioxide is -173±27 mV vs SHE, while the water oxidation to oxygen potential is +776±31 mV vs SHE. The change in anode

electron donor was detected by a sudden increase of the anode potential from -290±1 to +1010±38 mV vs SHE. If water was being used as the anode electron donor, the dose of acetate (or other organic carbon source) was no longer required. In consequence, the use of water free of organic matter at the anode compartment was evaluated. It would imply that groundwater treated at the cathode could be directly injected to the anode, and thus, the treatment would not require an addition of chemicals. Moreover, it would avoid possible acetate oxidation in the cathode compartment through the ion exchange membrane (Jung et al., 2007), which could affect water quality. A sustainable treatment of nitrate-polluted groundwater could be reached.

Three different electrode materials were evaluated to catalyze abiotic oxidation processes at the anode (graphite, stainless steel and Ti-MMO).

When either graphite (Chapter 5 (Pous et al., 2015b)) or stainless steel (Chapter 6) were used at the anode compartment without the presence of acetate, it was assumed that the oxidation of water to oxygen was occurring. Neither the use of graphite or stainless steel at the anode limited cathodic performance. Both materials were able to supply the electrons required for the biocathodic denitrification. However, a severe degradation of the anodic electrodes was observed in both cases. It suggested that oxidation of the electrode itself had been produced, rather than water oxidation to oxygen. Therefore, a periodical replacement of anode material would be needed if graphite or stainless steel were used.

Ti-MMO electrodes were seen as stable anode materials capable of supporting the biocathodic requirements of the current (Chapter 8). The Ti-MMO anodes are dimensionally stable anodes (DSA). Ti-MMO electrodes are able to promote chloride oxidation to hypochlorite (Tzedakis and Assouan, 2014), which ends-up generating free chlorine (equation 21). If the cathode effluent is fed into the anode compartment, it would allow a certain disinfection of cathodic bacteria that could have been detached from the cathode electrodes. For drinking-water purposes, it would reduce the requirements of chlorine dosing.

Other than in batch experiments, the production of free chlorine was demonstrated. Under continuous-flow conditions, free chlorine was not detected either because of its dilution or because of its consumption for disinfection or nitrite oxidation to nitrate. Nevertheless, no degradation of the Ti-MMO electrode was observed. Therefore, if an abiotic anode were to be used, Ti-MMO electrodes would be recommended over graphite or stainless steel.

9.2. Denitrifying microbiome

In a biological process, such as BES, the understanding of microorganisms involved is fundamental. However, the knowledge regarding microbial communities present in biocathodes of denitrifying bioelectrochemical systems is scarce. In consequence, in this PhD thesis, the microbial community in biocathodes has been analyzed several times using different techniques. Table 9.5 summarizes the predominant species.

The microbial community attached to graphite electrodes was analyzed through PCR-DGGE at the end of d-BES operation as MFC (Chapter 4 (Pous et al., 2013)). A microbial community was observed that dominated by *Betaproteobacteria*, especially by *Candidatus Nitrotoga arctica* (97%) and *Thauera* sp. (100%). The same analysis was conducted at the end of d-BES operation as MEC at a poised cathode potential of -123 mV vs SHE (Chapter 5 (Pous et al., 2015b)). It was observed that a microbial community dominated by the betaproteobacterium specie *Azovibrio restrictus* (98%) and the nitrospirae *Candidatus Nitrosospira defluvii* (100%) was present. Therefore, different species belonging to the same class were identified by operating under the two different electrochemical modes.

Although the PCR-DGGE analyses allowed for identification of the bacteria present inside the cathode, it did not allow for determination of bacterial roles in the process. This knowledge is fundamental for understanding and, consequently, operating denitrifying BES more efficiently. Moreover, denitrification is a complex process. It involves four reduction steps. Hence, the elucidation of which

microorganism (or group of microorganisms) is catalyzing each reaction is more relevant, but also more challenging.

For this reason, a goal was to reveal the structure-function relationship of a bioathodic denitrifying community (Chapter 6). To achieve this goal, cytometric fingerprinting using flow cytometry combined with T-RFLP was used (Koch et al., 2013a, 2013b). To the best of the author's knowledge, the application of flow cytometry had never been exploited in biocathodes of bioelectrochemical systems, but it had already been used for bioanodes (Harnisch et al., 2011). Additionally, the main aim of this thesis is the treatment of nitrate-polluted groundwater, and groundwater is restricting water for BES due to its low conductivity (Logan et al., 2006; Puig et al., 2012). For this reason, it was decided to use this technique in a denitrifying BES fed with synthetic water. Higher denitrification rates were expected, and thus the viability of flow cytometry could be better explored. The operational condition studied was a poised cathode potential of -123 mV vs SHE.

The identified microbial community was composed of 21 different subcommunities. Several of them presented no correlation with the bioelectrochemical process. It suggested that, from all the microbiome detected in a denitrifying biocathode, only some subcommunities were directly related to the bioelectrochemical denitrification. Results also suggested that different bacterial subcommunities were in charge of the different nitrate reduction steps to dinitrogen gas. A subcommunity mainly composed of the betaproteobacterium *Thiobacillus* sp. was mainly responsible for the nitrate reduction to nitrite. Nitrite and nitrous oxide reduction was catalyzed by a wider range of subcommunities.

Species of *Thiobacillus*, such as *Thiobacillus denitrificans*, are known as autotrophic denitrifiers and are able to use either ferrous iron (Fe^{2+}) (Hedrich et al., 2011; Straub et al., 2004, 1996), thiosulfate (Fernandez et al., 2008) or sulfide (Haaijer et al., 2012) as electron donors. Other microorganisms able to use Fe^{2+} as an electron donor, such as *Geobacter metallireducens* (Hedrich et al., 2011), are already known to use an electrode as an electron donor for nitrate reduction

(Gregory et al., 2004). Hence, *Thiobacillus* sp. could potentially perform bioelectrochemical reduction of nitrate.

Although the presence of *Thiobacillus* sp. had not been detected in denitrifying biocathodes before, its electroactivity had already been suggested (Kato et al., 2012). Kato et al. (2012) observed electrical currents between *Geobacter sulfurreducens* and *Thiobacillus denitrificans* through conductive minerals. It coupled acetate oxidation (by *Geobacter sulfurreducens*) and nitrate reduction (by *Thiobacillus denitrificans*). Therefore, the use of flow cytometry combined with T-RFLP allowed not only for analysis of the microorganism present in the biocathode per conventional techniques (as PCR-DGGE), but also allowed elucidation of which subcommunities were involved in bioelectrochemical denitrification.

Table 9.5. Predominant microorganisms found during the specific studies of this PhD thesis.

Electrochemical configuration	Molecular techniques	Phylum	Class	Order	Specie	Reference
MFC	PCR-DGGE	Proteobacteria	beta	Gallionellales	*Candidatus Nitrotoga arctica*	Chapter 4 (Pous et al., 2013)
				Rhodocyclales	*Thauera* sp.	
MEC with poised cathode potential of -123 mV vs SHE	PCR-DGGE	Proteobacteria	beta	Rhodocyclales	*Azovibrio restrictus*	Chapter 5 (Pous et al., 2015b)
				Nitrosomonadales	*Candidatus Nitrosospira defluvii*	
	Flow-cytometry and T-RFLP	Proteobacteria	beta	Hydrogenophilales	*Thiobacillus* sp.	Chapter 6
	T-RFLP	Proteobacteria	beta	Hydrogenophilales	*Thiobacillus* sp.	Chapter 7 (Pous et al., 2014)

Considering all results, it can be surmised that Proteobacteria-like species were enriched in the denitrifying biocathode regardless of the electrochemical operation applied (MFC or MEC at a poised cathode potential). A similar trend was observed in other denitrifying BES. Bacteria found in cathodes of denitrifying BES of different reported studies are shown in Table 9.6.

Research efforts have focused on analyzing the microorganisms present inside the biocathode after a certain operation time, and an enrichment of Proteobacteria-like species has been commonly observed in denitrifying biocathodes (Gregory et al., 2004; Park et al., 2006; Van Doan et al., 2013; Vilar-Sanz et al., 2013; Wrighton et al., 2010; Xiao et al., 2014). From them, orders of *Burkholderiales* (Park et al., 2006; Van Doan et al., 2013; Vilar-Sanz et al., 2013; Wrighton et al., 2010), *Rhizobiales* (Park et al., 2006; Vilar-Sanz et al., 2013; Wrighton et al., 2010) or *Xanthomonadales* (Gregory et al., 2004; Van Doan et al., 2013; Vilar-Sanz et al., 2013) have been observed in more than two studies. In systems where the denitrifying biocathode was coupled to an external nitrifying reactor (Virdis et al., 2008), species of phylum Firmicutes were also enriched (Wrighton et al., 2010), indicating that the coupling of the two processes lead to a more diverse community.

Table 9.6. Bacteria reported in denitrifying BES. Legend: A = autotrophic and H = heterotrophic.

Reference	Cathode medium	Electrochemical configuration	Phylum	Class	Order
Wrighton et al. (2010)	A	MFC	Proteobacteria	alpha	Rhizobiales
					Sphingomonadales
				beta	Burkholderiales
					Rhodocyclales
				delta	
				gamma	
Gregory et al. (2004)	A	MEC with poised cathode potential	Proteobacteria	delta	Desulfuromonadales
				gamma	Xanthomonadales
Park et al. (2006)	A	MEC with fixed current	Bacteroidetes	Flavobacteriia	Flavobacteriales
			Proteobacteria	alpha	Rhizobiales
					Sphingomonadales
				beta	Burkholderiales
				gamma	Enterobacteriales
Van Doan et al. (2013)	A	MEC with fixed current	Bacteroidetes	Flavobacteriia	Flavobacteriales
			Gemmatimonadetes	beta	Gemmatimonales
			Proteobacteria		Burkholderiales
				gamma	Aeromonadales
					Xanthomonadales
Cong et al. (2013)	H	MEC with fixed current	Bacteroidetes	Sphingobacteria	
			Proteobacteria	alpha	
				beta	Azoarcus
					Hydrogenophaga
					Thauera
Vilar-Sanz et al. (2013)	Either in A and H (but bacteria was found at different percentages)	MFC	Actinobacteria	Actinobacteridae	Actinomycetales
			Deinococcus	Deinococci	Thermales
			Proteobacteria	alpha	Rhizobiales
					Rhodobacterales
					Rhodospirillales
				beta	Burkholderiales
					Hydrogenophilales
					Nitrosomonadales
					Rhodocyclales
				gamma	Pseudomonadales
					Xanthomonadales
Wrighton et al. (2010)	Autotrophic cathode coupled to nitrifying reactor	MFC	Chloroflexi		
			Firmicutes	bacili	
				catabacter	
				clostridia	
				desulfotomaculum	
				mollicutes	
				symbiobacteria	

9.3. Extracellular electron transfer mechanism in a denitrifying biocathode

Regarding BES, a fundamental understanding is that of the extracellular electron transfer used by bacteria to transport the electrons from/to its cell to/from the electrode. It involves the transfer mechanism (direct or mediated electron transfer) and the thermodynamics of this process (redox potential at which the electron transfer takes place). Knowledge regarding biocathodic EET is scarce (Rosenbaum et al., 2011), but it is essential to characterize and consequently operate BES.

In this thesis, a new methodology for studying the extracellular electron transfer in biocathodes of BES was used (Chapter 7 (Pous et al., 2014)). Cathodic samples from a working d-BES (Chapter 6) were extracted to inoculate denitrifying microcosms. In microcosms, the smaller reactor size allowed a more sensitive electrochemical analysis. It is fundamental for studying autotrophic electroactive biofilms due to its lower biomass abundance compared to heterotrophic electroactive biofilms, which are the most studied in BES (Fricke et al., 2008; Srikanth et al., 2008).

Denitrifying microcosms were successfully grown, and electrochemically characterized. In the different microcosms, the same microbial composition was attached to the cathode electrode. The different cathodes were mainly composed of *Thiobacillus* sp., and its thermodynamics toward nitrate and nitrite reduction was elucidated. The biocathode presented a Nernstian current-potential dependency on nitrate and nitrite reduction. It was revealed that nitrate reduction to nitrite, considering the respective mid-point potentials, was catalyzed at -103 mV vs SHE (-0.30 V vs Ag/AgCl) and the further reduction of nitrite to nitric oxide at -503 mV vs SHE (-0.70 V vs Ag/AgCl).

From cytometric fingerprinting analyses (Chapter 6 and discussed in section 9.2), it was deduced that in the BES operated at a -123 mV vs SHE, a subcommunity, mainly composed of *Thiobacillus* sp., played a key role in nitrate reduction to nitrite. As demonstrated in microcosms, the reduction of NO_3^- by a biofilm mainly

composed of *Thiobacillus* sp. could be carried out from -103 mV vs SHE. But nitrite reduction was performed by a wider number of subcommunities, and *Thiobacillus* sp. was not predominant there.

Two hypotheses were formulated to explain the finding of the thermodynamics in nitrite reduction at -503 mV vs SHE in microcosms, when the reactor worked at a poised cathode potential of -123 mV vs SHE. i) The medium used to allow microorganism attachment in the microcosms was composed of NO_3^- and, therefore, bacteria able to catalyze nitrate were favored. ii) It was described that porous electrodes, as the graphite granules present in the BES, implied a heterogeneous distribution of the potential (Doherty et al., 1996), allowing both nitrate and nitrite reduction in the BES. Nevertheless, thermodynamics of the extracellular electron transfer mechanism in denitrifying biocathodes was explained. The methodology presented can be used to characterize biocathodes of reactor BES.

The reduction of nitrate at -103 mV vs SHE (-0,30 V vs Ag/AgCl) was similar to the values reported by Gregoire et al. (2014) in a work published at the same time as the results of Chapter 7 (October 2014). In a biocathode predominantly covered by betaproteobacteria (including *Rhodocyclales* and *Burkholderiales*), nitrate reduction occurred at a mid-point potential of +17 mV vs SHE (-0.18 V vs Ag/AgCl), and a Nerstian current-potential dependency was also observed. Hence, both works (Gregoire et al., 2014 and Pous et al., 2014 (Chapter 7 of this thesis)) suggested that denitrifying biocathodes uses of extracellular electron transfer mechanisms similar to microbial bioanodes (Rosenbaum et al., 2011).

9.4. Implications of this thesis

From the discussion above, it can be stated that bioelectrochemical systems have the potential to be a sustainable alternative for nitrate-polluted groundwater treatment.

Despite the low conductivity of groundwater, nitrate present in groundwater can be reduced to dinitrogen gas using BES. If operational conditions are adapted, BES can be an alternative for the bioremediation of other pollutants usually found in subsurface waters, such as sulfate (Coma et al., 2013), arsenite (Pous et al., 2015a), hexavalent uranium (Gregory and Lovley, 2005) or chlorinated compounds (Aulenta et al., 2008).

The operation of the bioelectrochemical system is a key factor in obtaining high denitrification rates without accumulation of intermediates (nitrite and nitrous oxide). In this thesis, the operation at a fixed cathode potential in a range from -103 and -203 mV vs SHE allowed successful nitrate-polluted groundwater treatment. The standards for drinking-water were met in terms of nitrates and nitrites, and minimizing N_2O emissions. Even effluents free of nitrate, nitrite or nitrous oxide can be achieved.

The operation at low hydraulic retention times promotes nitrate consumption rates without an increase of nitrite or nitrous oxide accumulations. However, at low HRT the effluent nitrate concentration increases.

Tubular designed BES rather than rectangular BES allowed higher overall denitrifying performances. It might enforce a better cathode potential and water flow distribution, and hence a better homogenization of nutrients (nitrate, inorganic carbon and other nutrients).

The use of a poised cathode potential allows for a treatment free of organic carbon or chemical doses. Consequently, a successful treatment can be achieved at a competitive operational cost without modifying characteristics of the water. The

use of abiotic oxidations at the anode creates a scenario where *in situ* disinfection processes, via the production of free chlorine using Ti-MMO anodes, are possible.

Strategies for monitoring reactor microbiomes of denitrifying BES from microbiological and electrochemical perspectives have been successfully evaluated. The use of flow cytometry combined with T-RFLP allowed for elucidation of the structure-function relationship of a denitrifying biocathode, thereby identifying the different subcommunities responsible for the different denitrification steps. The use of microcosms was shown as an effective way to characterize extracellular electron transfer of biocathodic biofilms. Concretely, the nitrate and nitrite reduction thermodynamics were described for a *Thiobacillus* sp. dominated cathode.

Chapter 10. Conclusions

Nitrate-polluted groundwater can be sustainably treated using denitrifying bioelectrochemical systems with competitive energy consumption and no chemical additions.

The nitrate treatment efficiency, denitrification rates and operational costs obtained during this work suggest that denitrifying BES could be a competitive technology for the treatment of nitrates in groundwater.

Different operational modes, BES configurations and alternative monitoring techniques were assessed to maximize the denitrifying BES capabilities. The main conclusions can be summarized as follows:

- The operation at a fixed cathode potential in a range from -103 and -203 mV vs SHE allowed successful treatment of nitrate-polluted groundwater. At -123 mV vs SHE, the highest conversions of nitrate to dinitrogen gas were achieved. By poising the cathode potential, no dose of chemicals (as acetate as anode electron donor) is required, allowing a treatment at a competitive estimated operational cost (between 0.38 and 0.20 $kWh \cdot m^{-3}_{treated}$ or $0.68 \cdot 10^{-2}$ and $1.27 \cdot 10^{-2}$ $kWh \cdot gN_{removed}^{-1}$).

- The operation at low hydraulic retention time increased the nitrate consumption rate (up to 700 $gN \cdot m^{-3} \cdot d^{-1}$ at 0.6 h) and decreased NO_2^- and N_2O accumulations. A linear correlation between the nitrate loading rate (modified by changing the HRT) and the nitrate consumption rate was found ($r^2 = 0.9989$), with slope of 0.5. In addition to nitrate consumption rate increasing, effluent nitrate concentrations increased as well.

- The microbiome monitoring of the denitrifying biocathode using flow cytometry combined with T-RFLP revealed that different subcommunities were in charge of the different denitrification steps. A subcommunity mainly composed of *Thiobacillus* sp. was the major contributor to NO_3^- reduction to NO_2^-. A wider group of subcommunities were involved in NO_2^- and N_2O reductions.

- Thermodynamics of the extracellular electron transfer mechanism in a denitrifying biocathode were revealed. A biofilm, mainly composed of *Thiobacillus* sp., catalyzed nitrate to nitrite at -103 mV vs SHE (-0.30 V vs Ag/AgCl) and the further reduction of nitrite to nitric oxide at -503 mV vs SHE (-0.70 V vs Ag/AgCl).
- Higher overall denitrifying performances were obtained when tubular BES was used (compared to rectangular BES). It suggested that a tubular design would be more appropiated for scaling-up.

The future directions for research in this area can have different perspectives. From the purely scientific research, a remarkable knowledge regarding denitrifying biocathodes has been obtained during the last years. Nevertheless, there are still knowledge gaps as the elucidation of whether direct or mediated electron transfer mechanisms take place in microbial denitrifying biocathodes, and in the field of microbial biocathodes in general. Furthermore, knowledge regarding the requirements of inorganic carbon consumed by biocathodic denitrifying microorganisms remains unknown.

From the perspective of applied research, the clear objective in the following years should be scaling-up the technology. The reproducibility of lab-scale results in pilot-scale plants is a key step for the succesful future of denitrifying bioelectrochemical systems in particular, but for microbial electrochemical technologies in general. In this sense, the work presented in this PhD thesis continues with the construction of a pilot plant for the treatment of 2.5-6.0 $m^3 \cdot d^{-1}$ of nitrate-polluted groundwater.

Chapter 11. References

Aelterman, P., Rabaey, K., Pham, H.T., Boon, N., Verstraete, W., 2006. Continuous electricity generation at high voltages and currents using stacked microbial fuel cells. Environ. Sci. Technol. 40 (10), 3388–3394. DOI:10.1021/es0525511.

Ali, M.B.S., Hamrouni, B., Dhahbi, M., 2010. Electrodialytic defluoridation of brackish water: effect of process parameters and water characteristics. Clean - Soil, Air, Water 38 (7), 623–629. DOI:10.1002/clen.200900301.

Anderson, L.J., Richardson, D.J., Butt, J.N., 2001. Catalytic protein film voltammetry from a respiratory nitrate reductase provides evidence for complex electrochemical modulation of enzyme activity. Bioelectrochemistry 40 (38), 11294–11307. DOI: 10.1021/bi002706b.

Ansys, 2009. Ansys fluent theory guide. pp. 49 - 53. Inc Northbrook IL.

APHA, 2005. Standard Methods for the Examination of Water and Wastewater, 19th ed. Washington DC, USA.

Aslan, S., Cakici, H., 2007. Biological denitrification of drinking water in a slow sand filter. J. Hazard. Mater. 148 (1-2), 253–258. DOI:10.1016/j.jhazmat.2007.02.012.

Aulenta, F., Gossett, J.M., Papini, M.P., Rossetti, S., Majone, M., 2005. Comparative study of methanol, butyrate, and hydrogen as electron donors for long-term dechlorination of tetrachloroethene in mixed anerobic cultures. Biotechnol. Bioeng. 91 (6), 743–753. DOI:10.1002/bit.20569.

Aulenta, F., Reale, P., Catervi, A., Panero, S., Majone, M., 2008. Kinetics of trichloroethene dechlorination and methane formation by a mixed anaerobic culture in a bio-electrochemical system. Electrochim. Acta 53 (16), 5300–5305. DOI:10.1016/j.electacta.2008.02.084.

Bagotzky, V.S., 1993. Fundamentals of electrochemistry. Plenum Press, New York.

Batlle-Vilanova, P., Puig, S., Gonzalez-Olmos, R., Vilajeliu-Pons, A., Bañeras, L., Balaguer, M.D., Colprim, J., 2014. Assessment of biotic and abiotic graphite

cathodes for hydrogen production in microbial electrolysis cells. Int. J. Hydrogen Energy 39 (3), 1297–1305. DOI:10.1016/j.ijhydene.2013.11.017.

Bertrand, P., Frangioni, B., Dementin, S., Sabaty, M., Arnoux, P., Guigliarelli, B., Pignol, D., Léger, C., 2007. Effects of slow substrate binding and release in redox enzymes: theory and application to periplasmic nitrate reductase. J. Phys. Chem. B 111 (34), 10300–10311. DOI:10.1021/jp074340j.

Butler, C.S., Clauwaert, P., Green, S.J., Verstraete, W., Nerenberg, R., 2010. Bioelectrochemical perchlorate reduction in a microbial fuel cell. Environ. Sci. Technol. 44 (12), 4685–4691. DOI:10.1021/es901758z.

Cai, J., Zheng, P., 2013. Simultaneous anaerobic sulfide and nitrate removal in microbial fuel cell. Bioresour. Technol. 128, 760–764. DOI:10.1016/j.biortech.2012.08.046.

Cai, J., Zheng, P., Qaisar, M., Xing, Y., 2014. Effect of operating modes on simultaneous anaerobic sulfide and nitrate removal in microbial fuel cell. J. Ind. Microbiol. Biotechnol. 41 (5), 795–802. DOI:10.1007/s10295-014-1425-4.

Carmona-Martínez, A.A., Pierra, M., Trably, E., Bernet, N., 2013. High current density via direct electron transfer by the halophilic anode respiring bacterium *Geoalkalibacter subterraneus*. Phys. Chem. Chem. Phys. 15 (45), 19699–19707. DOI:10.1039/c3cp54045f.

Chen, G.-W., Choi, S.-J., Lee, T.-H., Lee, G.-Y., Cha, J.-H., Kim, C.-W., 2008. Application of biocathode in microbial fuel cells: cell performance and microbial community. Appl. Microbiol. Biotechnol. 79 (3), 379–388. DOI:10.1007/s00253-008-1451-0.

Cheng, K.Y., Ginige, M.P., Kaksonen, A.H., 2012. Ano-cathodophilic biofilm catalyzes both anodic carbon oxidation and cathodic denitrification. Environ. Sci. Technol. 46 (18), 10372–10378. DOI:10.1021/es3025066.

Cheng, K.Y., Ho, G., Cord-Ruwisch, R., 2010. Anodophilic biofilm catalyzes cathodic oxygen reduction. Environ. Sci. Technol. 44 (1), 518–525. DOI:10.1021/es9023833.

Cheng, S., Xing, D., Call, D.F., Logan, B.E., 2009. Direct biological conversion of electrical current into methane by electromethanogenesis. Environ. Sci. Technol. 43 (10), 3953–3958. DOI:10.1021/es803531g.

Clauwaert, P., Desloover, J., Shea, C., Nerenberg, R., Boon, N., Verstraete, W., 2009. Enhanced nitrogen removal in bio-electrochemical systems by pH control. Biotechnol. Lett. 31 (10), 1537–1543. DOI:10.1007/s10529-009-0048-8.

Clauwaert, P., Rabaey, K., Aelterman, P., De Schamphelaire, L., Pham, T.H., Boeckx, P., Boon, N., Verstraete, W., 2007a. Biological denitrification in microbial fuel cells. Environ. Sci. Technol. 41 (9), 3354–3360. DOI:10.1021/es062580r.

Clauwaert, P., Van Der Ha, D., Boon, N., Verbeken, K., Verhaege, M., Rabaey, K., Verstraete, W., 2007b. Open air biocathode enables effective electricity generation with microbial fuel cells. Environ. Sci. Technol. 41 (21), 7564–7569. DOI:10.1021/es0709831.

Colprim, J., Balaguer, M.D., Puig, S., Pous, N., 2014. Bioelectrochemical water treatment and apparatus. WO2014/082989.

Coma, M., Puig, S., Pous, N., Balaguer, M.D., Colprim, J., 2013. Biocatalysed sulphate removal in a BES cathode. Bioresour. Technol. 130, 218–223. DOI:10.1016/j.biortech.2012.12.050.

Cong, Y., Xu, Q., Feng, H., Shen, D., 2013. Efficient electrochemically active biofilm denitrification and bacteria consortium analysis. Bioresour. Technol. 132, 24–27. DOI:10.1016/j.biortech.2013.01.004.

Darbi, A., Viraraghavan, T., Butler, R., Corkal, D., 2003. Column studies on nitrate removal from potable water. Water, Air, Soil Pollut. 150 (1-4), 235–254. DOI: 10.1023/A:1026149311106.

Dell'Acqua, S., Pauleta, S.R., Paes de Sousa, P.M., Monzani, E., Casella, L., Moura, J.J.G., Moura, I., 2010. A new CuZ active form in the catalytic reduction of N_2O by nitrous oxide reductase from *Pseudomonas nautica*. J. Biol. Inorg. Chem. 15 (6), 967–976. DOI:10.1007/s00775-010-0658-6.

Desloover, J., Puig, S., Virdis, B., Clauwaert, P., Boeckx, P., Verstraete, W., Boon, N., 2011. Biocathodic nitrous oxide removal in bioelectrochemical systems. Environ. Sci. Technol. 45 (24), 10557–10566. DOI:10.1021/es202047x.

Doherty, T., Sunderland, J.G., Roberts, E.P.L., Pickett, D.J., 1996. An improved model of potential and current distribution within a flow-through porous electrode. Electrochim. Acta 41 (4 SPEC.ISS.), 519–526. DOI: 10.1016/0013-4686(96)81774-9.

Duca, M., Koper, M.T.M., 2012. Powering denitrification: The perspectives of electrocatalytic nitrate reduction. Energ. Environ. Sci. 5 (12), 9726-9742. DOI: 10.1039/c2ee23062c.

Dutta, P.K.; Rabaey, K.; Yuan, Z.; Rozendal, R.A.; Keller, J., 2010. Electrochemical sulfide removal and recovery from paper mill anaerobic treatment effluent. Water Res. 44 (8), 2563-2571.. DOI: 10.1016/j.watres.2010.01.008.

El Midaoui, A., Elhannouni, F., Taky, M., Chay, L., Menkouchi Sahli, M.A., Echihabi, L., Hafsi, M., 2002. Optimization of nitrate removal operation from ground water by electrodialysis. Sep. Purif. Technol. 29 (3), 235–244. DOI:10.1016/S1383-5866(02)00092-8.

EPA, 2006. EPA, Environmental Protection Agency. Consumer Factsheet on Nitrates/Nitrites.

Ferguson, S.J., Richardson, D.J., 2004. The enzymes and bioenergetics of bacterial nitrate, nitrite, nitric oxide and nitrous oxide respiration, in: Zannoni, D. (Ed.), Respiration in Archaea and Bacteria, Advances in Photosynthesis and Respiration, Volume 16. Springer, Netherlands, pp. 169–206.

Fernandez, N., Sierra-Alvarez, R., Field, J.A., Amils, R., 2008. Microbial community dynamics in a chemolithotrophic denitrification reactor inoculated with methanogenic granular sludge. Chemosphere. 70 (3), 462–474. DOI:10.1016/j.chemosphere.2007.06.062.

Forster, P., Ramaswamy, V., Artaxo, P., Berntsen, T., Betts, R., Fahey, D.W., Haywood, J., Lean, J., Lowe, D.C., Myhre, G., Nganga, J., Prinn, R., Raga, G., Schulz, M., Van Dorland, R., 2007. Changes in atmospheric constituents and in radiative forcing, in: Solomon, S., Qin, D., Manning, M., Chen, Z., Marquis, M., Averyt, K.B., Tignor, M., Miller, H.L. (Eds.), Climate Change 2007: The Physical Science Basis. Contribution of Working Group I to the Fourth Assessment Report of the Intergovernmental Panel on Climate Change. Cambridge and New York.

Fricke, K., Harnisch, F., Schröder, U., 2008. On the use of cyclic voltammetry for the study of anodic electron transfer in microbial fuel cells. Energy Environ. Sci. 1 (1), 144–147. DOI:10.1039/b802363h.

Fu, F., Dionysiou, D.D., Liu, H., 2014. The use of zero-valent iron for groundwater remediation and wastewater treatment: A review. J. Hazard. Mater. 267, 194-205. DOI: 10.1016/j.jhazmat.2013.12.062.

Geelhoed, J.S., Stams, A.J.M., 2011. Electricity-assisted biological hydrogen production from acetate by *Geobacter sulfurreducens*. Environ. Sci. Technol. 45 (2), 815–820. DOI:10.1021/es102842p.

Ghafari, S., Hasan, M., Aroua, M.K., 2008. Bio-electrochemical removal of nitrate from water and wastewater - A review. Bioresour. Technol. 99 (10), 3965–3974. DOI:10.1016/j.biortech.2007.05.026.

Gregoire, K.P., Glaven, S.M., Hervey, J., Lin, B., Tender, L.M., 2014. Enrichment of a high-current density denitrifying microbial biocathode. J. . Electrochem. Soc. 161 (13), H3049-H3057. DOI: 10.1149/2.0101413jes.

Gregory, K.B., Bond, D.R., Lovley, D.R., 2004. Graphite electrodes as electron donors for anaerobic respiration. Environ. Microbiol. 6 (6), 596–604. DOI:10.1111/j.1462-2920.2004.00593.x.

Gregory, K.B., Lovley, D.R., 2005. Remediation and recovery of uranium from contaminated subsurface environments with electrodes. Environ. Sci. Technol. 39 (22), 8943–8947. DOI:10.1021/es050457e.

Groundwater Directive (GWD); 2006/118/EC of the European Parliament and of the Council of 12 December 2006 on the protection of groundwater against pollution and deterioration, 2006.

Gujer, W., Henze, M., Mino, T., Van Loosdrecht, M., 1999. Activated sludge model No. 3. Water Sci. Technol. 39 (1), 183–193. DOI:10.1016/S0273-1223(98)00785-9.

Haaijer, S.C.M., Crienen, G., Jetten, M.S.M., Op den Camp, H.J.M., 2012. Anoxic iron cycling bacteria from an iron sulfide- and nitrate-rich freshwater environment. Front. Microbiol. 3 (FEB), Article 26. DOI:10.3389/fmicb.2012.00026.

Harnisch, F., Freguia, S., 2012. A basic tutorial on cyclic voltammetry for the investigation of electroactive microbial biofilms. Chem. Asian J. 7 (3), 466–475. DOI:10.1002/asia.201100740.

Harnisch, F., Koch, C., Patil, S. A., Hübschmann, T., Müller, S., Schröder, U., 2011. Revealing the electrochemically driven selection in natural community derived microbial biofilms using flow-cytometry. Energy Environ. Sci. 4 (4), 1265–1267. DOI:10.1039/c0ee00605j.

Harnisch, F., Rabaey, K., 2012. The diversity of techniques to study electrochemically active biofilms highlights the need for standardization. ChemSusChem. 5 (6), 1027–1038. DOI:10.1002/cssc.201100817.

He, Z., Angenent, L.T., 2006. Application of bacterial biocathodes in microbial fuel cells. Electroanalysis. 18 (19-20), 2009–2015. DOI:10.1002/elan.200603628.

Hedrich, S., Schlömann, M., Johnson, D.B., 2011. The iron-oxidizing proteobacteria. Microbiology. 157 (6), 1551–1564. DOI:10.1099/mic.0.045344-0.

Huang, C.-P., Wang, H.-W., Chiu, P.-C., 1998. Nitrate reduction by metallic iron. Water Res. 32 (8), 2257–2264. DOI:10.1016/S0043-1354(97)00464-8.

Huang, L., Chen, J., Quan, X., Yang, F., 2010. Enhancement of hexavalent chromium reduction and electricity production from a biocathode microbial fuel cell. Bioprocess Biosyst. Eng. 33 (8), 937–945. DOI:10.1007/s00449-010-0417-7.

Jeremiasse, A.W., Hamelers, H.V.M., Buisman, C.J.N., 2010. Microbial electrolysis cell with a microbial biocathode. Bioelectrochemistry 78 (1), 39–43. DOI:10.1016/j.bioelechem.2009.05.005.

Jeremiasse, A.W., Hamelers, H.V.M., Croese, E., Buisman, C.J.N., 2012. Acetate enhances startup of a H_2-producing microbial biocathode. Biotechnol. Bioeng. 109 (3), 657–664. DOI:10.1002/bit.24338.

Jia, Y.-H., Tran, H.-T., Kim, D.-H., Oh, S.-J., Park, D.-H., Zhang, R.-H., Ahn, D.-H., 2008. Simultaneous organics removal and bio-electrochemical denitrification in microbial fuel cells. Bioprocess Biosyst. Eng. 31 (4), 315–21. DOI:10.1007/s00449-007-0164-6.

Jung, R.K., Cheng, S., Oh, S.-E., Logan, B.E., 2007. Power generation using different cation, anion, and ultrafiltration membranes in Microbial Fuel Cells. Environ. Sci. Technol. 41 (3), 1004–1009. DOI:10.1021/es062202m.

Karanasios, K.A., Vasiliadou, I.A., Pavlou, S., Vayenas, D.V., 2010. Hydrogenotrophic denitrification of potable water: a review. J. Hazard. Mater. 180 (1-3), 20–37. DOI:10.1016/j.jhazmat.2010.04.090.

Kato, S., Hashimoto, K., Watanabe, K., 2012. Microbial interspecies electron transfer via electric currents through conductive minerals. Proc. Natl. Acad. Sci. U. S. A. 109 (25), 10042–10046. DOI:10.1073/pnas.1117592109.

Kimura, K., Nakamura, M., Watanabe, Y., 2002. Nitrate removal by a combination of elemental sulfur-based denitrification and membrane filtration. Water Res. 36 (7), 1758–1766. DOI:10.1016/S0043-1354(01)00376-1.

Knobeloch, L., Salna, B., Hogan, A., Postle, J., Anderson, H., 2000. Blue babies and nitrate-contaminated well water. Environ. Health Perspect. 108 (7), 675–678.

Koch, C., Fetzer, I., Schmidt, T., Harms, H., Müller, S., 2013a. Monitoring functions in managed microbial systems by cytometric bar coding. Environ. Sci. Technol. 47 (3), 1753–1760. DOI:10.1021/es3041048.

Koch, C., Günther, S., Desta, A.F., Hübschmann, T., Müller, S., 2013b. Cytometric fingerprinting for analyzing microbial intracommunity structure variation and identifying subcommunity function. Nat. Protoc. 8 (1), 190–202. DOI:10.1038/nprot.2012.149.

Koch, C., Müller, S., Harms, H., Harnisch, F., 2014. Microbiomes in bioenergy production: from analysis to management. Curr. Opin. Biotechnol. 27, 65–72. DOI:10.1016/j.copbio.2013.11.006.

Kondaveeti, S., Lee, S.-H., Park, H.-D., Min, B., 2014. Bacterial communities in a bioelectrochemical denitrification system: the effects of supplemental electron acceptors. Water Res. 51, 25–36. DOI:10.1016/j.watres.2013.12.023.

Kondaveeti, S., Min, B., 2013. Nitrate reduction with biotic and abiotic cathodes at various cell voltages in bioelectrochemical denitrification system. Bioprocess Biosyst. Eng. 36 (2), 231–238. DOI:10.1007/s00449-012-0779-0.

Lane, D.J., 1991. 16S/23S rRNA sequencing, in: Sons, J.W. and (Ed.), Nucleic Acid Techniques in Bacterial Systematics. New York, USA, pp. 115–175.

Lee, K.-C., Rittmann, B.E., 2002. Applying a novel autohydrogenotrophic hollow-fiber membrane biofilm reactor for denitrification of drinking water. Water Res. 36 (8), 2040–2052. DOI:10.1016/S0043-1354(01)00425-0.

Lee, S.-H., Kondaveeti, S., Min, B., Park, H.-D., 2013. Enrichment of Clostridia during the operation of an external-powered bio-electrochemical denitrification system. Process Biochem. 48 (2), 306–311. DOI:10.1016/j.procbio.2012.11.020.

Liu, H., Grot, S., Logan, B.E., 2005. Electrochemically assisted microbial production of hydrogen from acetate. Environ. Sci. Technol. 39 (11), 4317–4320. DOI:10.1021/es050244p.

Liu, H., Logan, B.E., 2004. Electricity generation using an air-cathode single chamber microbial fuel cell in the presence and absence of a proton exchange membrane. Environ. Sci. Technol. 38 (14), 4040–4046. DOI:10.1021/es0499344.

Liu, H., Ramnarayanan, R., Logan, B.E., 2004. Production of electricity during wastewater treatment using a single chamber microbial fuel cell. Environ. Sci. Technol. 38 (7), 2281–2285. DOI:10.1021/es034923g.

Logan, B.E., Hamelers, B., Rozendal, R., Schröder, U., Keller, J., Freguia, S., Aelterman, P., Verstraete, W., Rabaey, K., 2006. Microbial fuel cells: methodology and technology. Environ. Sci. Technol. 40 (17), 5181–5192. DOI:10.1021/es0605016.

Lu, H., Chandran, K., 2010. Factors promoting emissions of nitrous oxide and nitric oxide from denitrifying sequencing batch reactors operated with methanol and ethanol as electron donors. Biotechnol. Bioeng. 106 (3), 390–398. DOI:10.1002/bit.22704.

Marshall, C.W., Ross, D.E., Fichot, E.B., Norman, R.S., May, H.D., 2012. Electrosynthesis of commodity chemicals by an autotrophic microbial community. Appl. Environ. Microbiol. 78 (23), 8412–8420. DOI:10.1128/AEM.02401-12.

Marsili, E., Baron, D.B., Shikhare, I.D., Coursolle, D., Gralnick, J.A., Bond, D.R., 2008. *Shewanella* secretes flavins that mediate extracellular electron transfer. Proc. Natl. Acad. Sci. U. S. A. 105 (10), 3968–3973. DOI:10.1073/pnas.0710525105.

Matějů, V., Čižinská, S., Krejčí, J., Janoch, T., 1992. Biological water denitrification - A review. Enzyme Microb. Technol. 14 (3), 170–183. DOI:10.1016/0141-0229(92)90062-S.

Maul, G.A., Kim, Y., Amini, A., Zhang, Q., Boyer, T.H., 2014. Efficiency and life cycle environmental impacts of ion-exchange regeneration using sodium, potassium, chloride, and bicarbonate salts. Chem. Eng. J. 254, 198–209. DOI:10.1016/j.cej.2014.05.086.

McAdam, E.J., Judd, S.J., 2008. Immersed membrane bioreactors for nitrate removal from drinking water: Cost and feasibility. Desalination. 231 (1-3), 52–60. DOI:10.1016/j.desal.2007.11.038.

Menció, A., Boy, M., Mas-Pla, J., 2011. Analysis of vulnerability factors that control nitrate occurrence in natural springs (Osona Region, NE Spain). Sci. Total Environ. 409 (16), 3049–3058. DOI:10.1016/j.scitotenv.2011.04.048.

Min, B., Logan, B.E., 2004. Continuous electricity generation from domestic wastewater and organic substrates in a flat plate microbial fuel cell. Environ. Sci. Technol. 38 (21), 5809–5814. DOI: 10.1021/es0491026.

Mohan, S.V., Srikanth, S., 2011. Enhanced wastewater treatment efficiency through microbially catalyzed oxidation and reduction: synergistic effect of biocathode microenvironment. Bioresour. Technol. 102 (22), 10210–10220. DOI:10.1016/j.biortech.2011.08.034.

Molognoni, D., Puig, S., Balaguer, M.D., Liberale, A., Capodaglio, A.G., Callegari, A., Colprim, J., 2014. Reducing start-up time and minimizing energy losses of microbial fuel cells using maximum power point tracking strategy. J. Power Sources 269, 403–411. DOI:10.1016/j.jpowsour.2014.07.033.

Müller, S., Nebe-von-Caron, G., 2010. Functional single-cell analyses: flow cytometry and cell sorting of microbial populations and communities. FEMS Microbiol. Rev. 34 (4), 554–587. DOI:10.1111/j.1574-6976.2010.00214.x.

Nevin, K.P., Woodard, T.L., Franks, A.E., Summers, Z.M., Lovley, D.R., 2010. Microbial electrosynthesis: feeding microbes electricity to convert carbon dioxide and water to multicarbon extracellular organic compounds. MBio 1 (2). DOI:10.1128/mBio.00103-10.

Nitrates Directive; 91/767/EU.

Ortiz, J.M., Expósito, E., Gallud, F., Garcís-García, V., Montiel, V., Alldaz, A., 2008. Desalination of underground brackish waters using an electrodialysis system powered directly by photovoltaic energy. Sol. Energy Mater. Sol. Cells 92 (12), 1677–1688. DOI:10.1016/j.solmat.2008.07.020.

Vitousek P.M., Aber, J.D., Howarth, R.W., Likens, G.E., Matson, P.A., Schindler, D.W., Schlesinger, W.H., Tilman, D.G., 1997. Human alteration of the global nitrogen cycle: sources and consequences. Ecol. Appl. 7 (3), 737–750.

Pan, Y., Ni, B.-J., Bond, P.L., Ye, L., Yuan, Z., 2013. Electron competition among nitrogen oxides reduction during methanol-utilizing denitrification in wastewater treatment. Water Res. 47 (10), 3273–3281. DOI:10.1016/j.watres.2013.02.054.

Pant, D., Van Bogaert, G., Diels, L., Vanbroekhoven, K., 2010. A review of the substrates used in microbial fuel cells (MFCs) for sustainable energy production. Bioresour. Technol. 101 (6), 1533–1543. DOI:10.1016/j.biortech.2009.10.017.

Parameswaran, P., Bry, T., Popat, S.C., Lusk, B.G., Rittmann, B.E., Torres, C.I., 2013. Kinetic, electrochemical, and microscopic characterization of the thermophilic, anode-respiring bacterium *Thermincola ferriacetica*. Environ. Sci. Technol. 47 (9), 4934–4940. DOI:10.1021/es400321c.

Park, H.I., Choi, Y.-J., Pak, D., 2005a. Autohydrogenotrophic denitrifying microbial community in a glass beads biofilm reactor. Biotechnol. Lett. 27 (13), 949–953. DOI:10.1007/s10529-005-7654-x.

Park, H.I., Kim, D.K., Choi, Y.-J., Pak, D., 2005b. Nitrate reduction using an electrode as direct electron donor in a biofilm-electrode reactor. Process Biochem. 40 (10), 3383–3388. DOI:10.1016/j.procbio.2005.03.017.

Park, H.I., Kim, J.S., Kim, D.K., Choi, Y.-J., Pak, D., 2006. Nitrate-reducing bacterial community in a biofilm-electrode reactor. Enzyme Microb. Technol. 39 (3), 453–458. DOI:10.1016/j.enzmictec.2005.11.028.

Potter, M.C., 1911. Effects accompanying the decomposition of organic compounds. Proc Roy Soc L. B 84, 260–276.

Pous, N., Casentini, B., Rossetti, S., Fazi, S., Puig, S., Aulenta, F., 2015a. Anaerobic arsenite oxidation with an electrode serving as the sole electron acceptor: A novel approach to the bioremediation of arsenic-polluted groundwater. J. Hazard. Mater. 283, 617–622. DOI:10.1016/j.jhazmat.2014.10.014.

Pous, N., Koch, C., Colprim, J., Puig, S., Harnisch, F., 2014. Extracellular electron transfer of biocathodes: Revealing the potentials for nitrate and nitrite reduction of denitrifying microbiomes dominated by *Thiobacillus* sp. Electrochem. commun. 49, 93–97. DOI:10.1016/j.elecom.2014.10.011.

Pous, N., Puig, S., Coma, M., Balaguer, M.D., Colprim, J., 2013. Bioremediation of nitrate-polluted groundwater in a microbial fuel cell. J. Chem. Technol. Biotechnol. 88 (9), 1690–1696. DOI:10.1002/jctb.4020.

Pous, N., Puig, S., Dolors Balaguer, M., Colprim, J., 2015b. Cathode potential and anode electron donor evaluation for a suitable treatment of nitrate-contaminated groundwater in bioelectrochemical systems. Chem. Eng. J. 263, 151–159. DOI:10.1016/j.cej.2014.11.002.

Puig, S., Coma, M., Desloover, J., Boon, N., Colprim, J., Balaguer, M.D., 2012. Autotrophic denitrification in microbial fuel cells treating low ionic strength waters. Environ. Sci. Technol. 46 (4), 2309–2315. DOI:10.1021/es2030609.

Puig, S., Serra, M., Coma, M., Balaguer, M.D., Colprim, J., 2011a. Simultaneous domestic wastewater treatment and renewable energy production using microbial fuel cells (MFCs). Water Sci. Technol. 64 (4), 904–909. DOI:10.2166/wst.2011.401.

Puig, S., Serra, M., Coma, M., Cabré, M., Balaguer, M.D., Colprim, J., 2010. Effect of pH on nutrient dynamics and electricity production using microbial fuel cells. Bioresour. Technol. 101 (24), 9594–9599. DOI:10.1016/j.biortech.2010.07.082.

Puig, S., Serra, M., Coma, M., Cabré, M., Dolors Balaguer, M., Colprim, J., 2011b. Microbial fuel cell application in landfill leachate treatment. J. Hazard. Mater. 185 (2-3), 763–767. DOI:10.1016/j.jhazmat.2010.09.086.

Puig, S., Serra, M., Vilar-Sanz, A., Cabré, M., Bañeras, L., Colprim, J., Balaguer, M.D., 2011c. Autotrophic nitrite removal in the cathode of microbial fuel cells. Bioresour. Technol. 102 (6), 4462–4467. DOI:10.1016/j.biortech.2010.12.100.

Qu, J., Fan, M., 2010. The current state of water quality and technology development for water pollution control in China. Crit. Rev. Environ. Sci. Technol. 40 (6), 519–560. DOI:10.1080/10643380802451953.

Rabaey, K., Angenent, L., Schröder, U., Keller, J., 2009. Bioelectrochemical systems: From extracellular electron transfer to biotechnological application. International water association publishing, London.

Rabaey, K., Lissens, G., Siciliano, S.D., Verstraete, W., 2003. A microbial fuel cell capable of converting glucose to electricity at high rate and efficiency. Biotechnol. Lett. 25 (18), 1531–1535. DOI:10.1023/A:1025484009367.

Rabaey, K., Ossieur, W., Verhaege, M., Verstraete, W., 2005. Continuous microbial fuel cells convert carbohydrates to electricity. Water Sci. Technol. 52 (1-2), 515–523.

Real Decreto 140/2003. Criterios sanitarios de la calidad del agua de consumo humano.

Rieger, P., 1994. Electrochemistry, Second. ed. Chapman and Hall, Inc., U.S.A.

Rosenbaum, M., Aulenta, F., Villano, M., Angenent, L.T., 2011. Cathodes as electron donors for microbial metabolism: which extracellular electron transfer mechanisms are involved? Bioresour. Technol. 102 (1), 324–333. DOI:10.1016/j.biortech.2010.07.008.

Ross, D.E., Flynn, J.M., Baron, D.B., Gralnick, J.A., Bond, D.R., 2011. Towards electrosynthesis in shewanella: energetics of reversing the Mtr pathway for reductive metabolism. PLoS One. 6 (2), e16649. DOI:10.1371/journal.pone.0016649.

Rozendal, R.A., Jeremiasse, A.W., Hamelers, H.V.M., Buisman, C.J.N., 2008. Hydrogen production with a microbial biocathode. Environ. Sci. Technol. 42 (2), 629–634. DOI:10.1021/es071720+.

Safe drinking water act (SDWA); P.L. 93 – 523.

Sakakibara, Y., Kuroda, M., 1993. Electric prompting and control of denitrification. Biotechnol. Bioeng. 42 (4), 535–537.

Sakakibara, Y., Nakayama, T., 2001. A novel multi-electrode system for electrolytic and biological water treatments: electric charge transfer and application to denitrification. Water Res. 35 (3), 768–78. DOI: 10.1016/S0043-1354(00)00327-4.

Schmidt, C.M., Fisher, A.T., Racz, A.J., Lockwood, B.S., Huertos, M.L., 2011. Linking denitrification and infiltration rates during managed groundwater recharge. Environ. Sci. Technol. 45 (22), 9634–9640. DOI:10.1021/es2023626.

Schröder, U., 2007. Anodic electron transfer mechanisms in microbial fuel cells and their energy efficiency. Phys. Chem. Chem. Phys. 9 (21), 2619–2629. DOI:10.1039/b703627m.

Schröder, U., 2011. Discover the possibilities: microbial bioelectrochemical systems and the revival of a 100-year–old discovery. J. Solid State Electrochem. 15 (7-8), 1481–1486. DOI:10.1007/s10008-011-1395-7.

Schumann, J., Koch, C., Günther, S., Fetzer, I., Müller, S., 2014. FlowCyBar: Analyze flow cytometric data using gate information. R package version 1.2.1.

Shi, L., Rosso, K.M., Zachara, J.M., Fredrickson, J.K., 2012. Mtr extracellular electron-transfer pathways in Fe(III)-reducing or Fe(II)-oxidizing bacteria: a genomic perspective. Biochem. Soc. Trans. 40 (6), 1261–1267. DOI:10.1042/BST20120098.

Shrimali, M., Singh, K.P., 2001. New methods of nitrate removal from water. Environ. Pollut. 112 (3), 351–359. DOI: 10.1016/S0269-7491(00)00147-0.

Soares, M.I.M., 2000. Biological denitrification of groundwater. Water. Air. Soil Pollut. 123 (1-4), 183–193.

Sprague, L.A., Hirsch, R.M., Aulenbach, B.T., 2011. Nitrate in the Mississippi River and its tributaries, 1980 to 2008: are we making progress? Environ. Sci. Technol. 45 (17), 7209–7216. DOI:10.1021/es201221s.

Srikanth, S., Marsili, E., Flickinger, M.C., Bond, D.R., 2008. Electrochemical characterization of *Geobacter sulfurreducens* cells immobilized on graphite paper electrodes. Biotechnol. Bioeng. 99 (5), 1065–73. DOI:10.1002/bit.21671.

Straub, K.L., Benz, M., Schink, B., Widdel, F., 1996. Anaerobic, nitrate-dependent microbial oxidation of ferrous iron. Appl. Environ. Microbiol. 62 (4), 1458–1460.

Straub, K.L., Schönhuber, W.A., Buchholz-Cleven, B.E.E., Schink, B., 2004. Diversity of ferrous iron-oxidizing, nitrate-reducing bacteria and their involvement in oxygen-independent iron cycling. Geomicrobiol. J. 21 (6), 371–378. DOI:10.1080/01490450490485854.

Thieme Chemistry (Hrsg.): RÖMPP Online - Version 3.5. Georg Thieme Verlag KG. Stuttgart 2009.

Tong, Y., He, Z., 2013. Nitrate removal from groundwater driven by electricity generation and heterotrophic denitrification in a bioelectrochemical system. J. Hazard. Mater. 262, 614–619. DOI:10.1016/j.jhazmat.2013.09.008.

Torres, C.I., Lee, H.-S., Rittmann, B.E., 2008. Carbonate species as OH- carriers for decreasing the pH gradient between cathode and anode in biological fuel cells. Environ. Sci. Technol. 42 (23), 8773–8777. DOI: 10.1021/es8019353.

Turner, S., Pryer, K.M., Miao, V.P., Palmer, J.D., 1999. Investigating deep phylogenetic relationships among cyanobacteria and plastids by small subunit rRNA sequence analysis. J. Eukaryot. Microbiol. 46 (4), 327–38.

Twomey, K.M., Stillwell, A.S., Webber, M.E., 2010. The unintended energy impacts of increased nitrate contamination from biofuels production. J. Environ. Monit. 12 (1), 218–224. DOI:10.1039/b913137j.

Tzedakis, T., Assouan, Y., 2014. One-flow feed divided electrochemical reactor for indirect electrolytic production of hypochlorite from brine for swimming pool treatment-experimental and theoretical optimization. Chem. Eng. J. 253, 427–437. DOI:10.1016/j.cej.2014.05.001.

Van Doan, T., Lee, T.K., Shukla, S.K., Tiedje, J.M., Park, J., 2013. Increased nitrous oxide accumulation by bioelectrochemical denitrification under autotrophic conditions: kinetics and expression of denitrification pathway genes. Water Res. 47 (19), 7087–7097. DOI:10.1016/j.watres.2013.08.041.

Van Grinsven, H.J.M., Rabl, A., De Kok, T.M., 2010. Estimation of incidence and social cost of colon cancer due to nitrate in drinking water in the EU: a tentative cost-benefit assessment. Environ. Health. 9 (1), 58. DOI:10.1186/1476-069X-9-58.

Vilar-Sanz, A., Puig, S., García-Lledó, A., Trias, R., Balaguer, M.D., Colprim, J., Bañeras, L., 2013. Denitrifying bacterial communities affect current production

and nitrous oxide accumulation in a microbial fuel cell. PLoS One. 8 (5), e63460. DOI:10.1371/journal.pone.0063460.

Virdis, B., Rabaey, K., Yuan, Z., Keller, J., 2008. Microbial fuel cells for simultaneous carbon and nitrogen removal. Water Res. 42 (12), 3013–3024. DOI:10.1016/j.watres.2008.03.017.

Virdis, B., Rabaey, K., Yuan, Z., Rozendal, R.A., Keller, J., 2009. Electron fluxes in a microbial fuel cell performing carbon and nitrogen removal. Environ. Sci. Technol. 43 (13), 5144–5149. DOI:10.1021/es8036302.

Wan, D., Liu, H., Qu, J., Lei, P., Ziao, S., Hou, Y., 2009. Using the combined bioelectrochemical and sulfur autotrophic denitrification system for groundwater denitrification. Bioresource Technol. 100 (1), 142-148. DOI: 10.1016/j.biortech.2008.05.042.

Wang, A.-J., Cheng, H.-Y., Liang, B., Ren, N.-Q., Cui, D., Lin, N., Kim, B.H., Rabaey, K., 2011. Efficient reduction of nitrobenzene to aniline with a biocatalyzed cathode. Environ. Sci. Technol. 45 (23), 10186–10193. DOI:10.1021/es202356w.

Water Framework Directive (WFD); 2000/60/EC.

Weyer, P.J., Cerhan, J.R., Kross, B.C., Hallberg, G.R., Kantamneni, J., Breuer, G., Jones, M.P., Zheng, W., Lynch, C.F., 2001. Municipal drinking water nitrate level and cancer risk in older women: the Iowa women's health study. Epidemiology 12 (3), 327–338. DOI:10.1097/00001648-200105000-00013.

WHO, 2007. Nitrate and nitrite in drinking-water: Background document for development of WHO Guidelines for drinking-water quality.

WHO, 2011. Nitrate and nitrite in drinking-water: Background document for development of WHO Guidelines for drinking-water quality.

Wijma, H.J., Jeuken, L.J.C., Verbeet, M.P., Armstrong, F.A., Canters, G.W., 2006. A random-sequential mechanism for nitrite binding and active site reduction in

copper-containing nitrite reductase. J. Biol. Chem. 281 (24), 16340–16346. DOI:10.1074/jbc.M601610200.

Wrighton, K.C., Virdis, B., Clauwaert, P., Read, S.T., Daly, R.A., Boon, N., Piceno, Y., Andersen, G.L., Coates, J.D., Rabaey, K., 2010. Bacterial community structure corresponds to performance during cathodic nitrate reduction. ISME J. 4 (11), 1443–1455. DOI:10.1038/ismej.2010.66.

Xafenias, N., Zhang, Y., Banks, C.J., 2013. Enhanced performance of hexavalent chromium reducing cathodes in the presence of *Shewanella oneidensis* MR-1 and lactate. Environ. Sci. Technol. 47 (9), 4512–4520. DOI:10.1021/es304606u.

Xiao, Y., Zheng, Y., Wu, S., Yang, Z.-H., Zhao, F., 2014. Bacterial community structure of autotrophic denitrification biocathode by 454 pyrosequencing of the 16S rRNA gene. Microb. Ecol. DOI:10.1007/s00248-014-0492-4.

Zhang, Y., Angelidaki, I., 2012. Bioelectrode-based approach for enhancing nitrate and nitrite removal and electricity generation from eutrophic lakes. Water Res. 46 (19), 6445–6453. DOI:10.1016/j.watres.2012.09.022.

Zhang, Y., Angelidaki, I., 2013. A new method for in situ nitrate removal from groundwater using submerged microbial desalination-denitrification cell (SMDDC). Water Res. 47 (5), 1827–1836. DOI:10.1016/j.watres.2013.01.005.

Zhao, Y., Zhang, B., Feng, C., Huang, F., Zhang, P., Zhang, Z., Yang, Y., Sugiura, N., 2012. Behavior of autotrophic denitrification and heterotrophic denitrification in an intensified biofilm-electrode reactor for nitrate-contaminated drinking water treatment. Bioresour. Technol. 107, 159–165. DOI:10.1016/j.biortech.2011.12.118.

Zhou, M., Fu, W., Gu, H., Lei, L., 2007. Nitrate removal from groundwater by a novel three-dimensional electrode biofilm reactor. Electrochim. Acta 52 (19), 6052–6059. DOI:10.1016/j.electacta.2007.03.064.